Interdisciplinary Research Centre

in

Materials for High Performance Applications

Final Proceedings of The EOARD/IRC-sponsored International Workshop on Gamma Aluminide Alloy Technology

held from 1 to 3 May 1996
at The IRC in Materials for High Performance Applications
The University of Birmingham

SECTION THREE

THE UNIVERSITY OF BIRMINGHAM

UNIVERSITY OF WALES SWANSEA

THE UNIVERSITY OF BIRMINGHAM AND UNIVERSITY OF WALES SWANSEA CONSORTIUM

Funded by the Engineering and Physical Sciences Research Council

Final Proceedings of The EOARD/IRC-sponsored International Workshop on Gamma Aluminide Alloy Technology

held from 1 to 3 May 1996
at The IRC in Materials for High Performance Applications
The University of Birmingham

SECTION THREE

The organisers wish to thank the United States Air Force European Office of Aerospace Research and Development for its contributions to the success of this conference

√

Gamma Alloy Technology: Fundamentals and Development

Young-Won Kim
UES-Materials & Processes
Dayton, OH, USA

Fundamentals
Processing
Microstructural Evolution
Structure/Property Relationships
Designing Microstructures
Component-Specific Alloy Design
Forming and Application
Summary and Future Direction

(April 1996)

Fundamentals

Phase Relations and Transformations

Microstructural Evolution

Deformation Mechanism

Alloying Effects

Deformation and Fracture Behavior

Environmental Resistance

Alpha Decomposition

At Very Slow Cooling Rate

At Intermediate Cooling Rates

Lamellar Structure Formation

- Stacking Fault Mechanism
- Gamma Precipitation and Growth

Ordering

- No Compositional Changes Involved
- Compositional Changes Involved

Effects of Composition and Cooling Rate

At Fast Cooling Rates

Widmanstätten Structures

Massively-Transformed Gamma

Formation of α_2 Phase

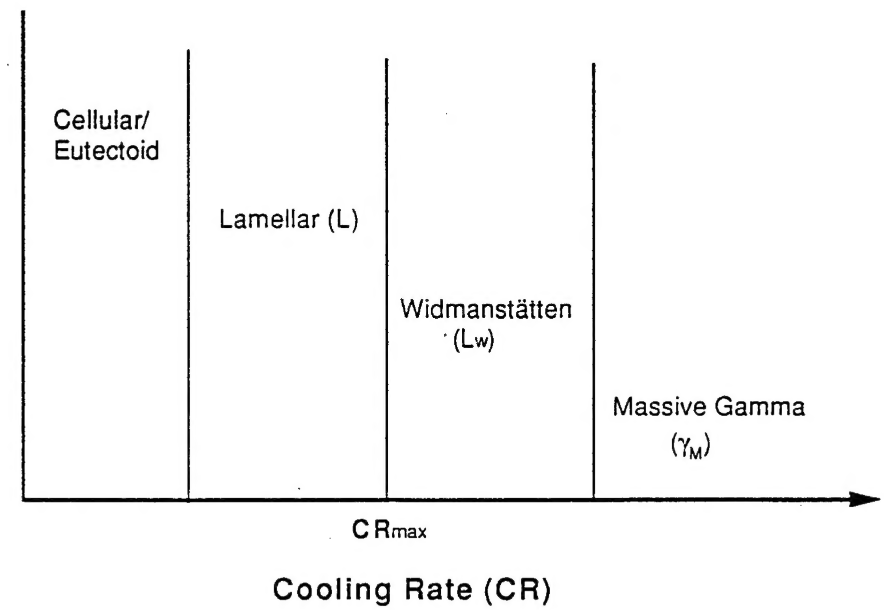
Cellular/
Eutectoid
Lamellar (L)
Widmanstätten
(Lw)
Massive Gamma
(γ_M)
C Rmax
Cooling Rate (CR)

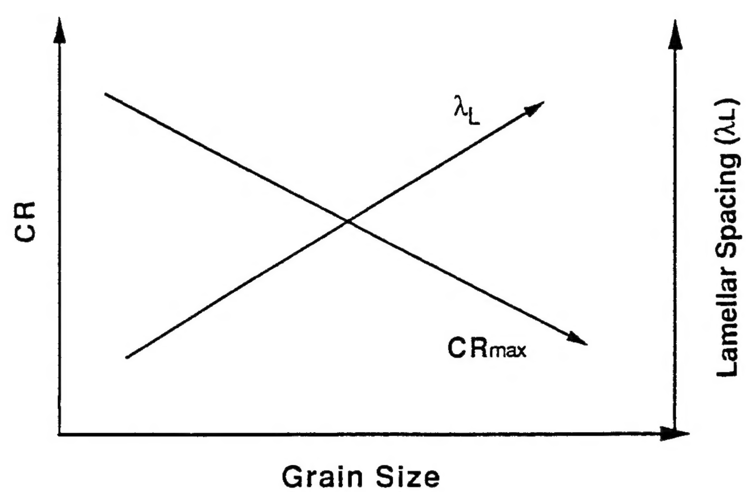
CR
λ_L
C Rmax
Lamellar Spacing (λL)
Grain Size

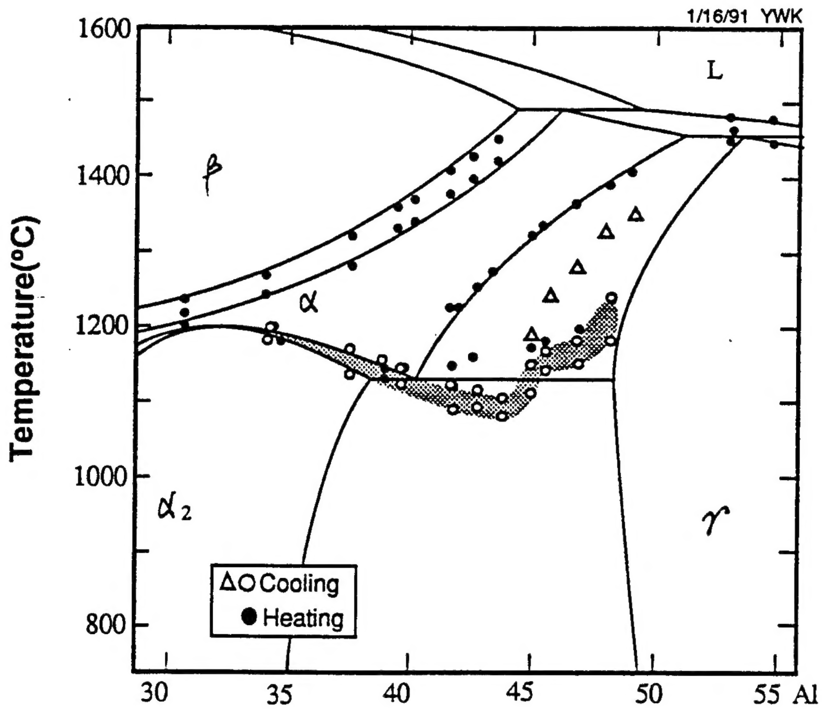

DTA Data at 30°C/min

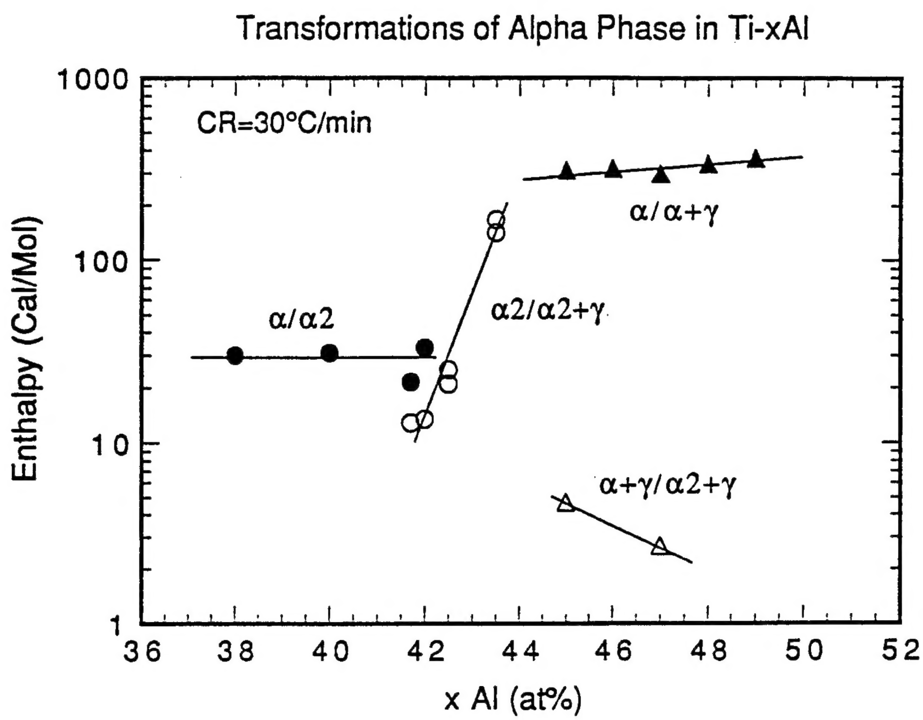

Transformations of Alpha Phase in Ti-xAl
CR=30°C/min
Enthalpy (Cal/Mol)
x Al (at%)
α/α+γ
α2/α2+γ
α/α2
α+γ/α2+γ
1000
100
10
1
36
38
40
42
44
46
48
50
52

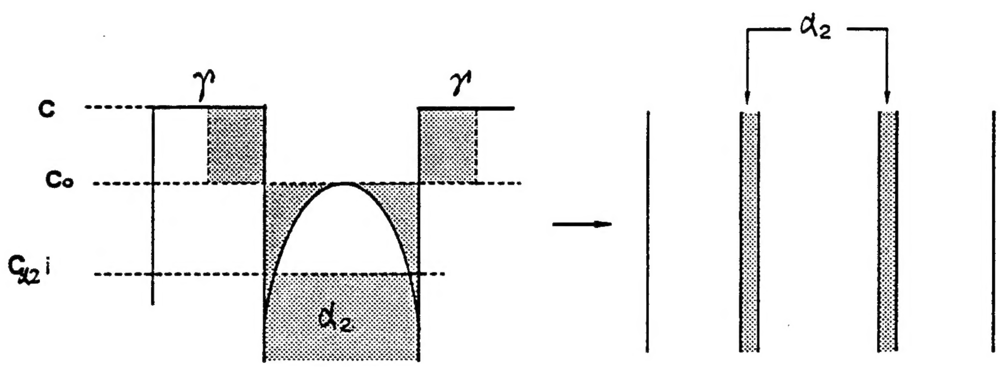

γ
γ
C
Co
α2
α2

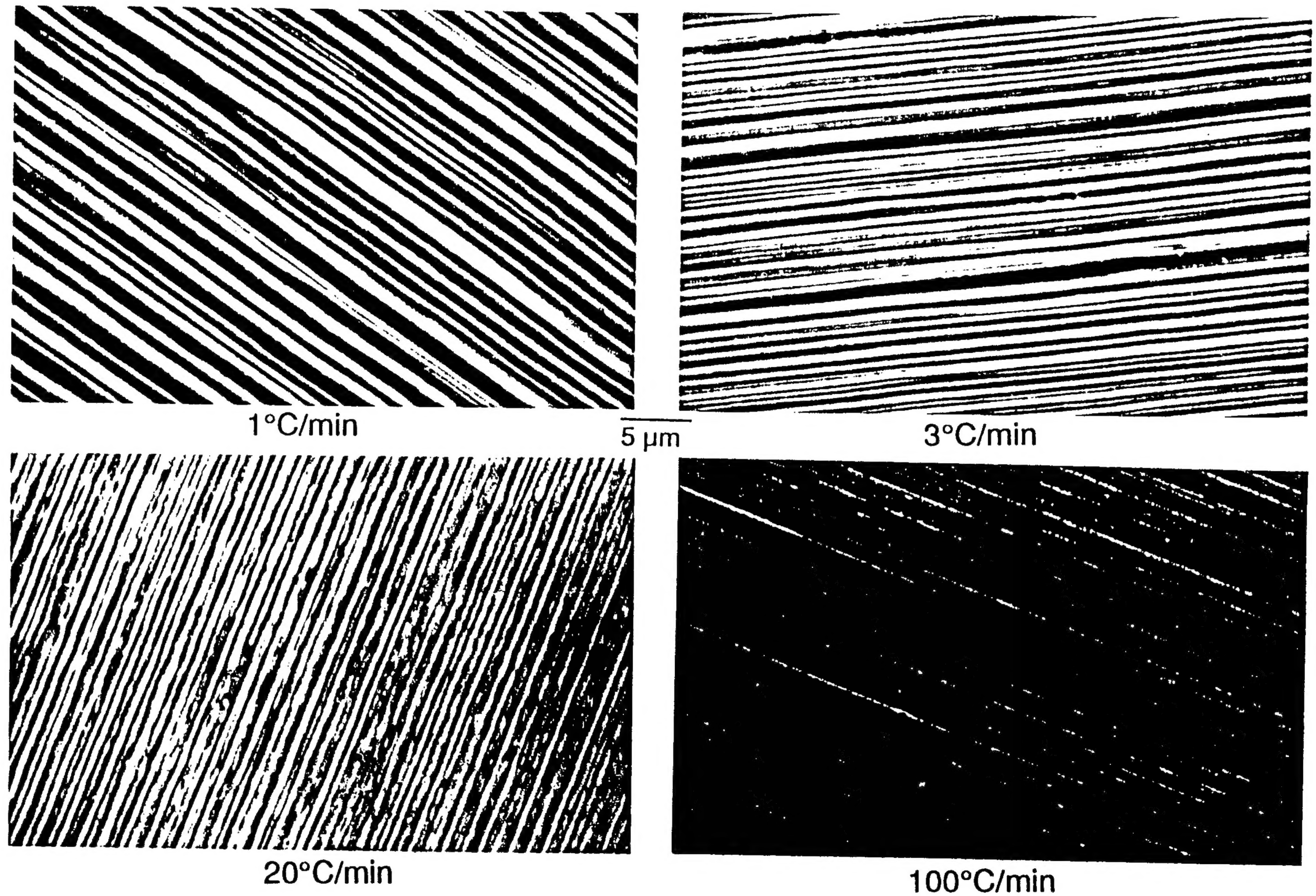

Ti-43Al : Homogenized and DTA Cooled

Cooling Rate vs Lamellar Spacing
(Ti-47Al)

0.2 °C/min

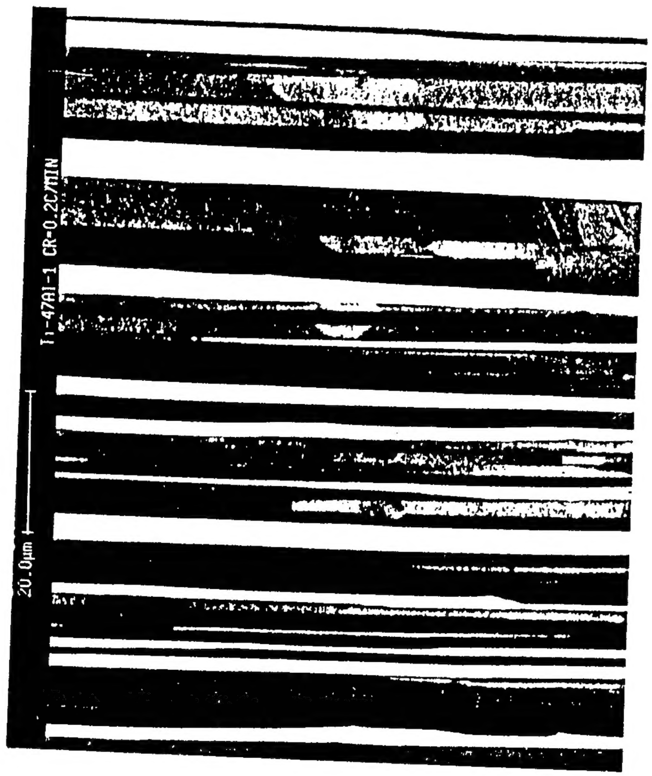

50°C/min

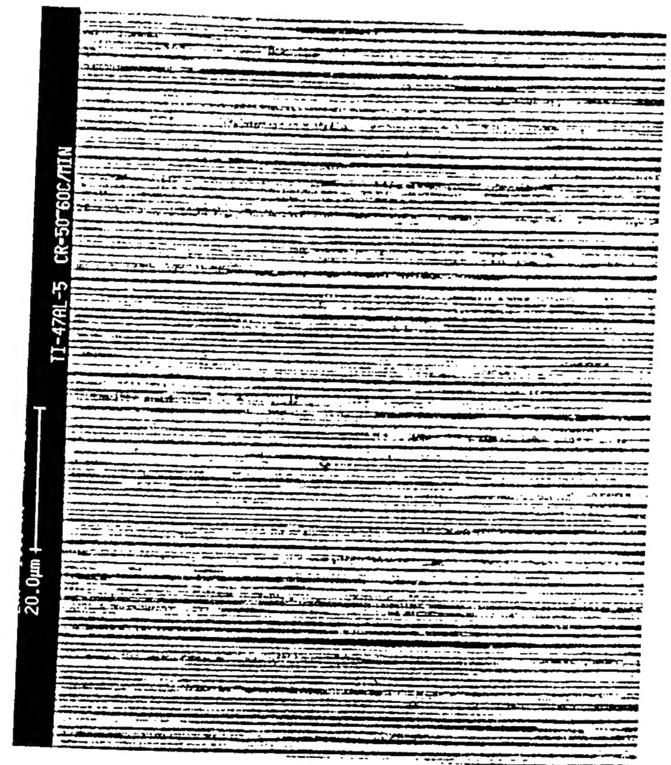

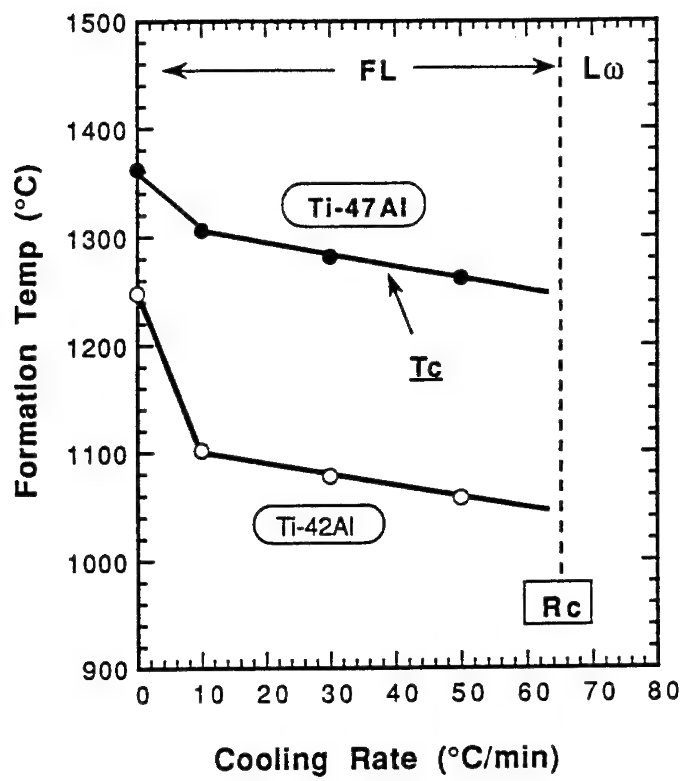

Kim (94)

Cooling Rate (R) vs Lamellar Spacing (λ)

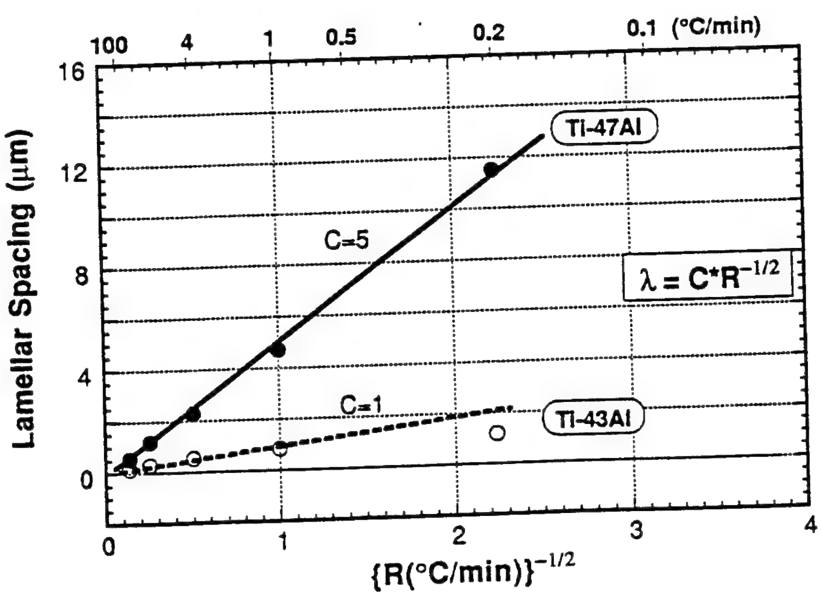

Kim (9

3

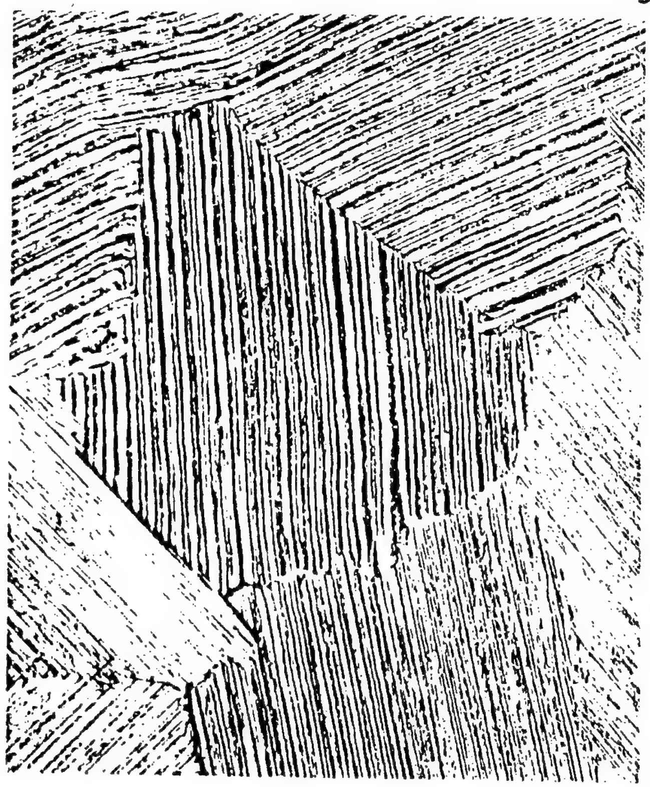

TI-43AL: COOLED AT 5°C/MIN

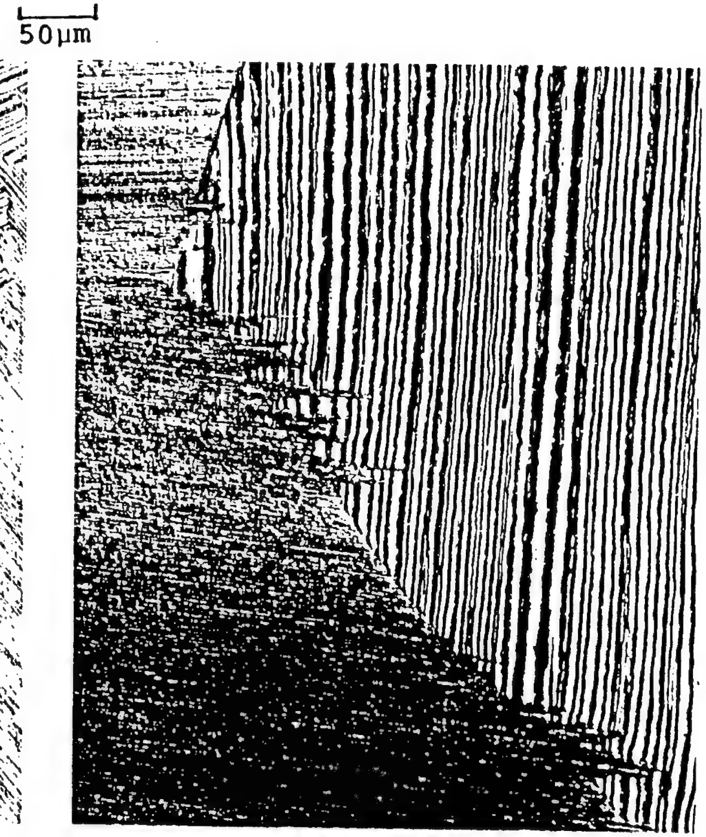

TI-47AL: COOLED AT 30°C/MIN

DTA SPECIMENS OF HOMOGENIZED ALLOYS

20μm

Ti-47Al-1.1 wt%Ox

1350°C/6 hr + 1000°C/24 hr/WQ

Ti-51Al-1.1 wt%Ox

1350°C/6 hr/FC

Cast alloys

Processing Routes for Gamma Alloys

Kim (90-95)

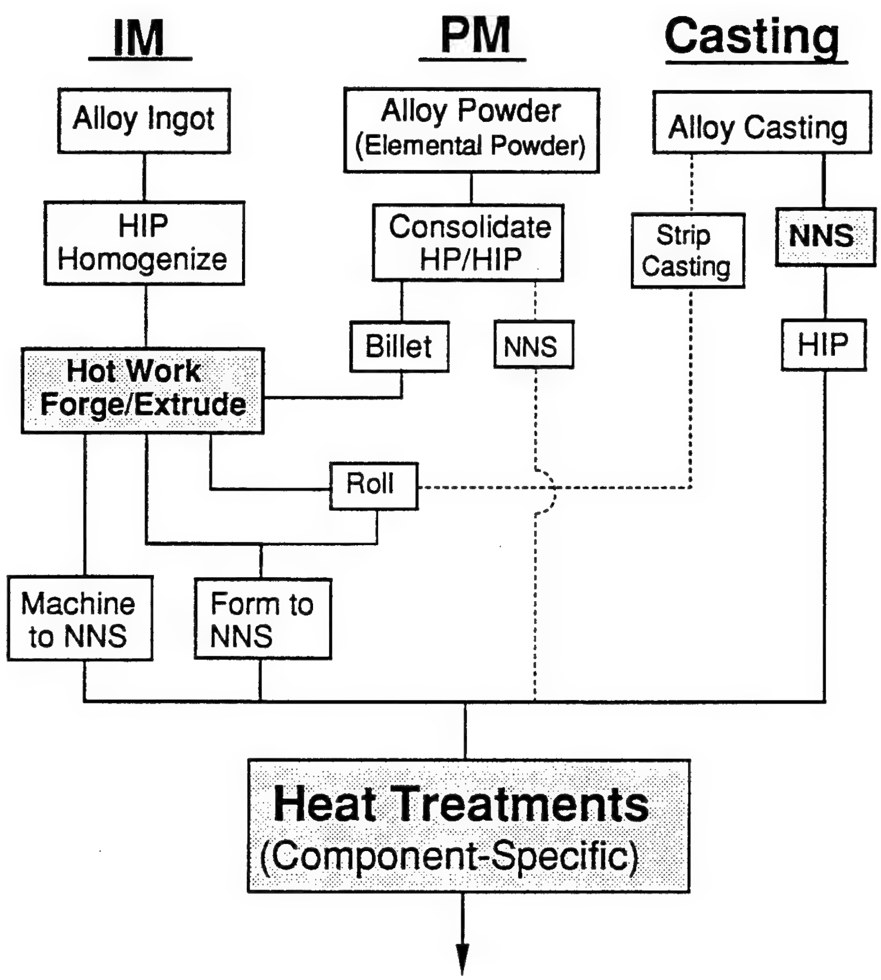

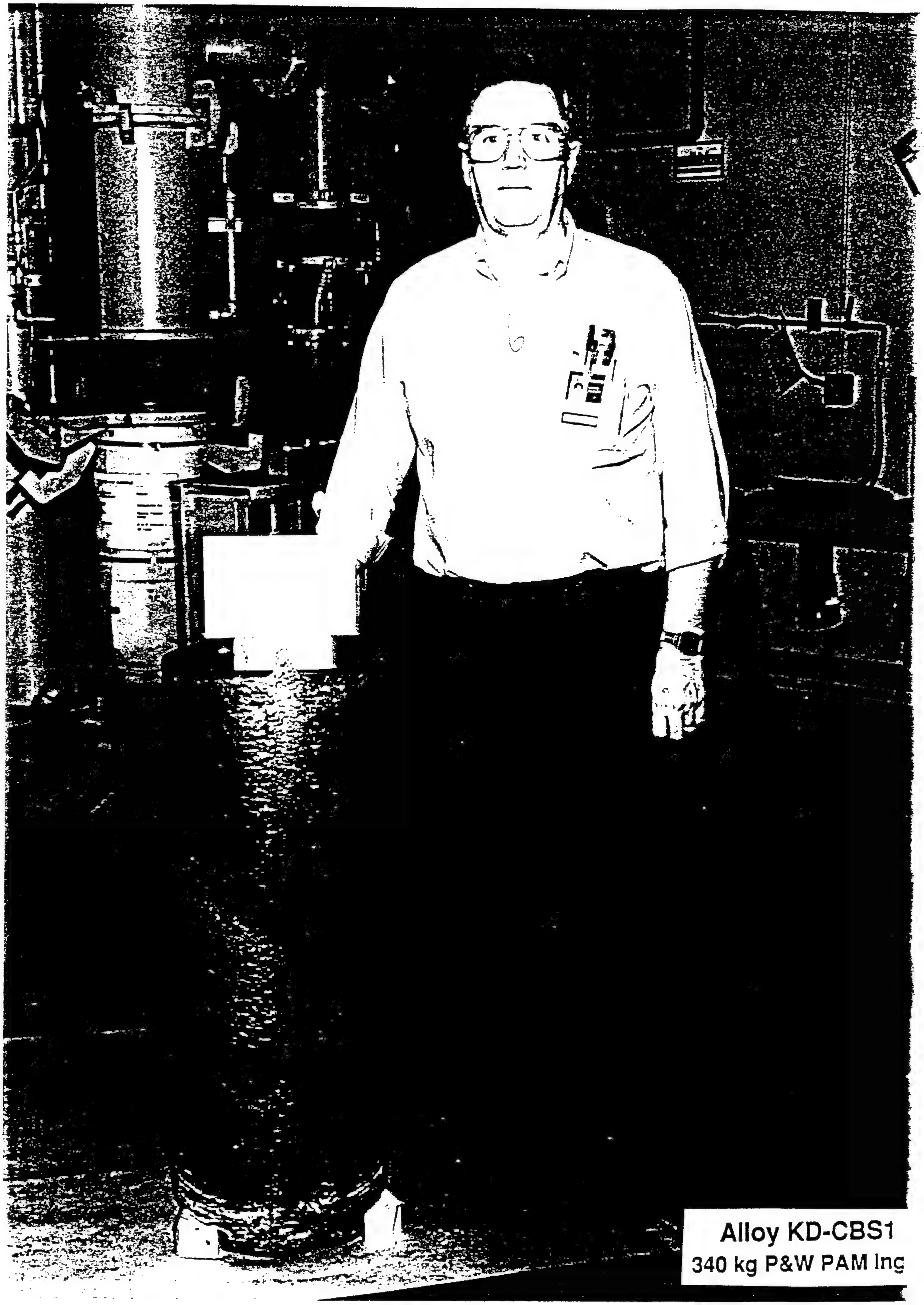

Alloy KD-CBS1
340 kg P&W PAM Ing

Microstructural Evolution and Control

Principle

Phase Relation and Transformation

In Practice

Formation/Growth Kinetics, Distribution and Morphology Depend on Starting Microstructural and Compositional Conditions.

Controlling Factors

Temperature and Time
Heating Rate, Cooling Rate, and Scheme
Aging Method and Condition

Starting Material

Cast Product
Ingot Wrought-Processed Material
PM Processed Material
Material Processed by Other Processes

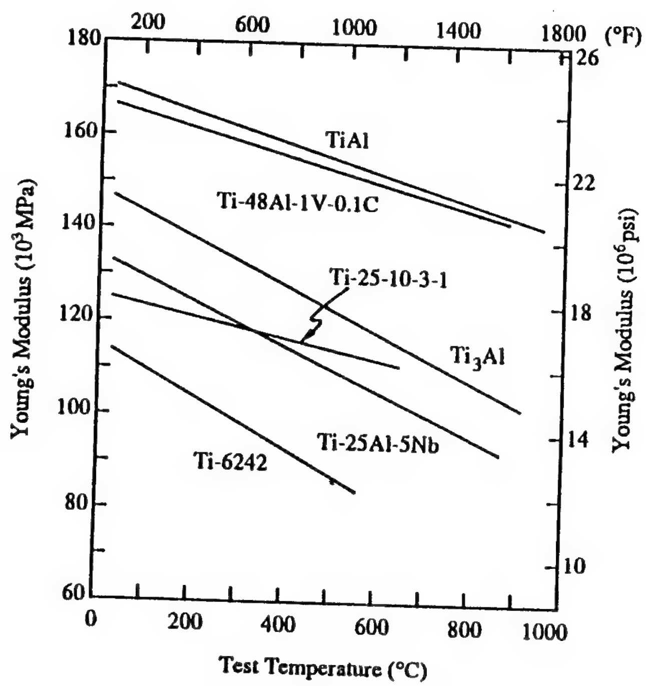

Young's Modulus (10^3 MPa)
Young's Modulus (10^6 psi)
Test Temperature (°C)
(°F)
TiAl
Ti-48Al-1V-0.1C
Ti-25-10-3-1
Ti_3Al
Ti-25Al-5Nb
Ti-6242

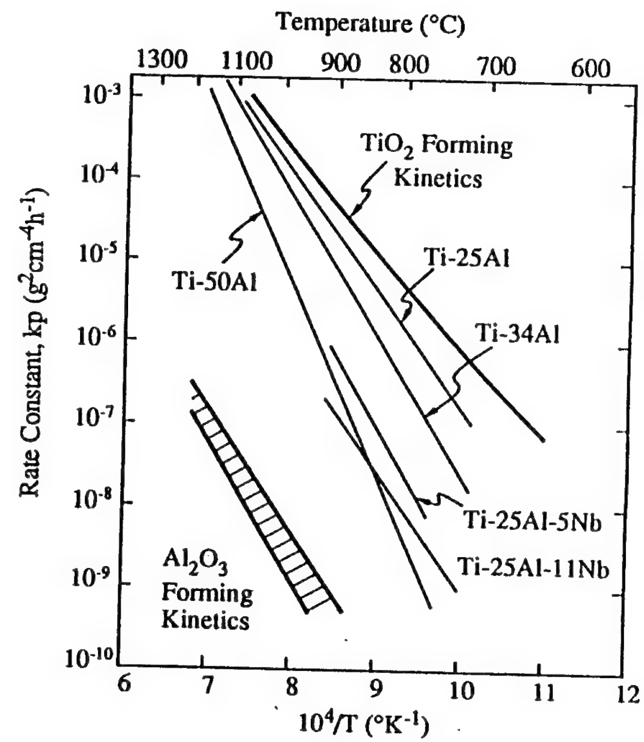

Temperature (°C)
Rate Constant, kp ($g^2cm^{-4}h^{-1}$)
$10^4/T$ (°K^{-1})
TiO_2 Forming Kinetics
Ti-50Al
Ti-25Al
Ti-34Al
Ti-25Al-5Nb
Ti-25Al-11Nb
Al_2O_3 Forming Kinetics

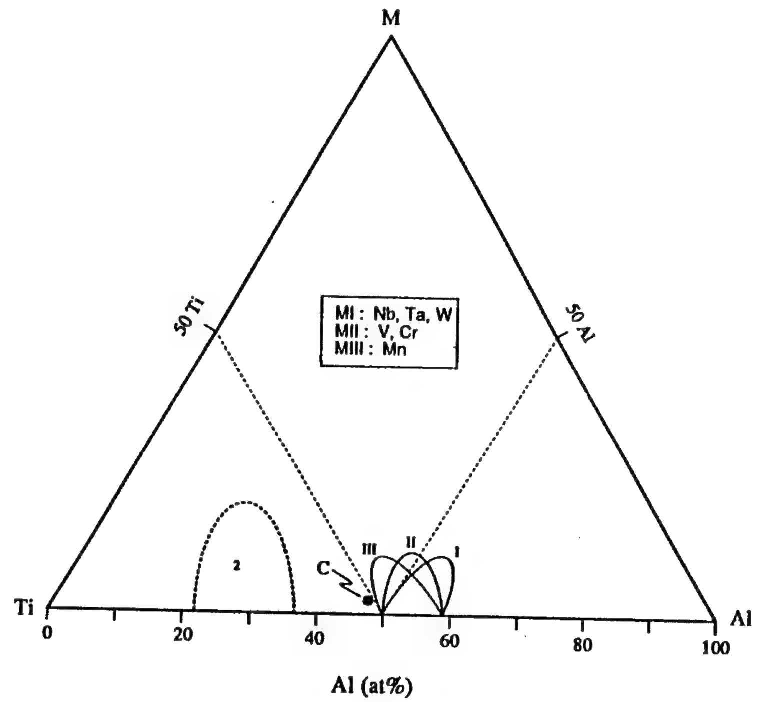
M
Ti
Al
50 Ti
50 Al
MI : Nb, Ta, W
MII : V, Cr
MIII : Mn
2
C
III
II
I
0
20
40
60
80
100
Al (at%)

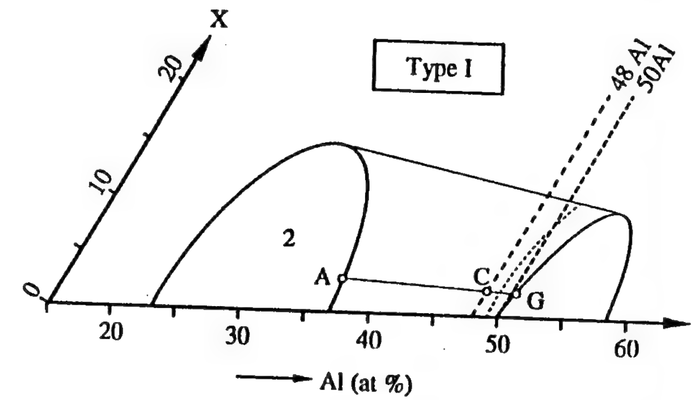
Type I
X
0
10
20
2
A
C
G
48 Al
50Al
20
30
40
50
60
Al (at %)

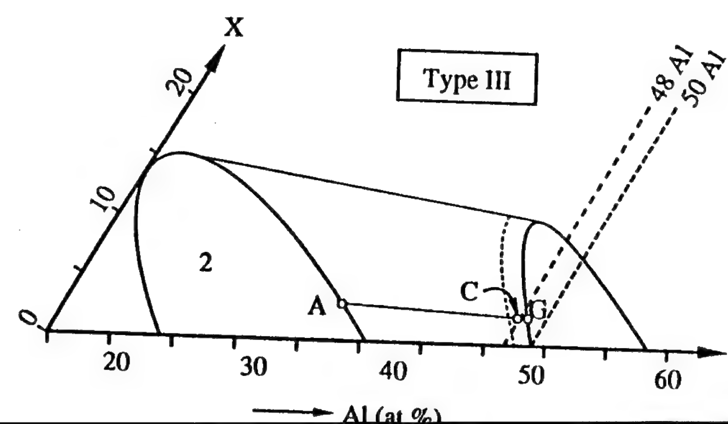
Type III
X
0
10
20
2
A
C
G
48 Al
50 Al
20
30
40
50
60

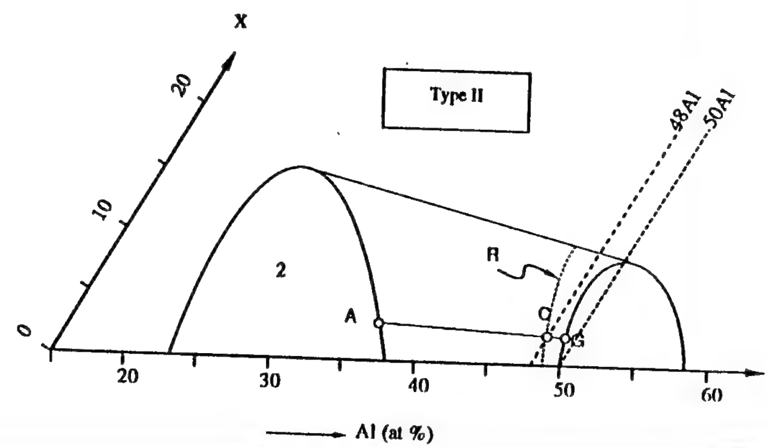
Type II
x
0
10
20
2
A
R
C
G
48Al
50Al
20
30
40
50
60
Al (at %)

Processing

Ingot Preparation

Methods: ISM; PAM; VAR; VAR-Skull
Size Limitations (?)
Compositional/Microstructural Issues

NNS Casting

Investment vs. Permanent-Mold
Issues: Refinement; Porosity/Hip-Cycle
Thin-Section Casting

Wrought Processing

Primary: Conversion; Mill Production
Secondary: Forming, Rolling, etc.
Heat-Treatment Cycles
Joining; Machining

Other Processes

Processing Routes for Gamma Alloys

Kim (90-95)

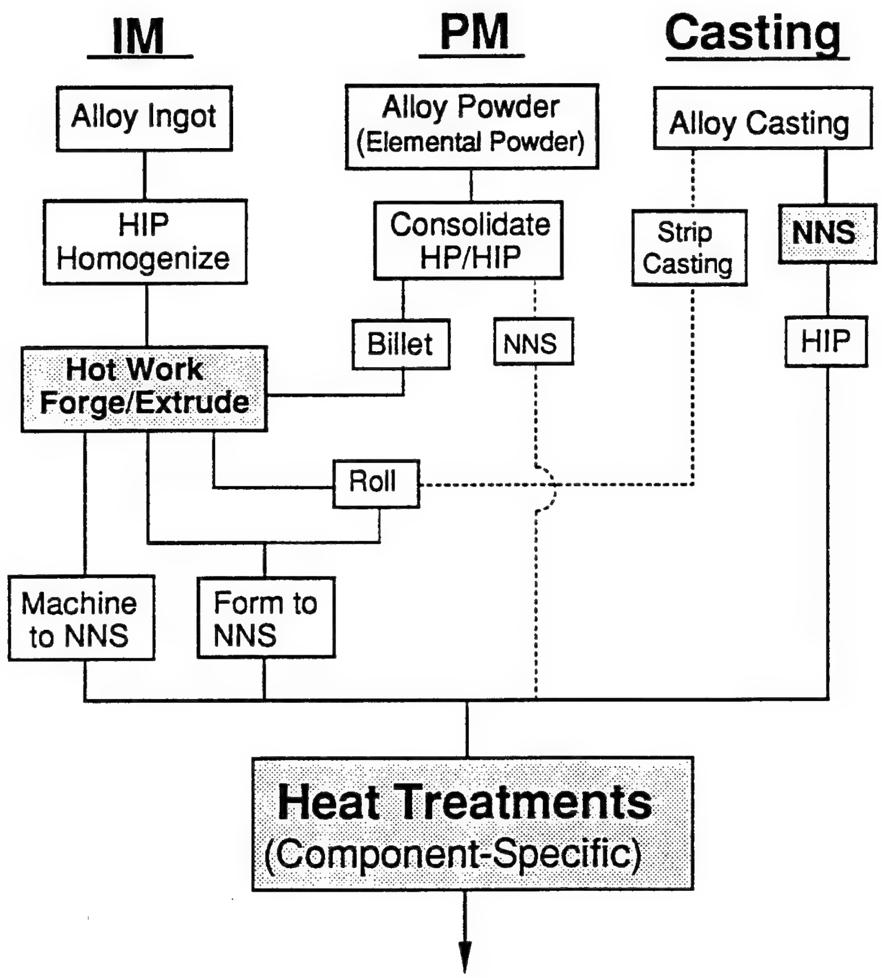

Microstructure Control in Castings

Standard Alloys

Ti-47Al-(1-2)Cr-(2-4)(Nb,Ta,W)-(0-0.2)Si

As-Cast Microstructures

Non-uniform; Lamellar Base

Controlled Microstructures

Refining and Uniformization
Practical: Casting Duplex
Desired: NL; Refined FL

Boride-Containing Alloys

XD Gamma Alloys

Ti-(45, 47)Al-4(Cr,Mn)-2Nb-0.8TiB2
TMT-Type Microstructures

Others: IHI; GKSS
Inoculation by Borides

Microstructures in Castings

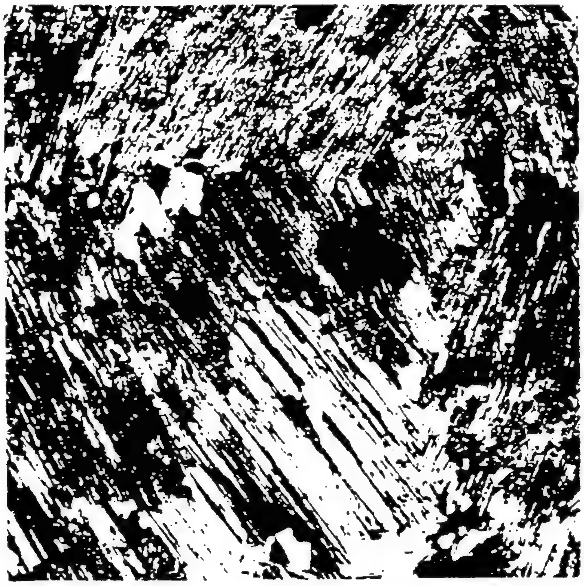

Cast and HIP'ed

200 µm

Casting Duplex

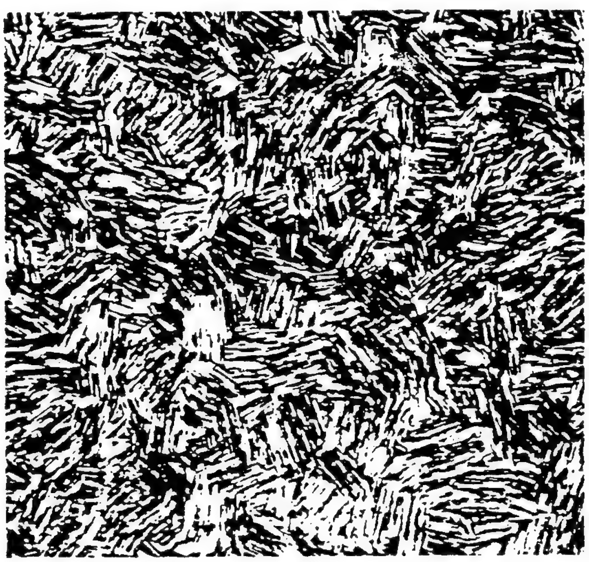

XD (HIP'ed)

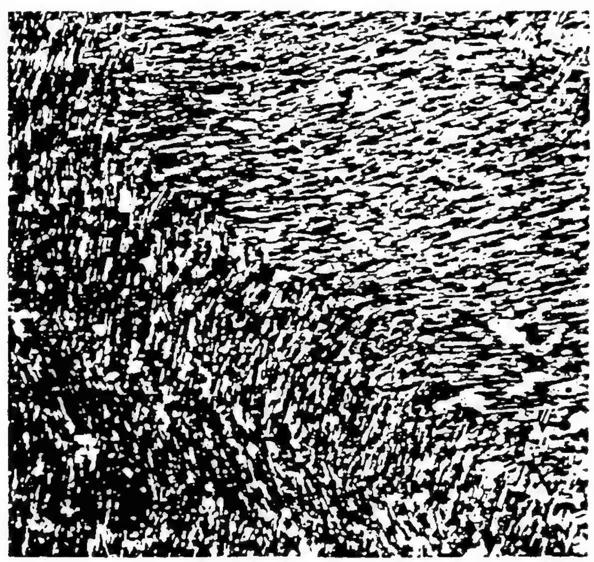

GKSS, As Cast

Casting RFL

As-Cast

100 μm

Tα-ΔT Treated

[redacted]

309-1A: 1320/2h 200X

309-09: 1440/½h 200X

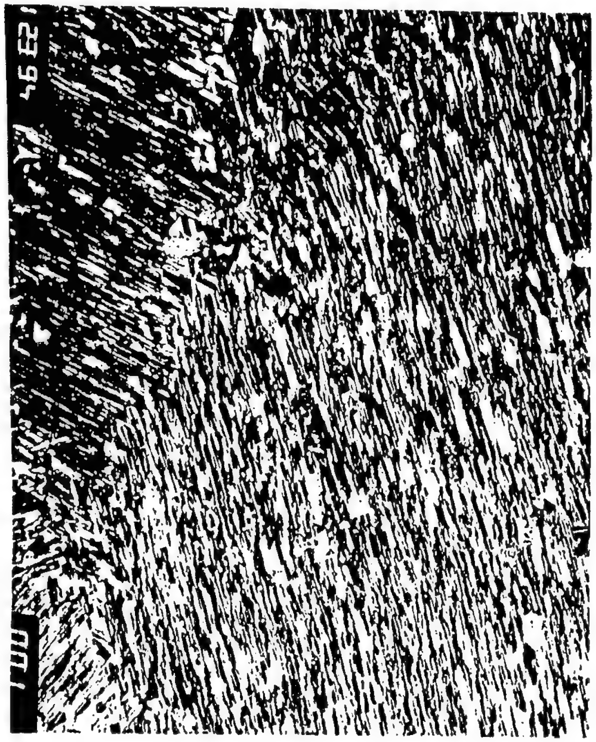

GKSS 100x As RECIEVED. P.L

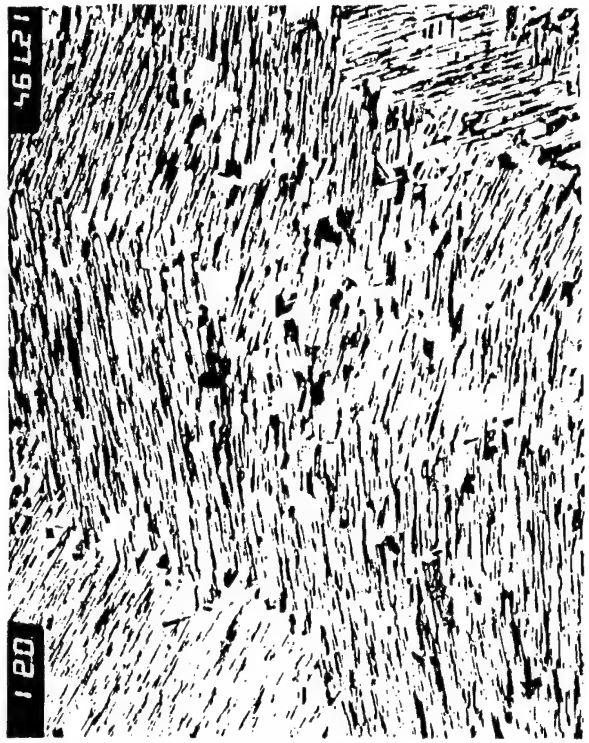

GKSS-3 1320/2Hr/FC/1000 100x P.L.

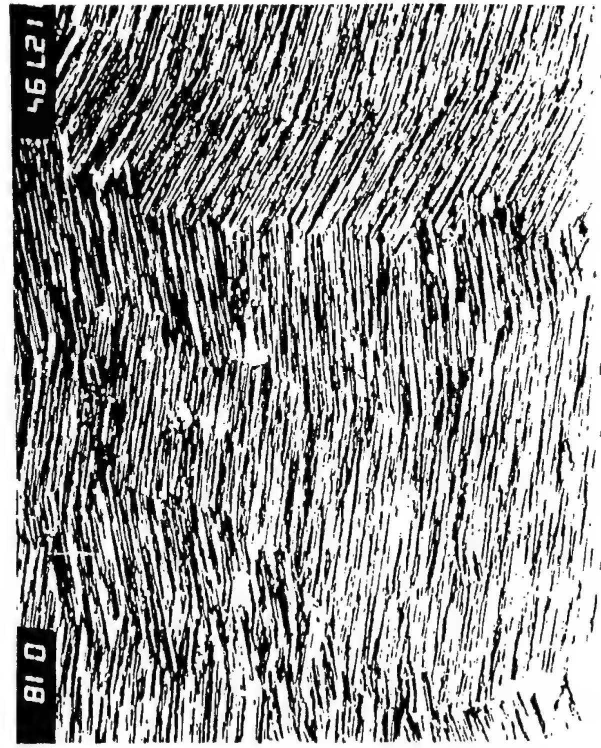

GKSS-2 1350/40m/FC/1000 100x P.L.

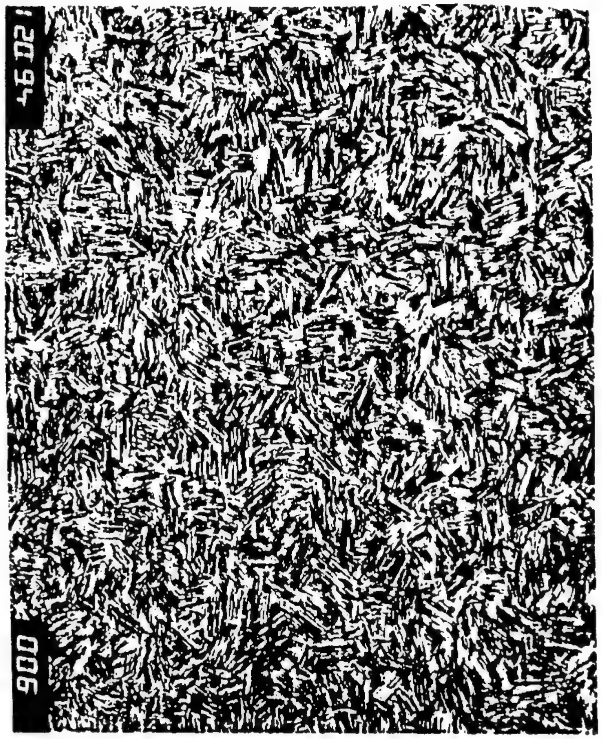

XD-01 50x Cast

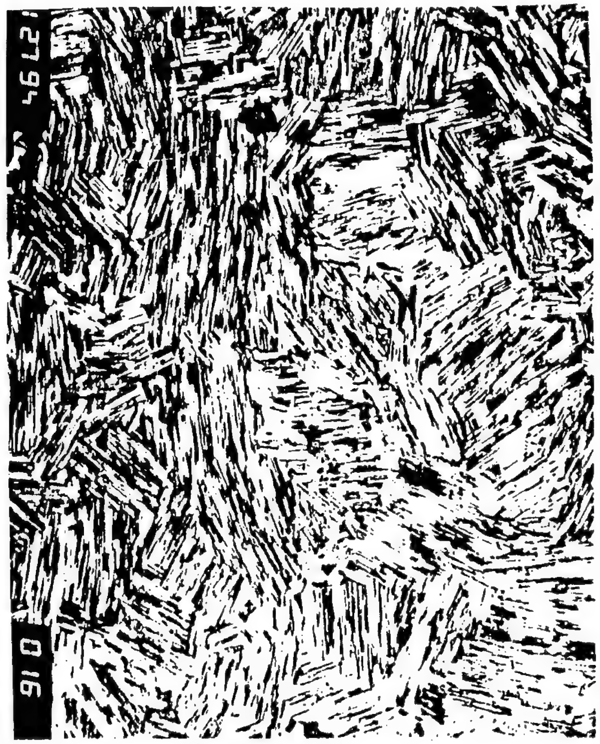

XD01-3 1320°/2Hr/FC/1000 100x P.L.

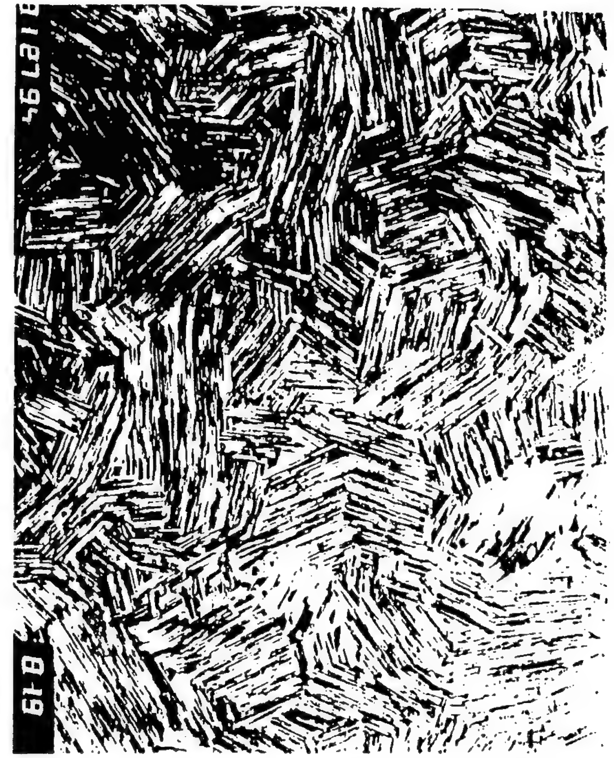

XD01-2 1370°/40min/F.C/1000 100x P.L.

Microstructure Control in Wrought Alloys

Standard Alloys

Ti-47Al-(0-3)(Cr,Mn,V)-(0-6)(Nb,Ta,Mo,W)

As-Processed Microstructures

- Fine Mixture of Gamma and Alpha-2

Heat Treatments Yield

- Standard Microstructures

Standard Microstructures

Types

- Near-Gamma (NG)
- Duplex (DP)
- Nearly-Lamellar (NL)
- Fully-Lamellar (FL)

Inverse El/K1c Relationship

Difficulties in Designing

Effort on Fundamental Understanding

Designed Microstructures

2

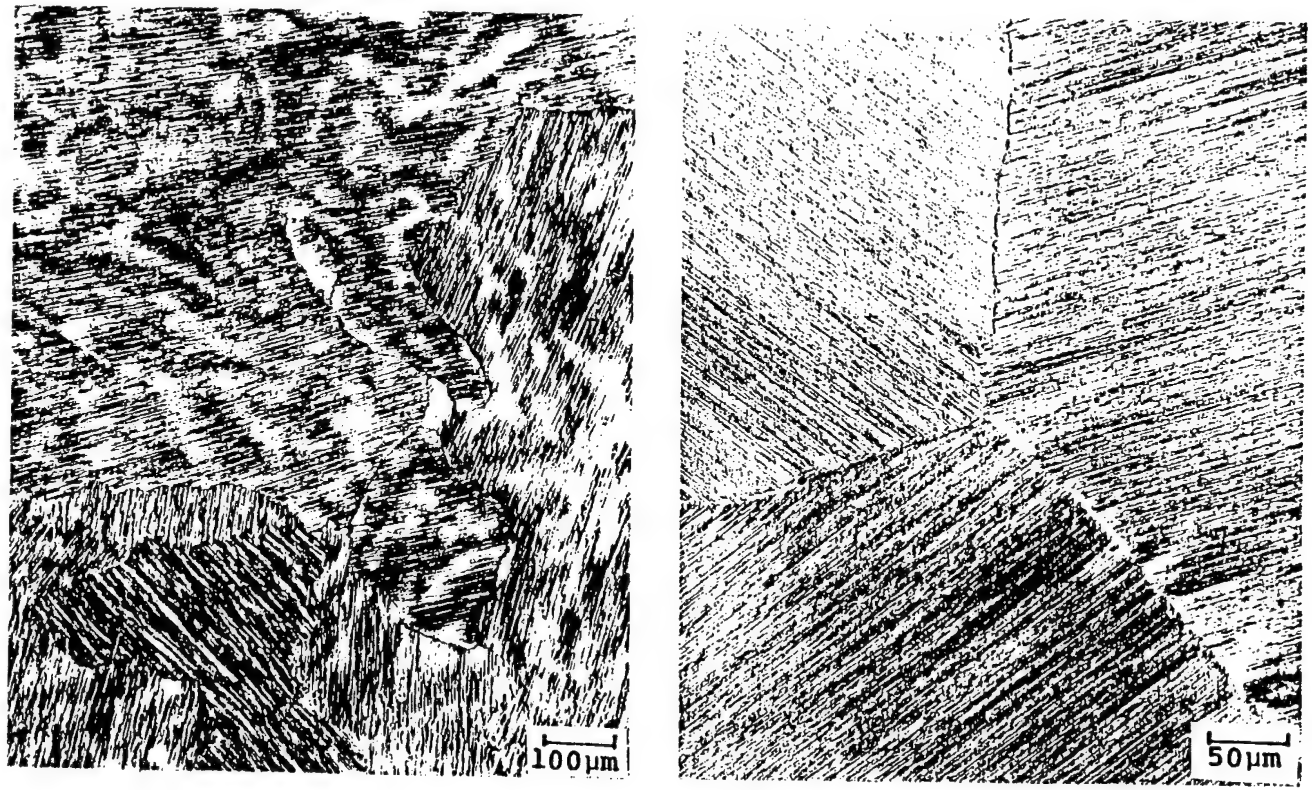

1300°C/1 HR/OQ + 900°C/1 HR/AC   1380°C/2 HR/CC + 1180°C/30 MIN/AC

TI-46AL ALLOY CIGAR

3

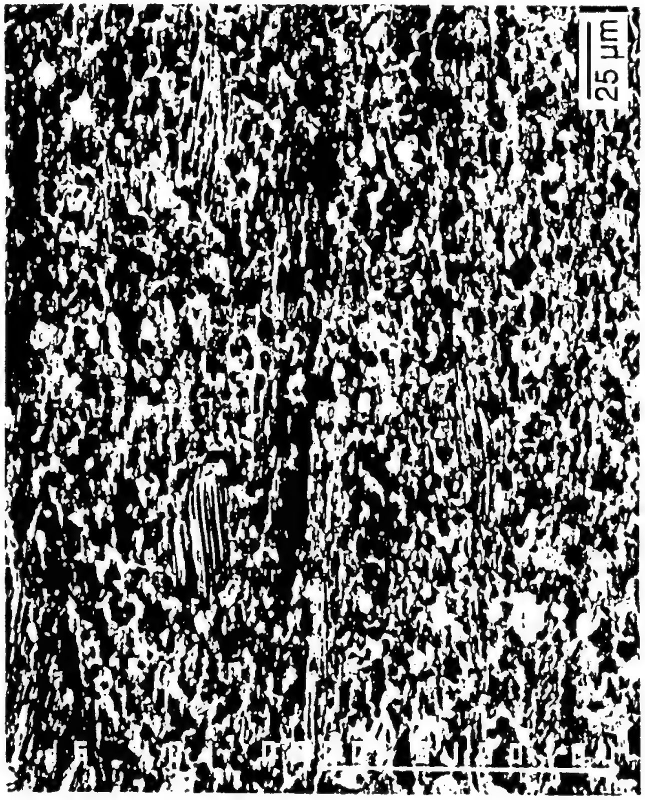

K5 (Ti-46.2Al-2Cr-3Nb-0.2W)

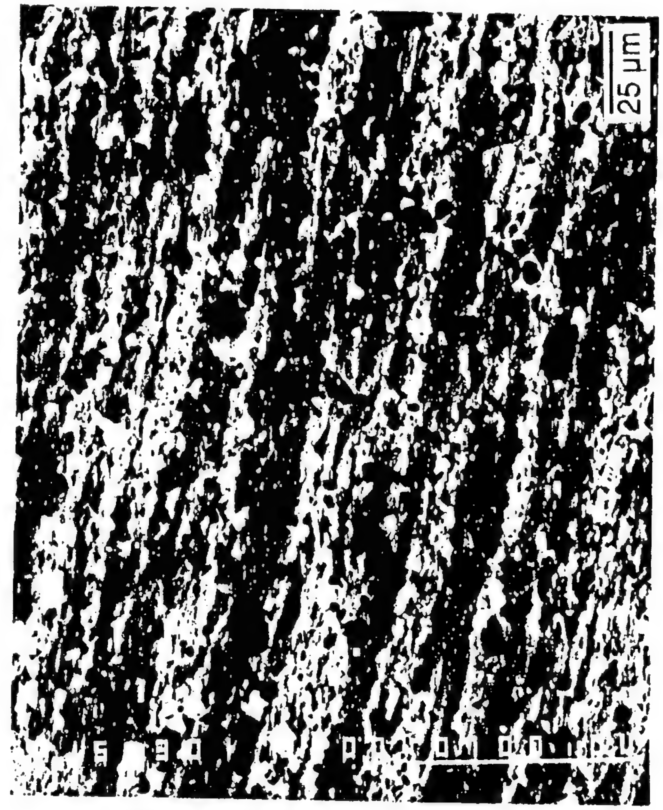

K5WSB (K5+0.3W+0.2Si+0.1B)

Alloy K5's: **Isothermally-Forged** (1150°C/70/70)

2

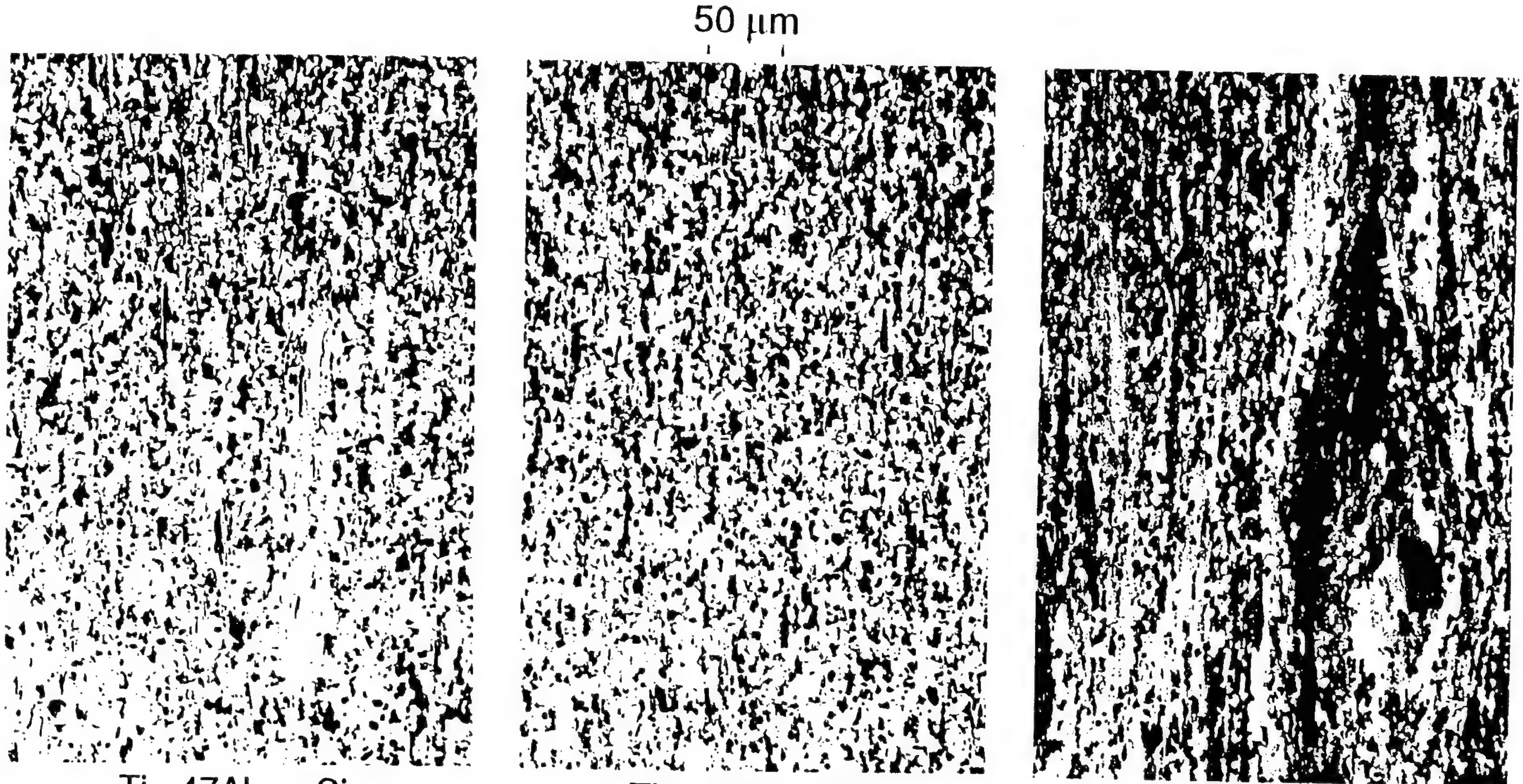

Ti - 47Al - x_1Si

Ti - 47Al - x_2Si

Ti - 48Al - x_2Si

Isothermally forged(85%) microstructures

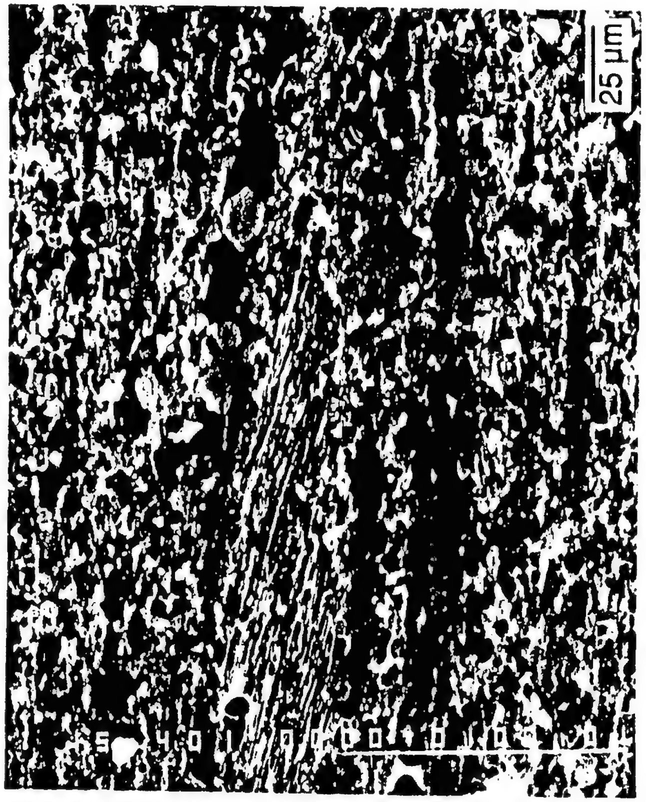

1150°C/70/70

1270°C/3h/FC

Alloy K5: **Isothermally-Forged and Duplex-Treated**

Tα-70°C / 4hr / AC 10 μm Tα-70°C / 24 hr / AC

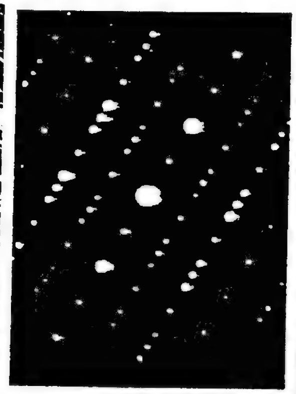

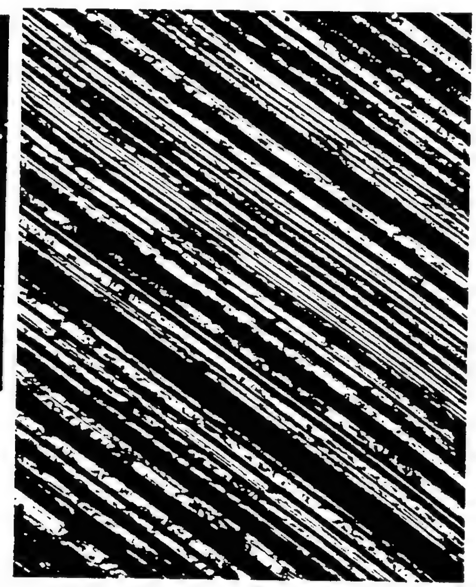

1 μm

Lamellar Structures : Light-to-Gray Areas

Alloy G1 : Forged + (α+γ) Treated + Air Cooled

Microstructures of Gamma Alloys

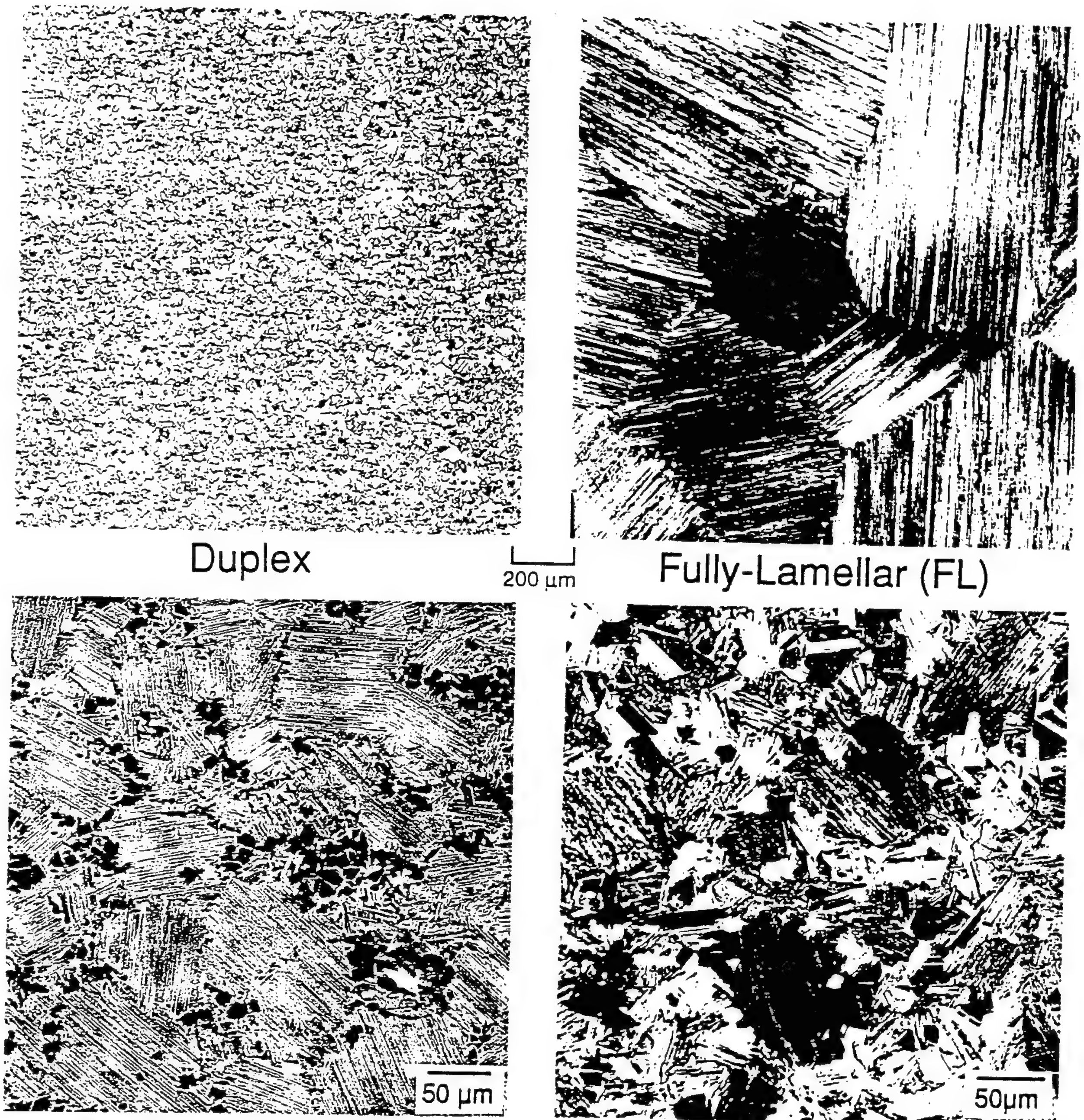

Duplex

Fully-Lamellar (FL)

Nearly-Lamellar (NL)

NL

3

Alloy K5 (Ti-46.5Al-2Cr-3Nb-0.2W)

Duplex

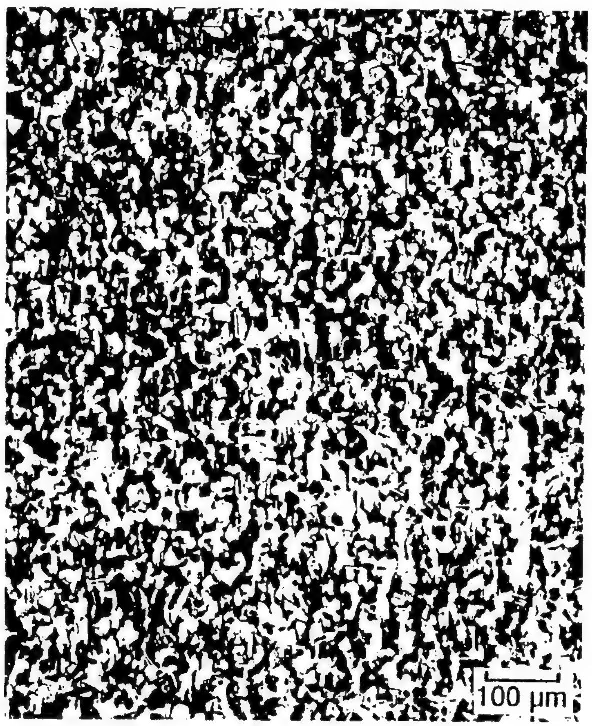

HW + (α+γ)-Treated

Fully-Lamellar

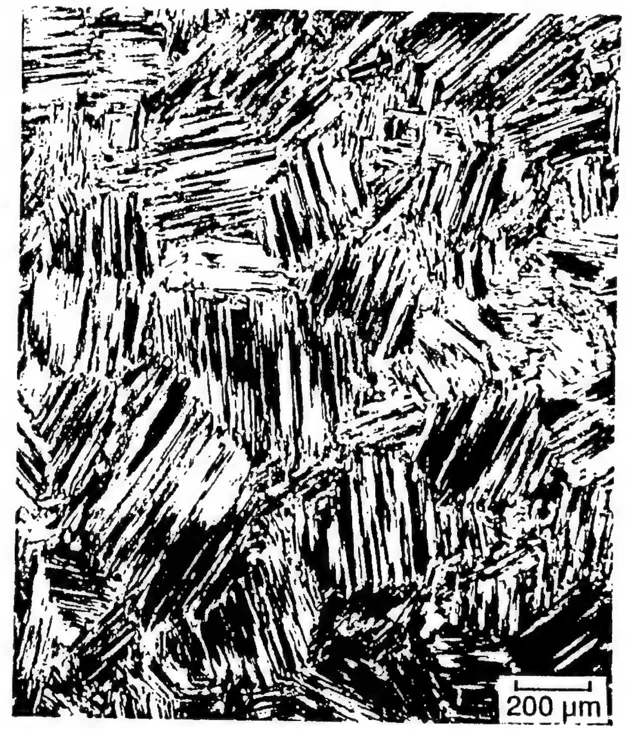

HW + α-Treated

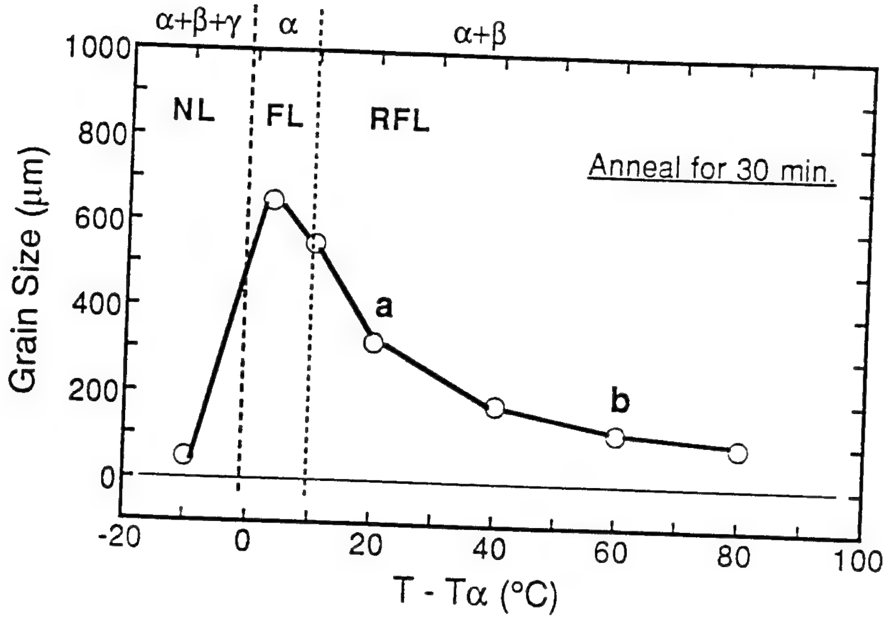

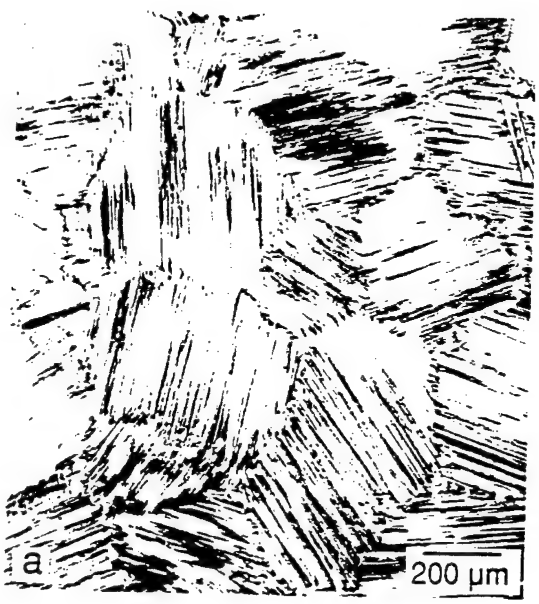

Lamellar Grain Size Control in Wrought Alloy K5

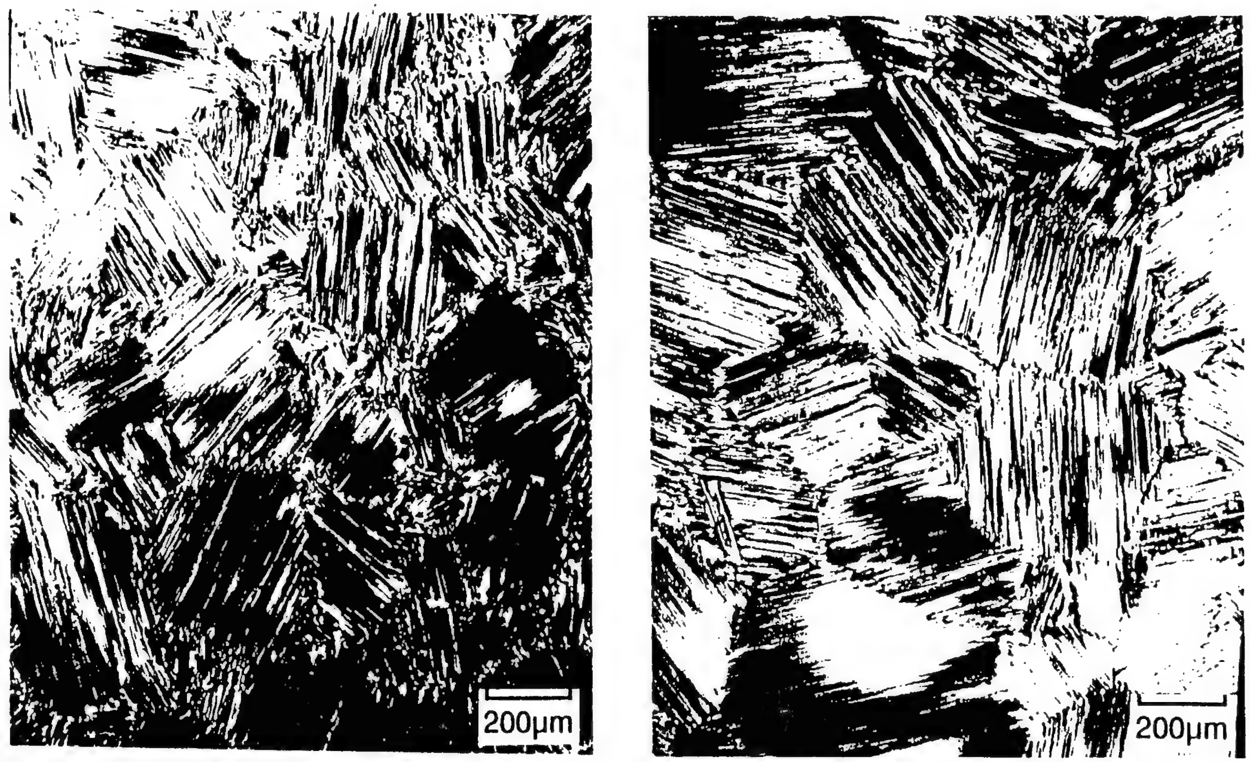

Cooling Condition Effect on RFL of Alloy K5

Alloy K5. Ti-46.4Al-2.1Cr-3Nb-0.2W

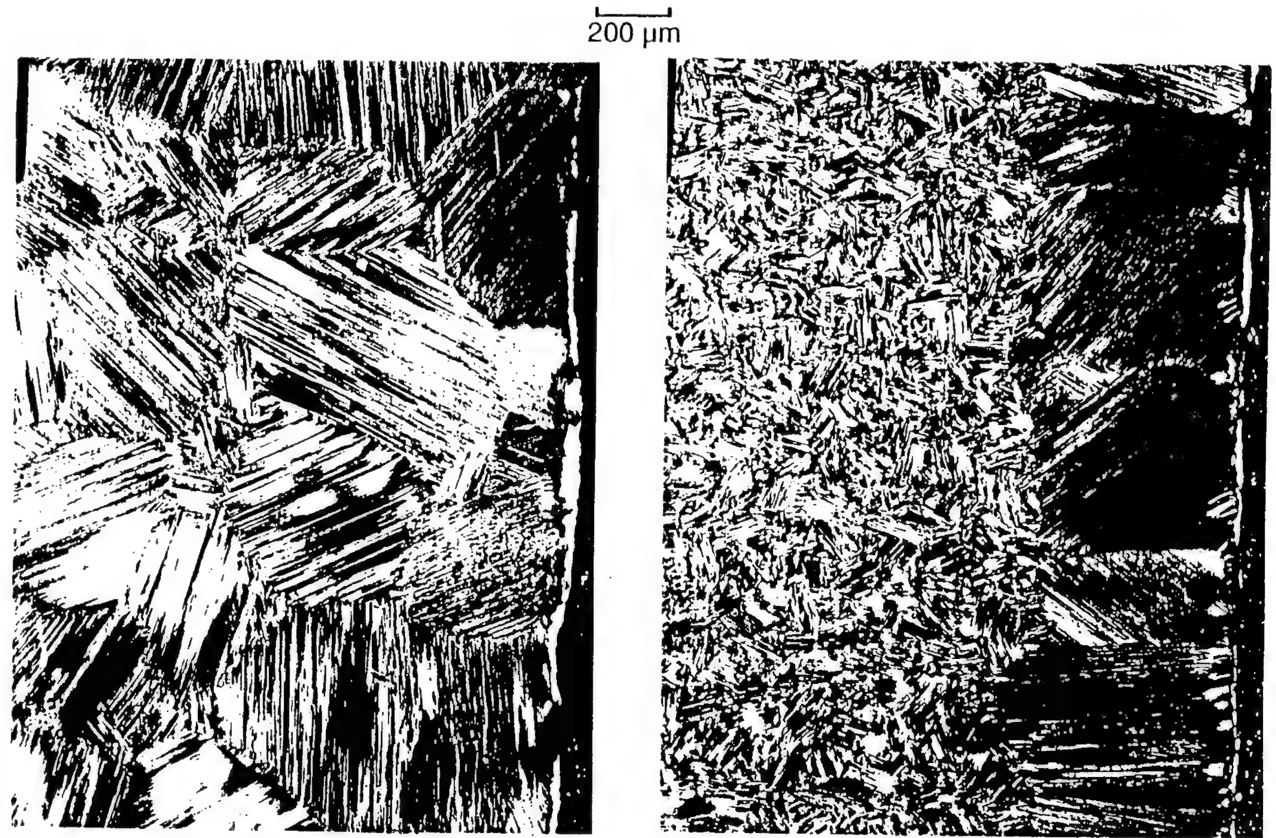

K5L-19 K5L-12

Wrought Alloy K5 after High Temperature Treatments

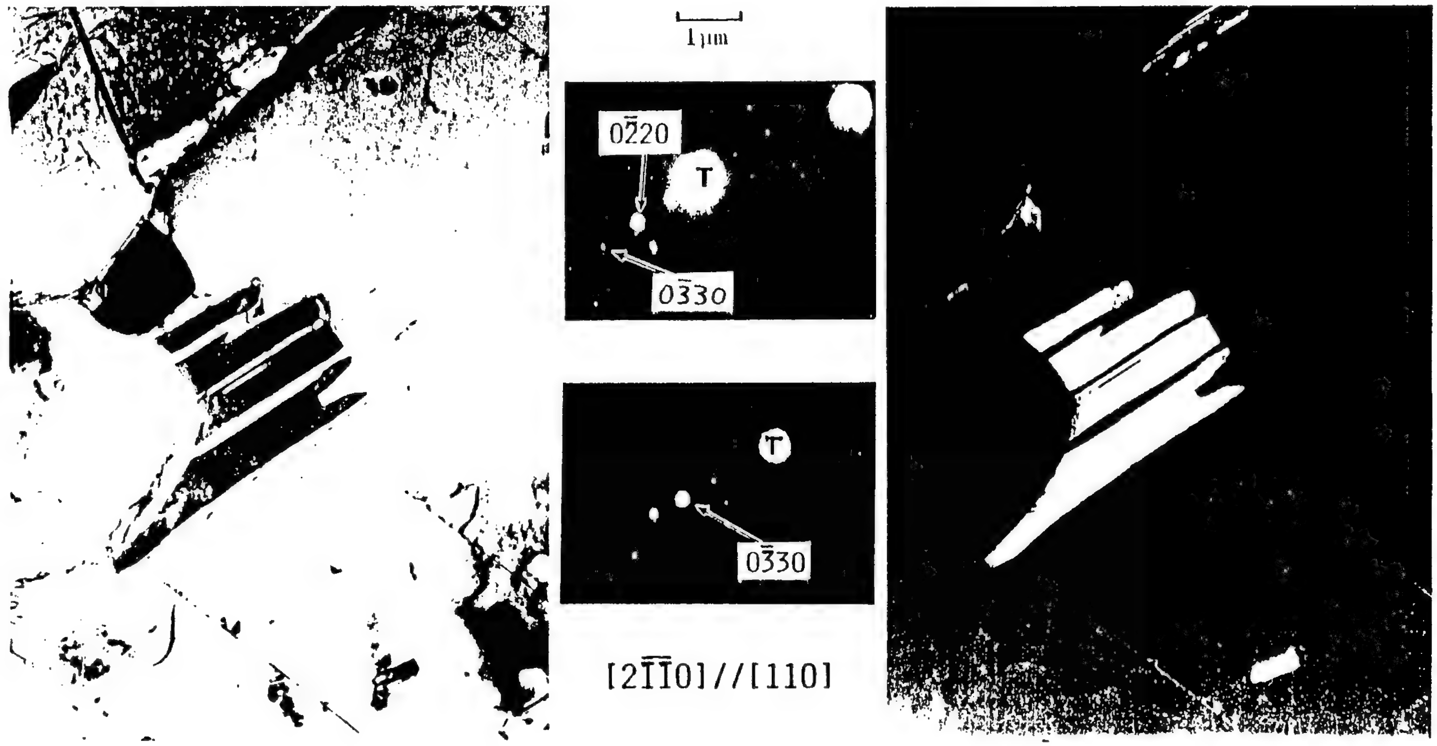

<u>ALLOY G16</u> FORGED (88%) AND HEAT TREATED (1200°C/2 HR/AC + 1000°C/24 HR/AC)

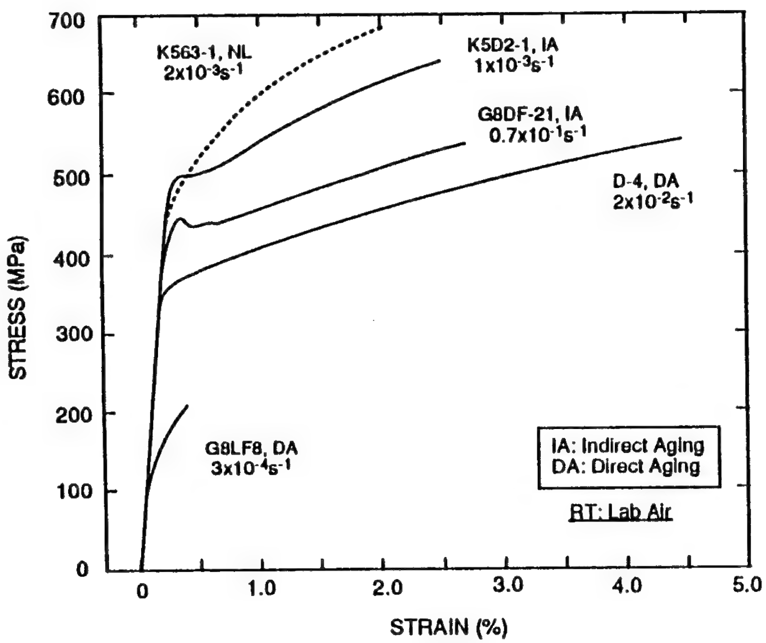

RT Tensile Curves in Duplex/NL Microstructures

YWK(92-94)

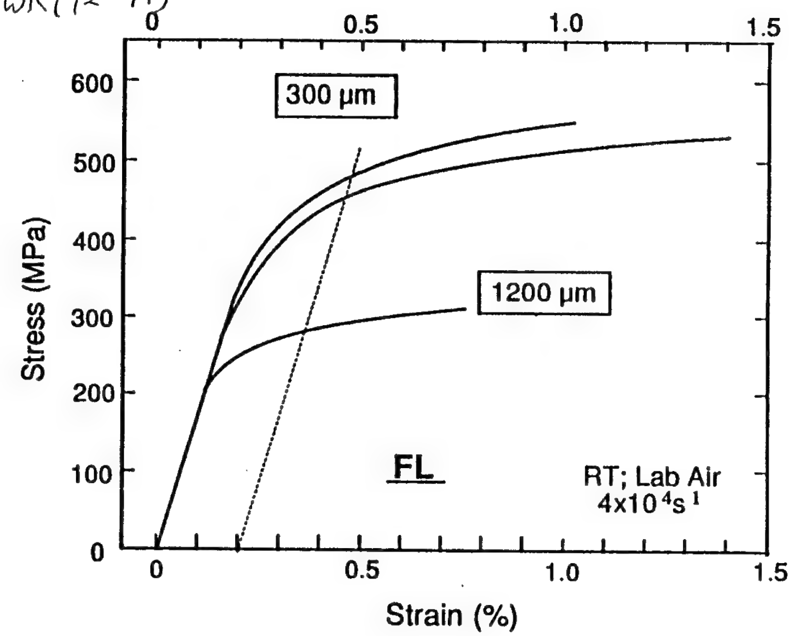

Directly Aged

Indirectly Aged

Duplex Microstructures in Alloy G1

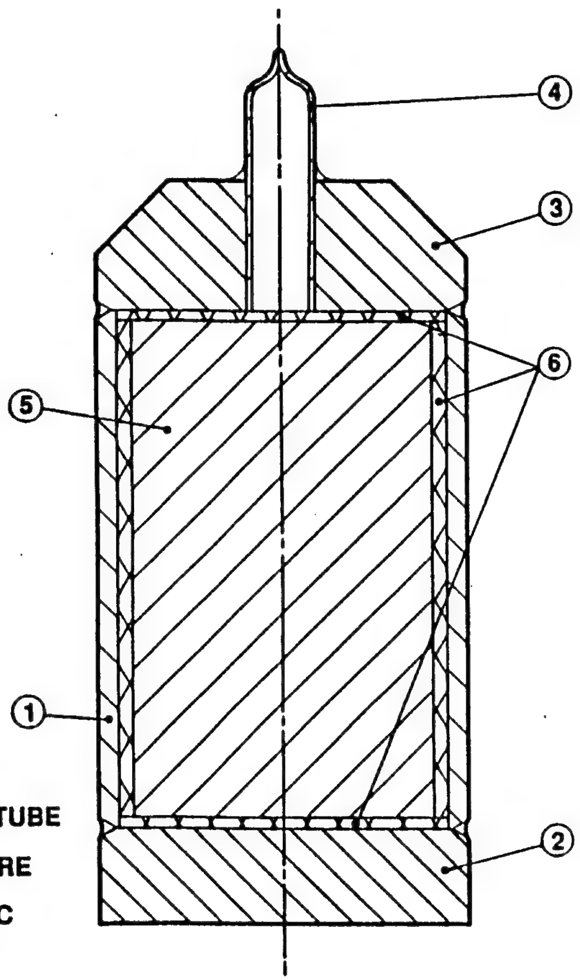

Goetz (92)

① CAN
② TAIL CAP
③ NOSE CAP
④ EVACUATION TUBE
⑤ BILLET OR CORE
⑥ SILICA FABRIC (SILTEMP)

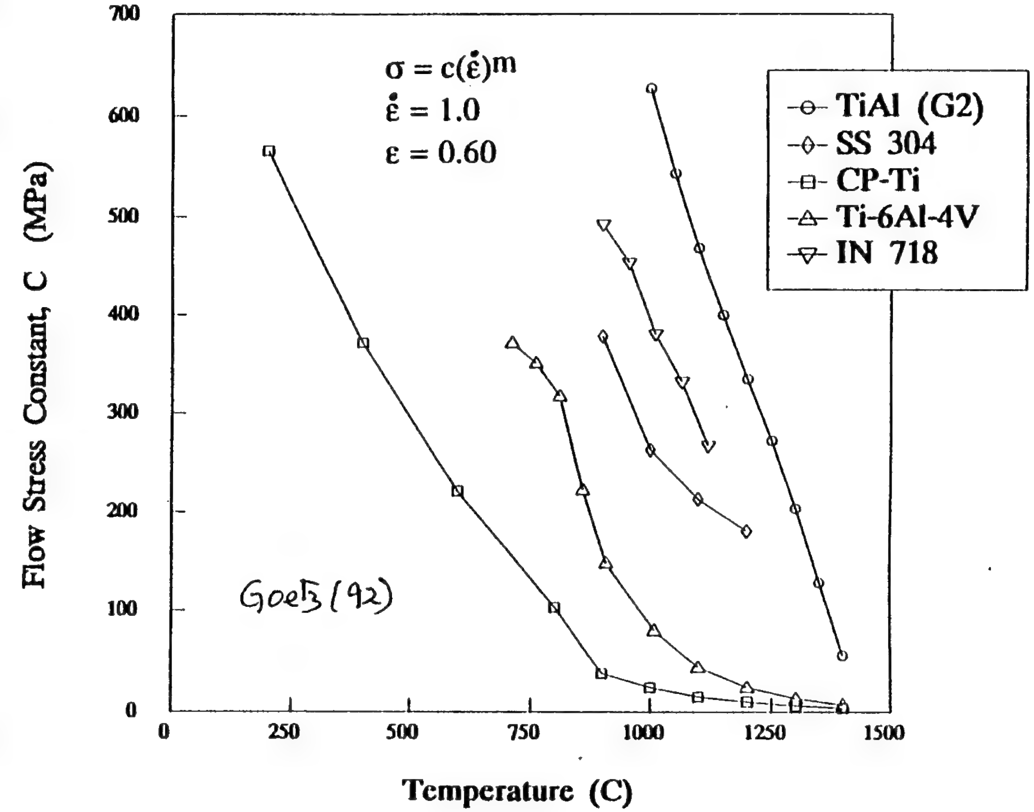

Structure/Property Relationships

General Mechanical Behavior

Tensile
Fracture Toughness
Creep
Fatigue; FCG,

Inverse Ductility/FT Relationship

Deformation and Fracture Behavior

Tensile Loading
Cyclic Loading
Creep Loading

Damage Tolerance and Life Prediction

Microstructure Optimization

Alloy K5 Duplex

1270°C/4h/AC/RT

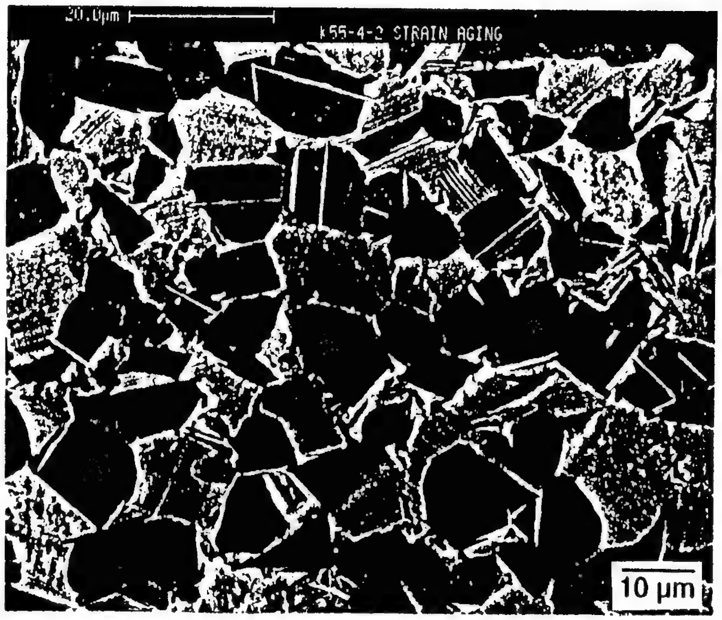

Weak Yield Point

1270°C/4h/FC/900°C/AC
+ 900°C/48h/AC

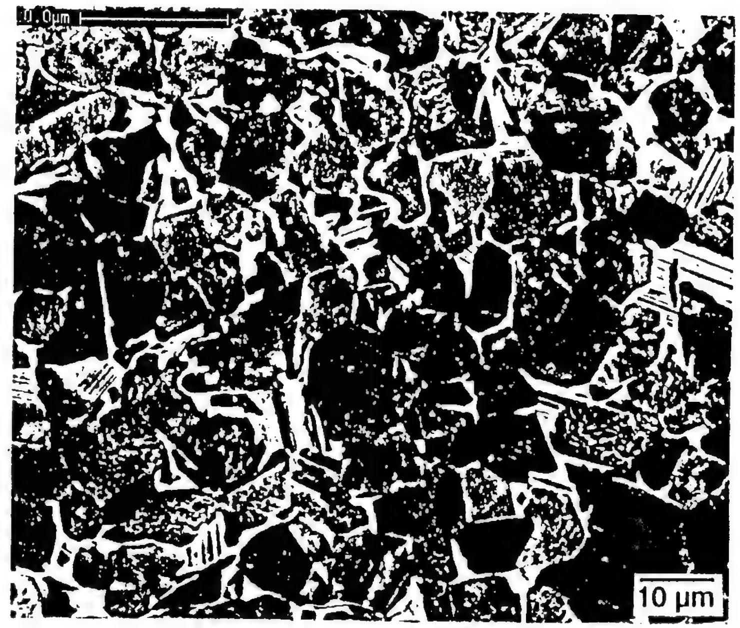

Pronounced Yield Point

K5 Duplex: ε_t=0.5%

Weak Yield Point

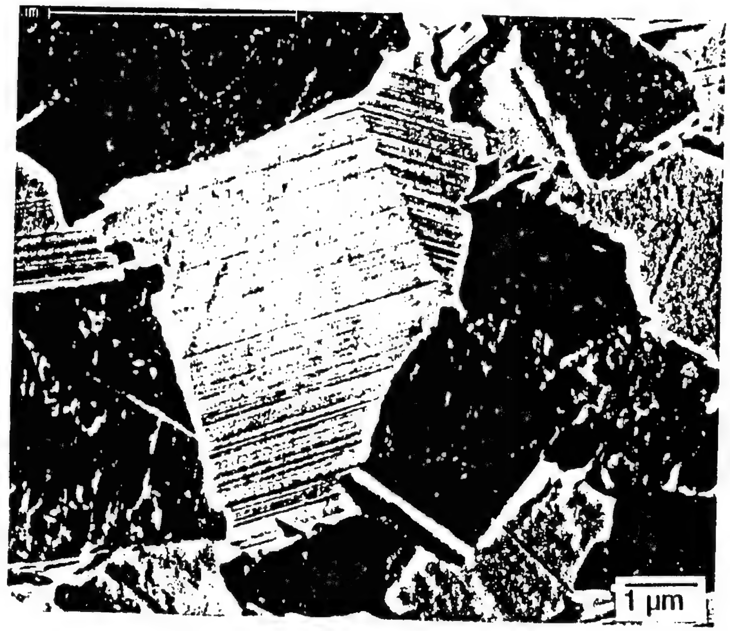

1270°C/4h/AC/RT

Strong Yield Point

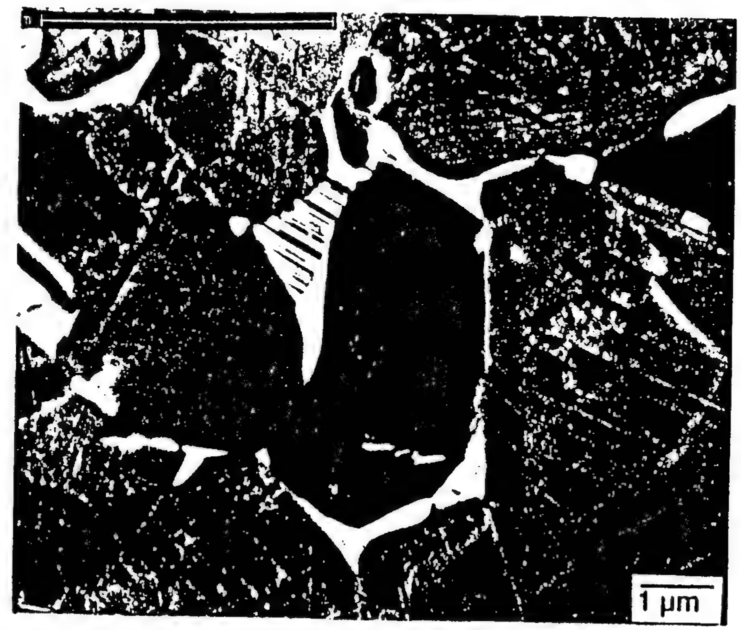

1270°C/4h/FC/900°C/AC + 900°C/48h/AC

Duplex (+) Treatment and Cooling

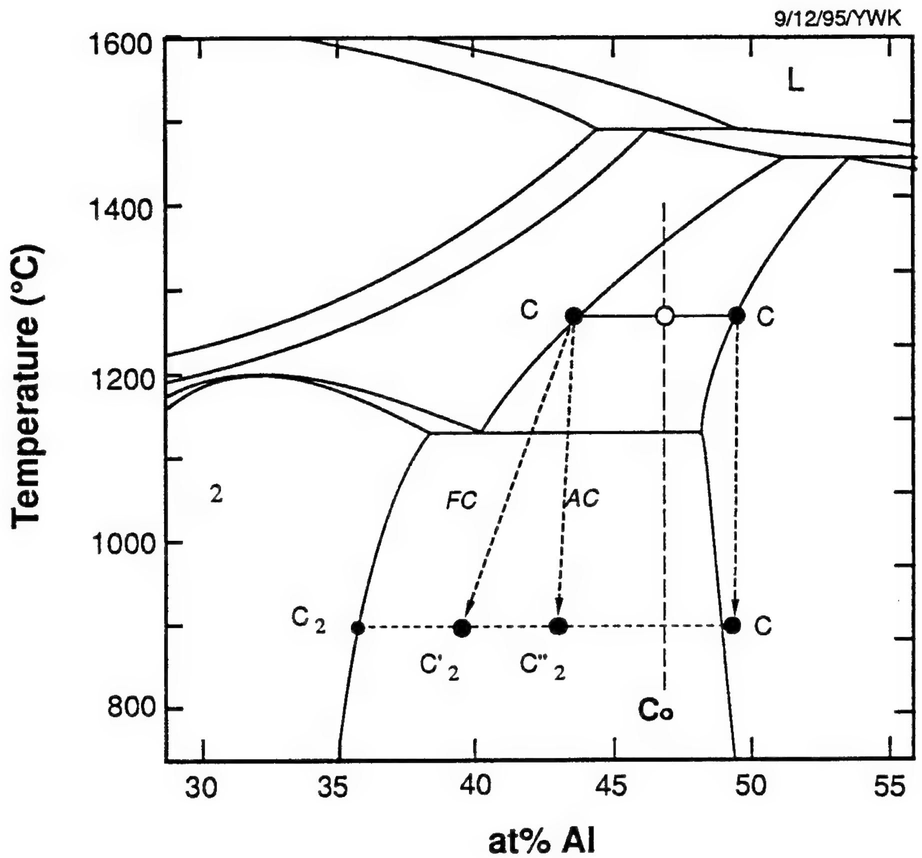

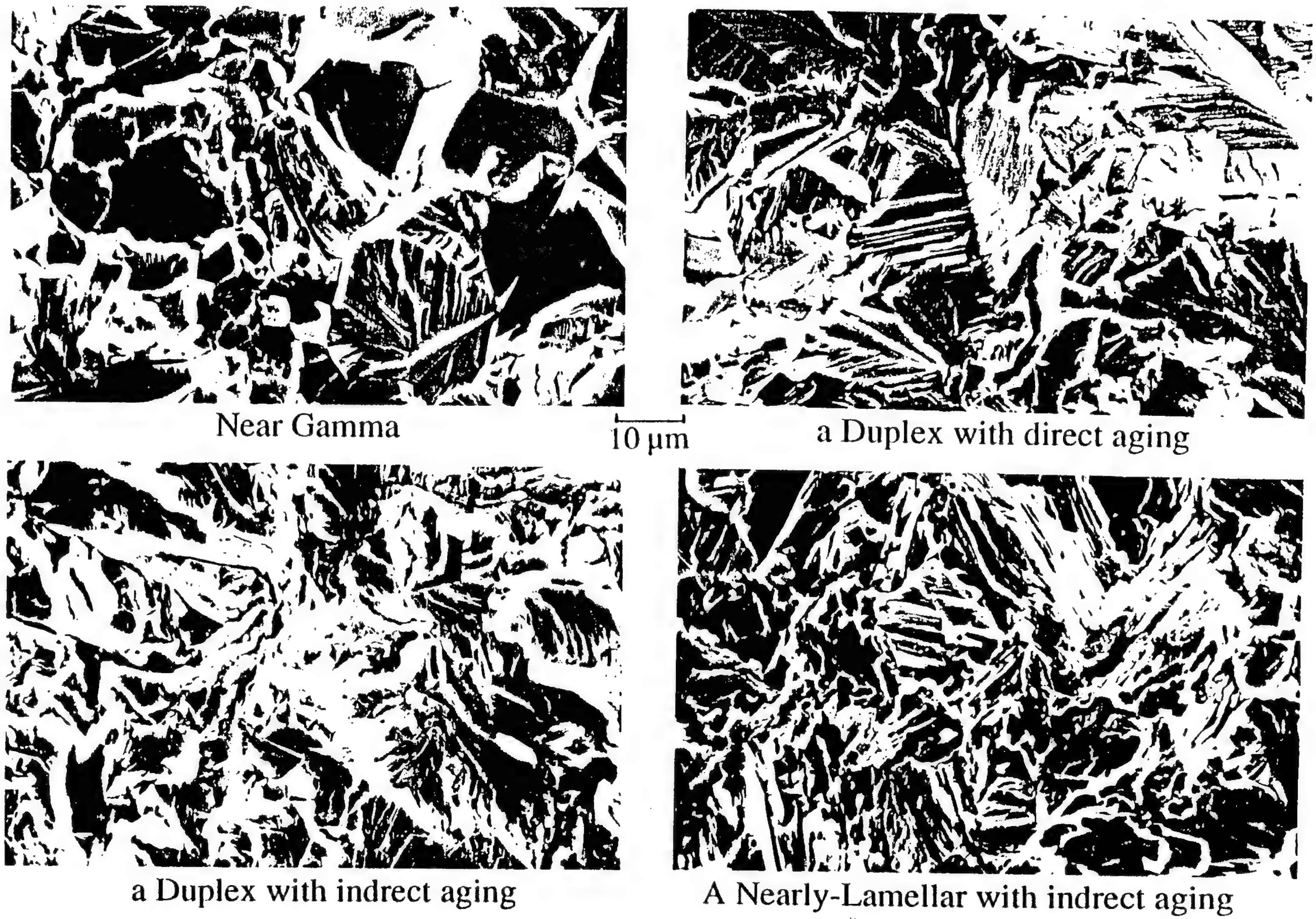

Tensile Fracture Surfaces of Alloy G1 in Various Microstructural Conditions

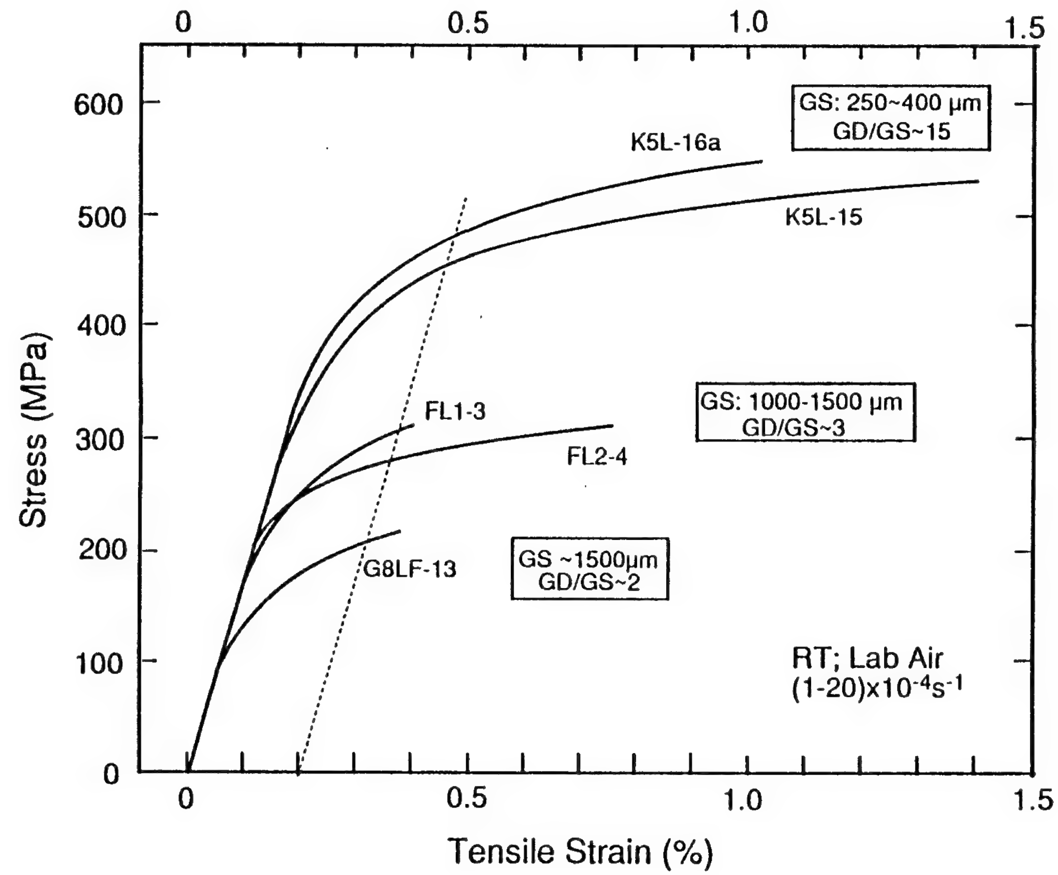

Tensile Curves of Fully-Lamellar Gamma Materials

ε_1/σ_1 = 0.3 %/ 427 MPa

ε_3/σ_3 = 0.55 %/ 493 MPa

Alloy K5 RFL Flat Gage Tensile Specimen Surface Deformed at RT
(σ_o/σ_y=328/474 MPa ; λ_L=0.3 μm)

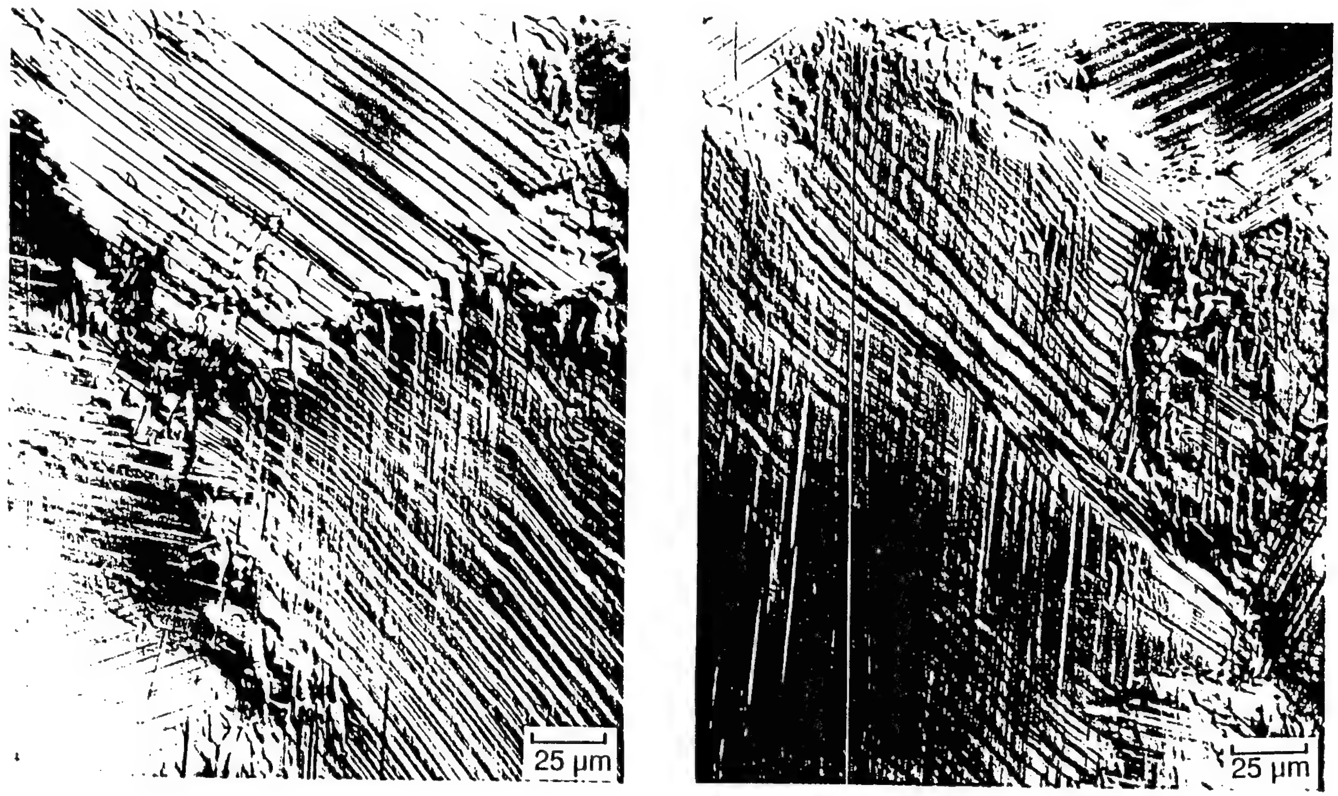

RT Tensile Deformation/Strain-Accomodation Observed on Electropolished Surfaces of Alloy K5 RFL Specimens at σ/ε=528 MPa/1.21% (σ_0/ε_0=328/0.19)

4

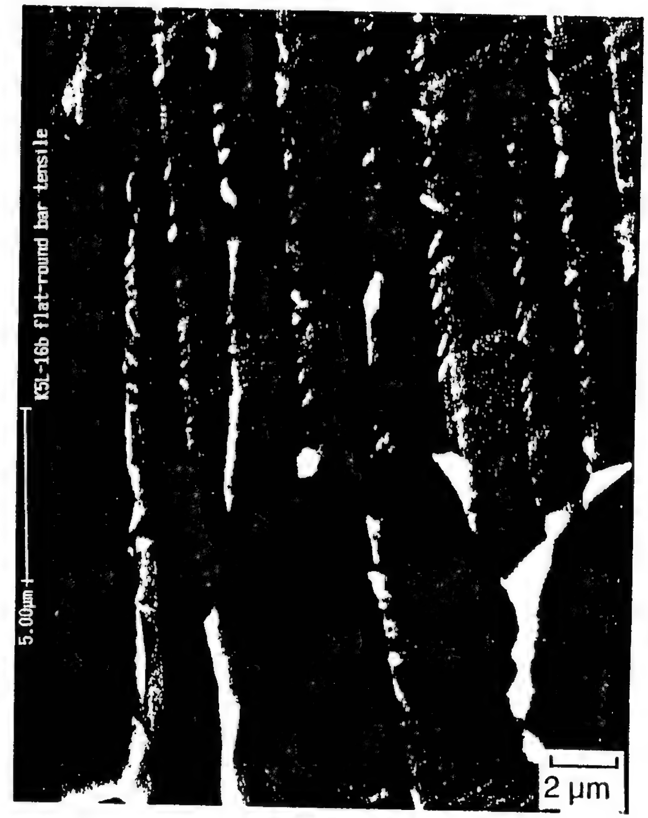

BSE Image of RT Tensile Deformation/Strain-Accomodation near GB's on Surfaces of Alloy K5 RFL Specimens at σ/ε=528 MPa/1.21% (ε_0=0.19)

4

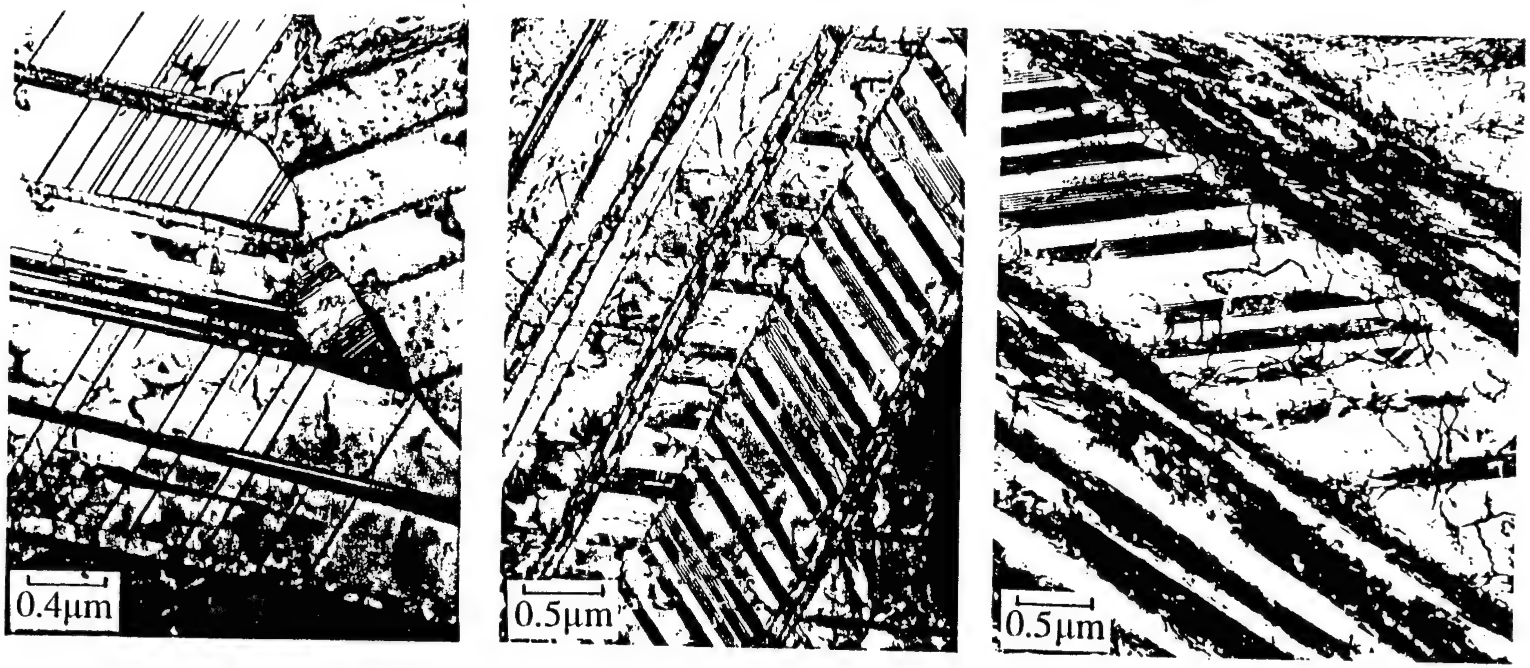

Deformed Microstructure of Alloy G1 at 1.9% Tensile Strain

Alloy K5 RFL Tensile Specimen Flat Gage Surface Deformed at RT

σ_5/ε_5 =524 MPa/0.78% (σ_0/ε_0=328/0.19)

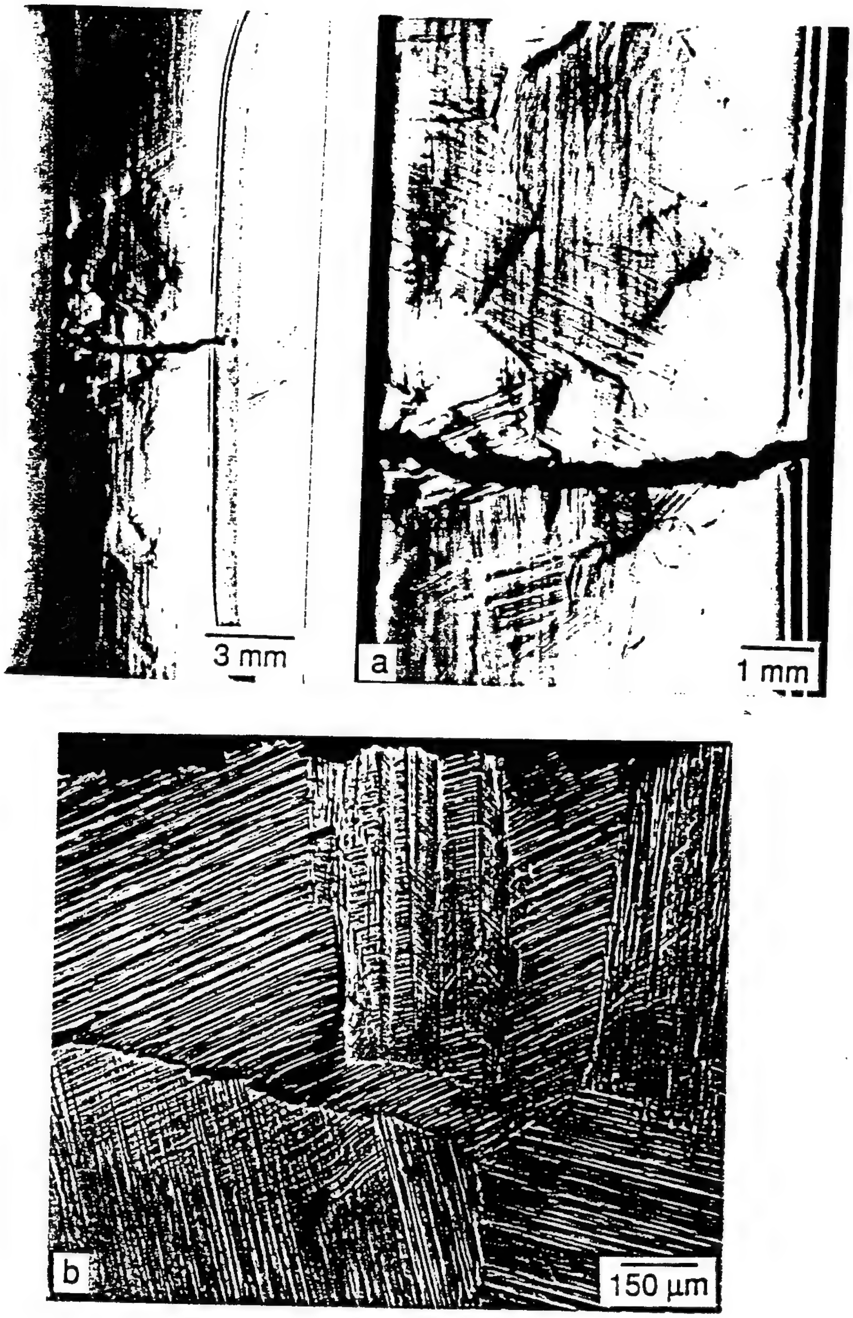
3 mm
a
1 mm
b
150 µm

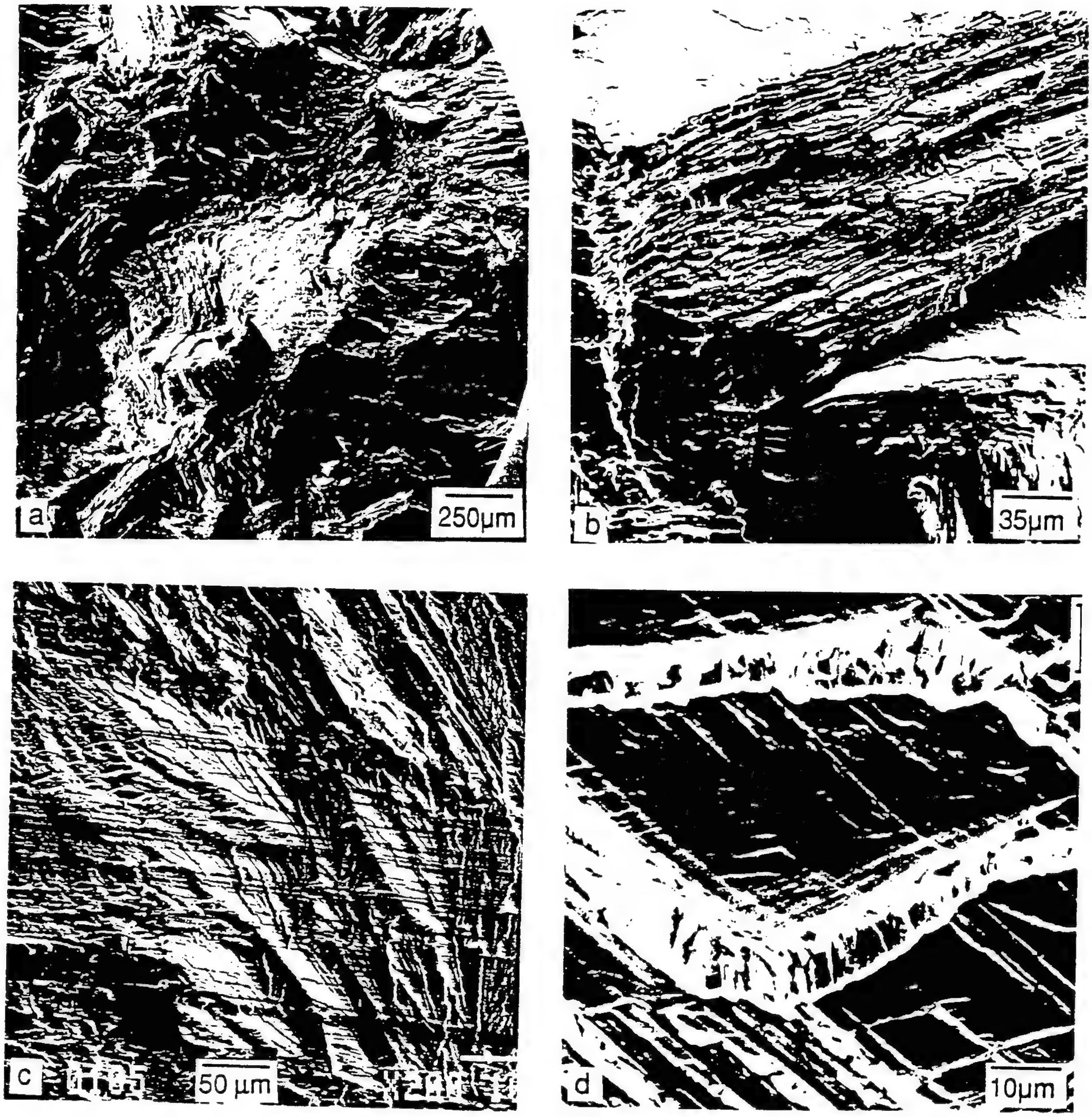

RT Tensile Transgranular Fracture of FL Gamma Alloys: (a) Overall, (b) Interlamellar and Translamellar, (c, d) Translamellar Cleavage with Interlamellar Deformation

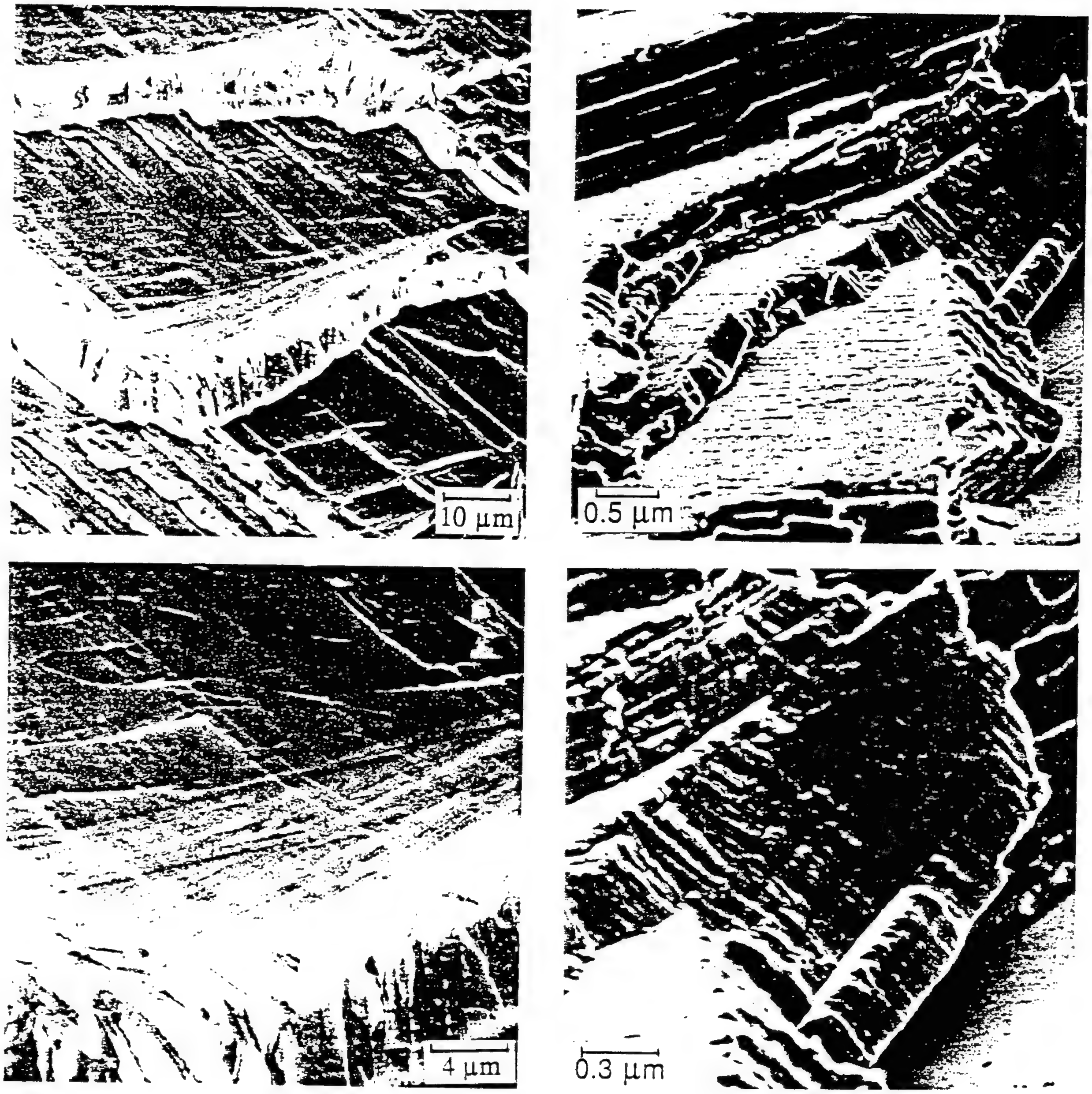

Fully-Lamellar

Duplex

RT Tensile Fracture Features of TiAl alloys in FL and Duplex Microstructural Conditions

Grain-Size//Yield-Stress Relations in TiAl

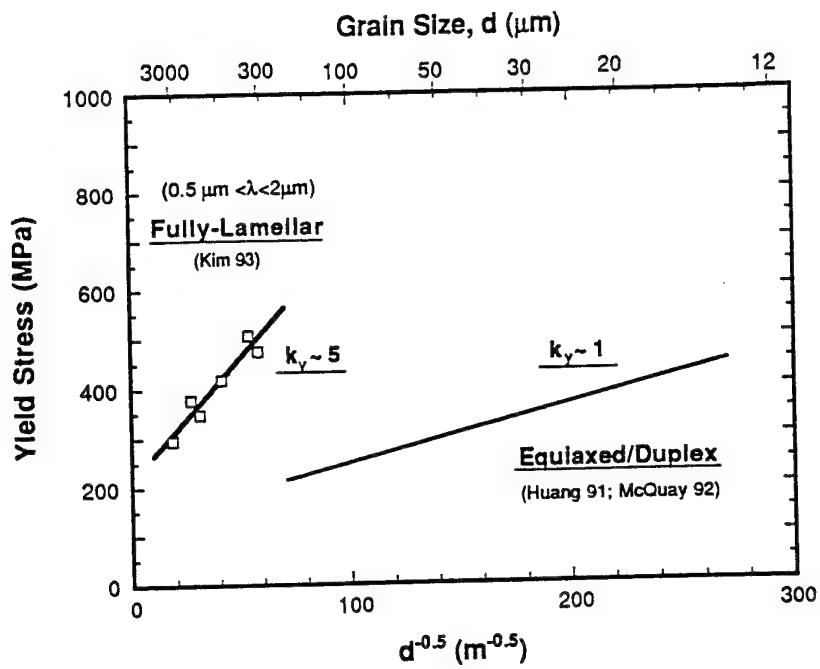

Specimen/Grain Size Effect on Tensile Properties

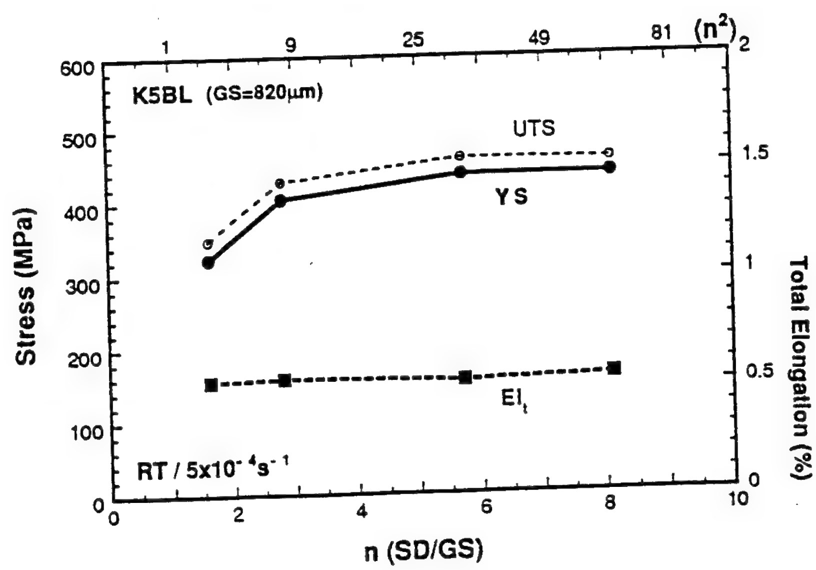

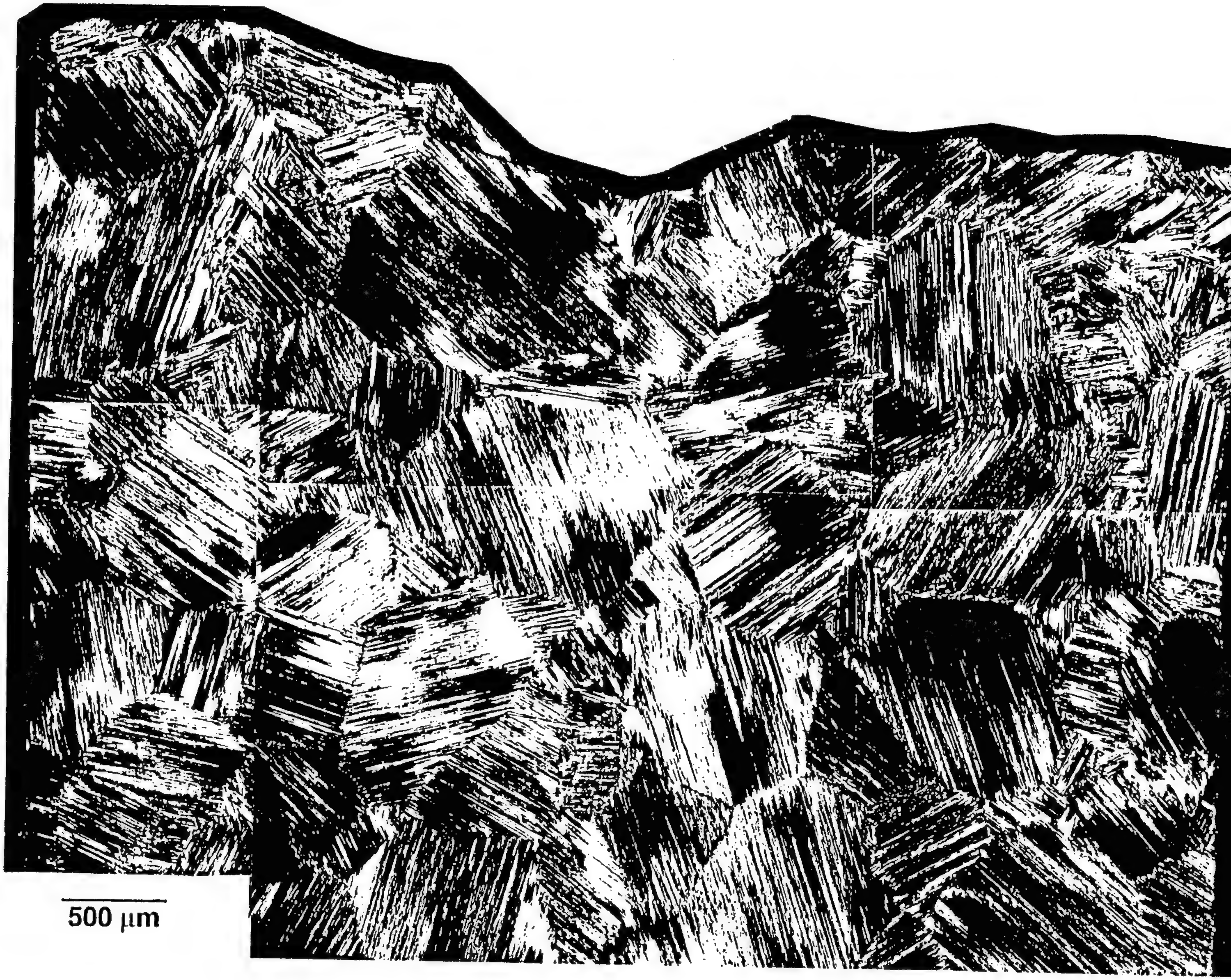

Specimen-Diameter/Grain-Size = 8.2:1

SD/GS=1.5:1

Corrected Hall-Petch Relation in FL TiAl

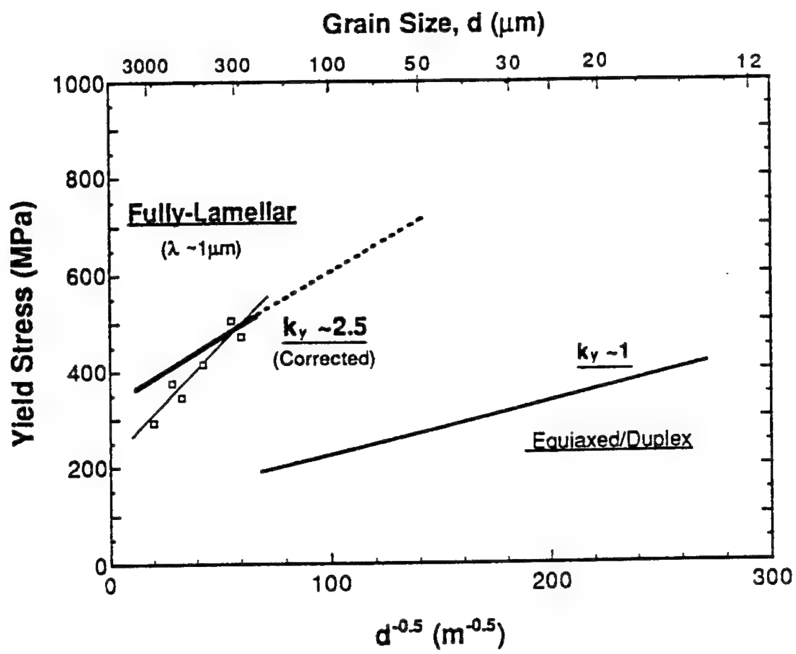

Hall-Petch Relations in TiAl Alloys

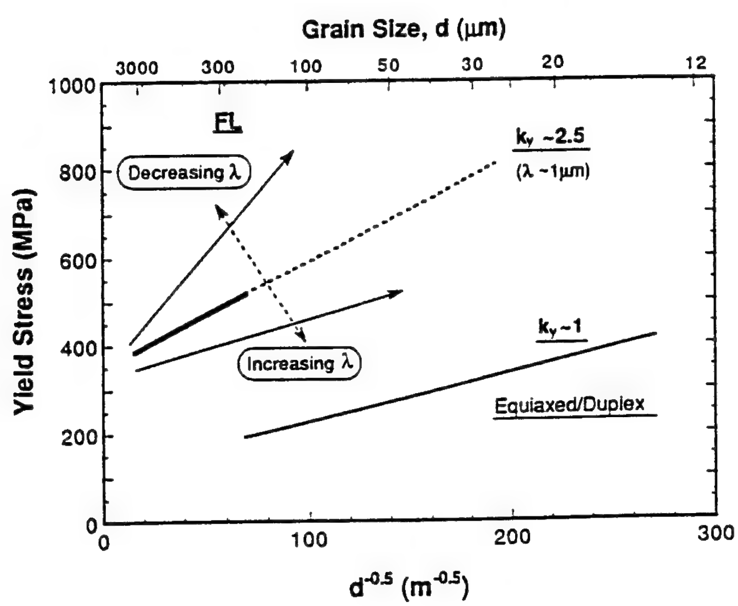

Hall-Petch Relations in TiAl Alloys

Duplex Material

$$\sigma_y = \sigma'_o = k_d d^{-1/2}$$

k_d ~1 MPa√m

Relatively isotropic

Fully-Lamellar Material

$$\sigma_y = \sigma_o + k_{d\lambda} d^{-1/2}$$

$k_{d\lambda} = 2.5$ MPa√m (for $\lambda = 1\ \mu m$)

Combined Effect of d and λ

$$k_{dy} = k_d \left(\tau^*_{avg} / \tau^*_s\right) = f_{tn}(\lambda)$$

Yielding of the $(\gamma+\alpha_2)$ Lath Structure

Ti-(46.5-47)Al- (4-6)(Cr,V,Nb,M)

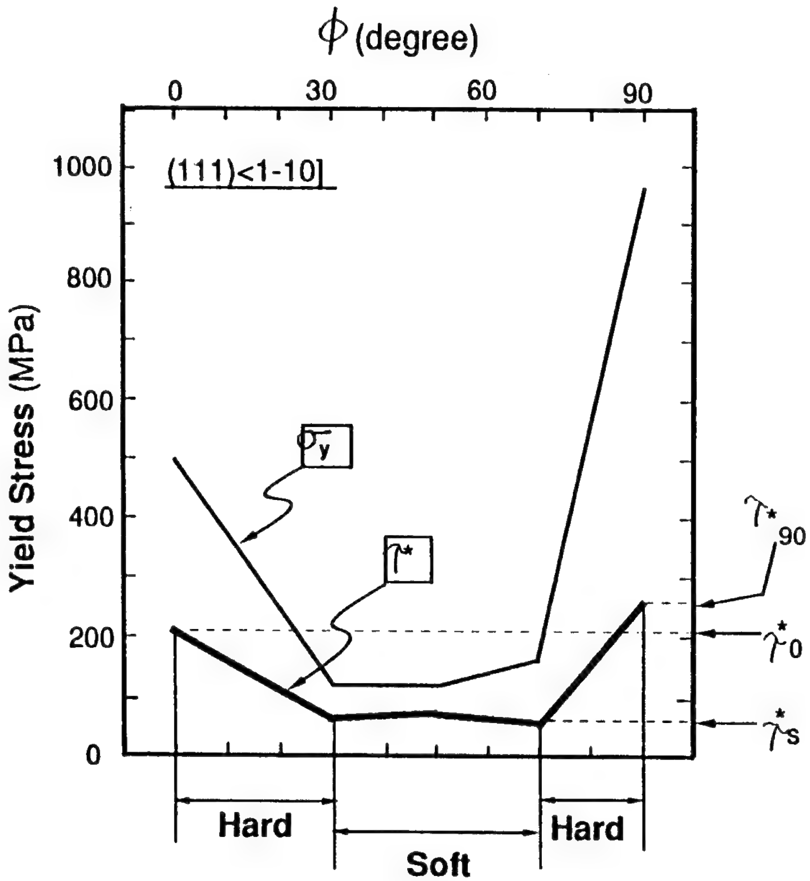

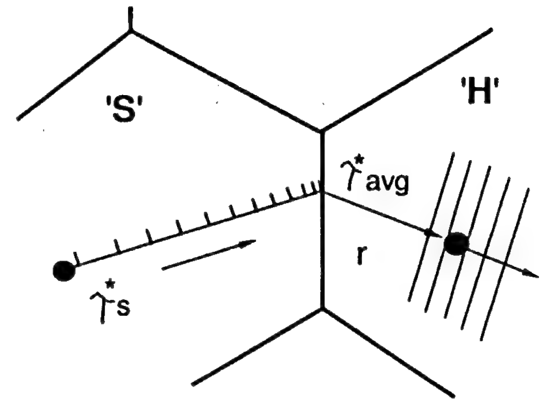

$$\tau^*_{avg} = \frac{\tau^*_{90} + \tau^*_0 + 2\tau^*_s}{4} \qquad (\sim 2.5\ \tau^*_s\ )$$

τ^*_{avg} :	Stress required to activate and move dislocations across lath boundaries

$$\boxed{k_d = k_d\ (\tau^*_{avg} / \tau^*_s)} \qquad (\sim 2.5k_d)$$

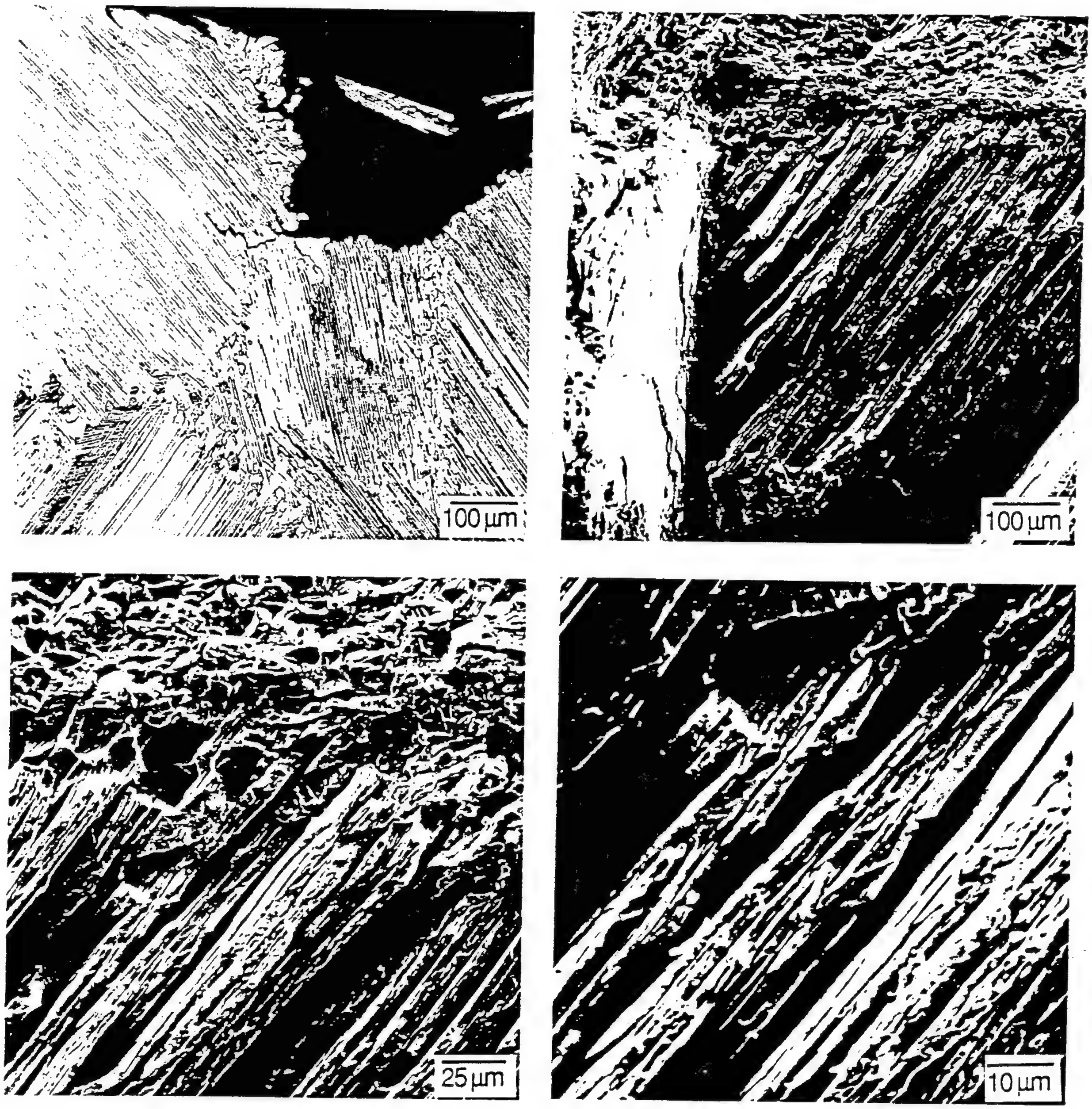

Tensile Fracture of FL Alloy G5 at 750°C

Tensile Properties of Alloy K5

(Dependence on Microstructure, Temperature and Strain Rate)

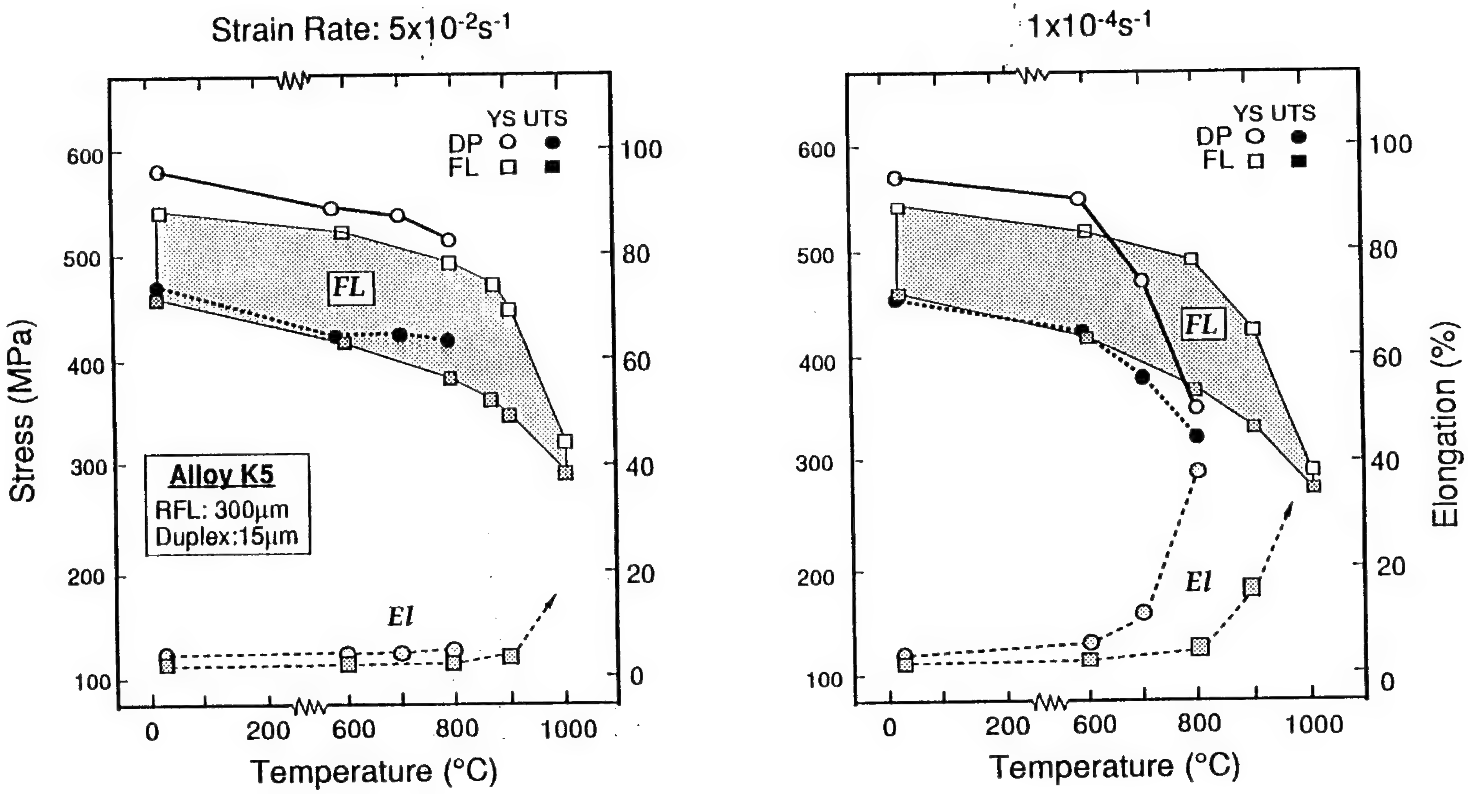

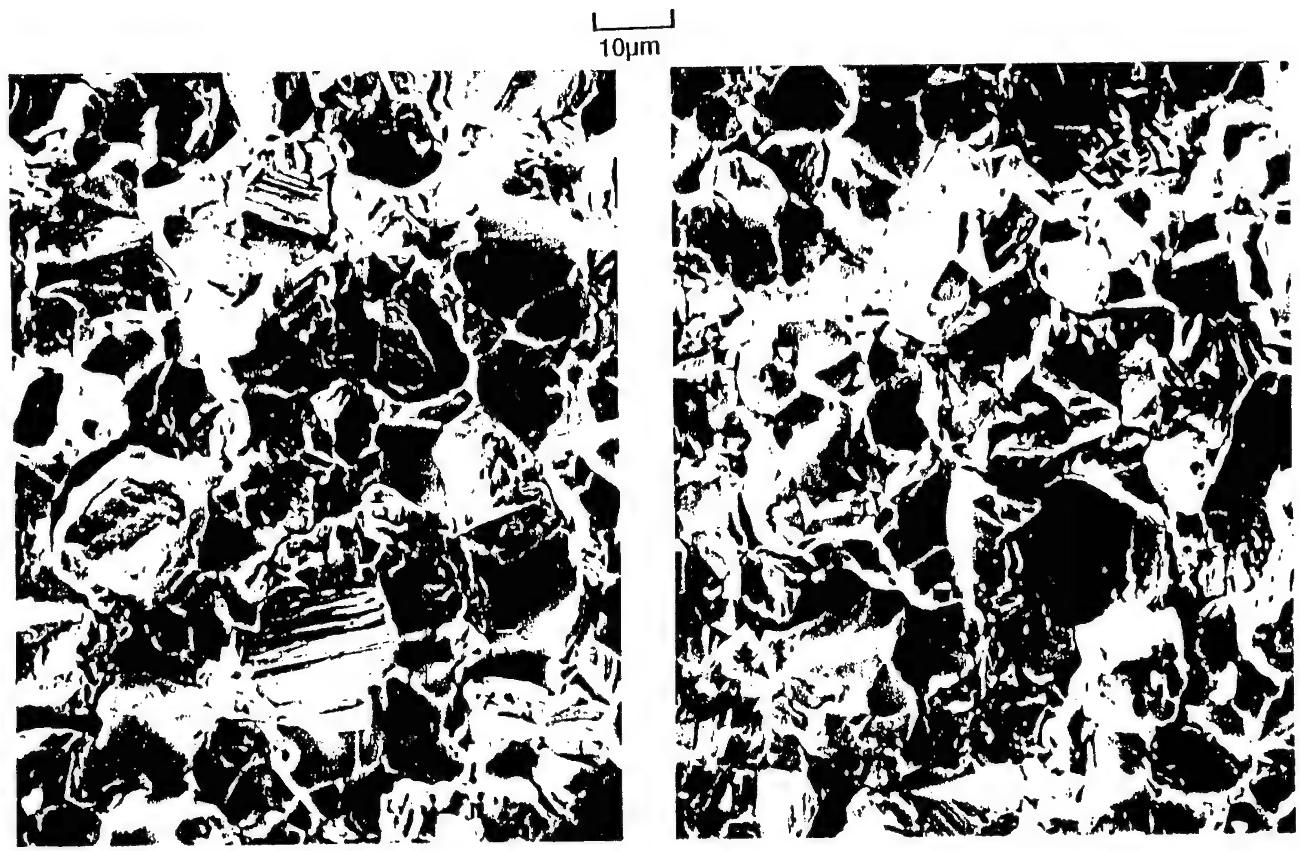

Tensile Fracture of Alloy K5 (Duplex) in Air at 600°C
[YS/UTS/El : 396/545/3.6]

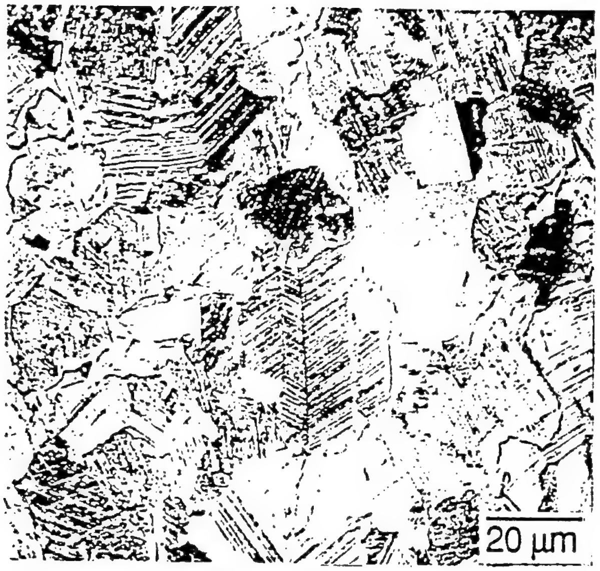

Far Below Fracture Surface

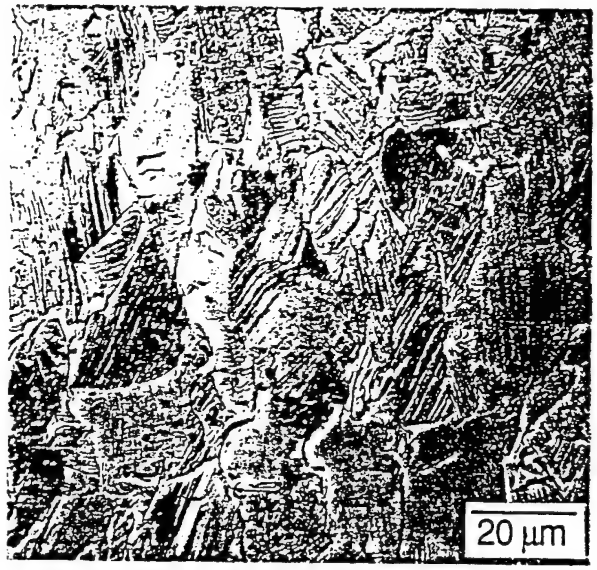

Just Below Fracture Surface

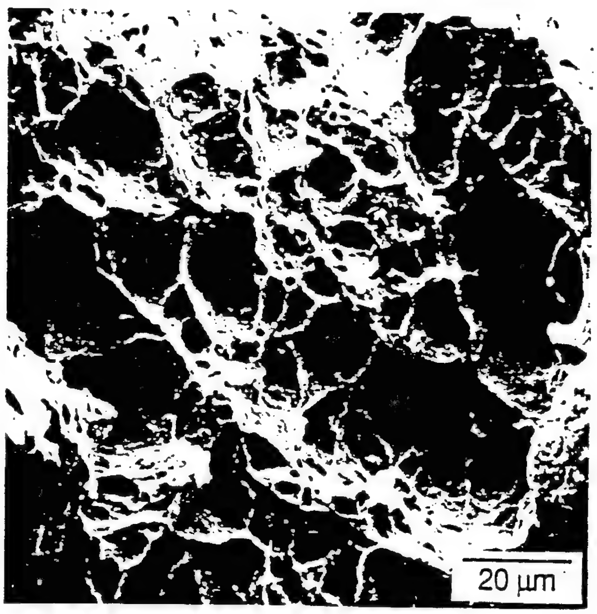

Near Cl site

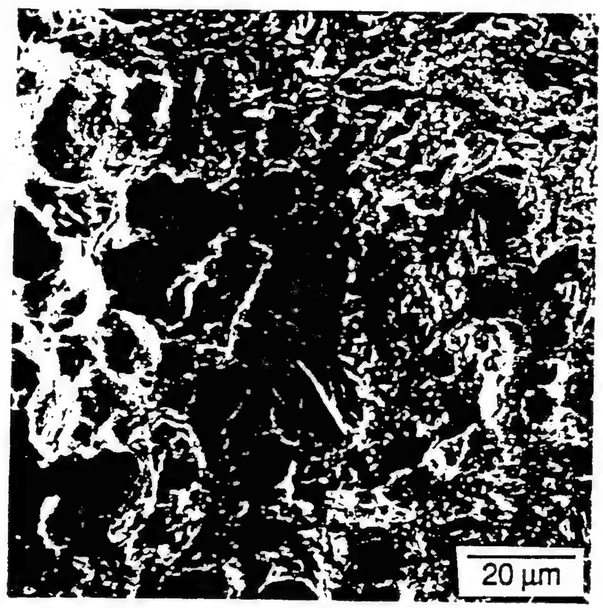

Away From Cl

Tensile Deformation and Fracture of a Duplex Alloy K5 at 800°C in Air

Temperature Effect on Fracture Mode

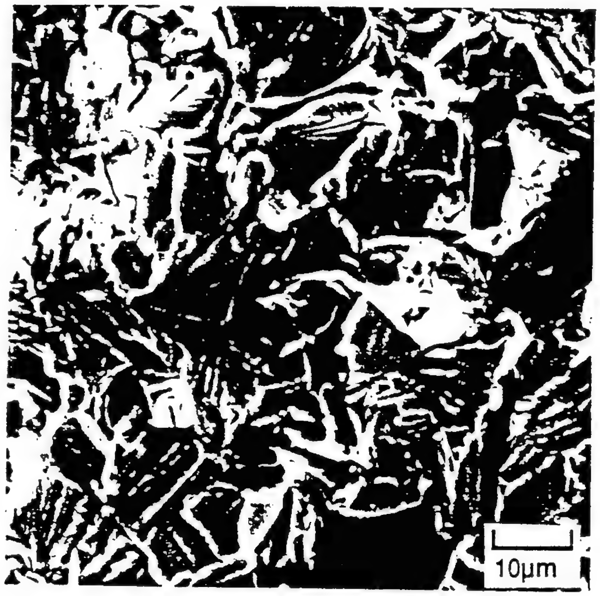

Duplex at RT

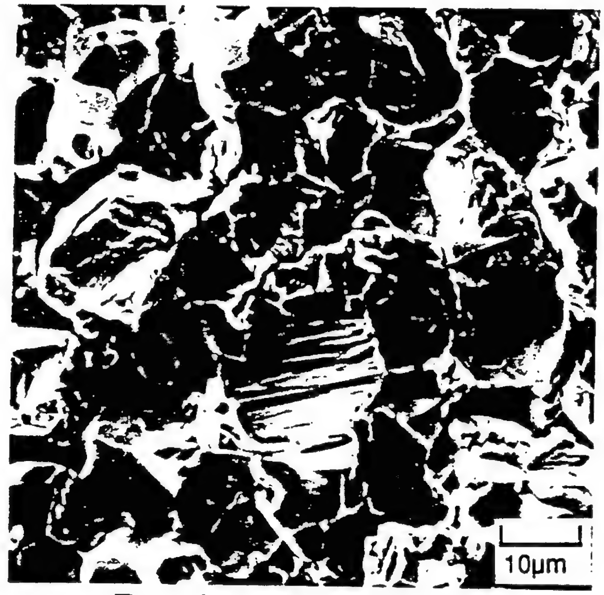

Duplex at 600°C

RFL at RT

250µm

RFL at 800°C

Tensile Properties of Alloy K5

(Dependence on Microstructure, Temperature and Strain-Rate)

K5-Duplex

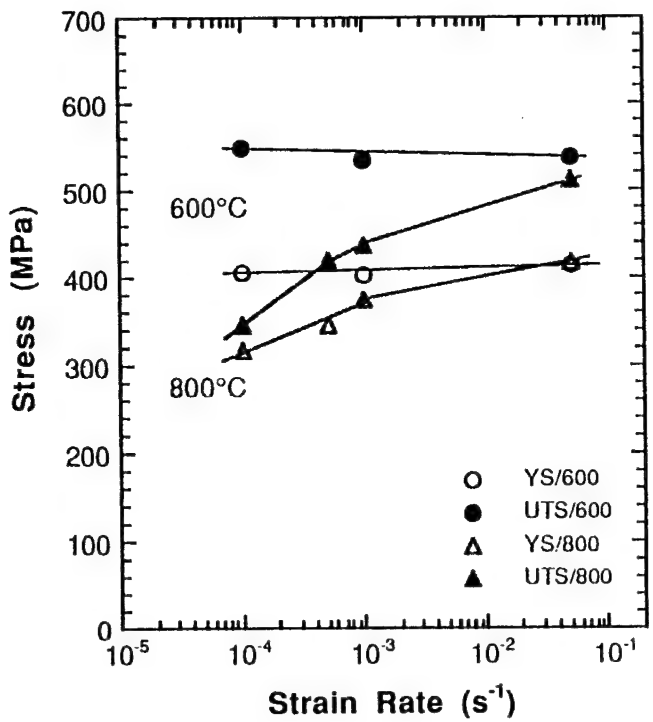

K5-RFL

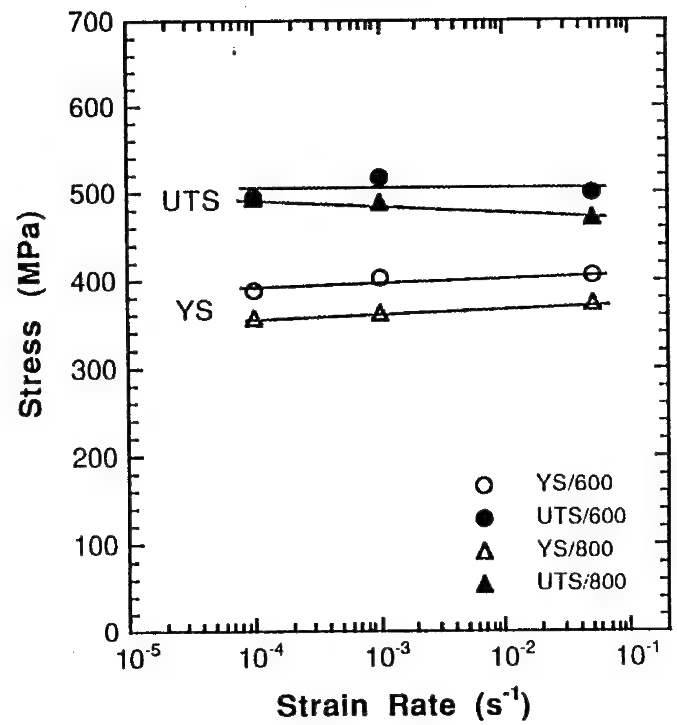

Effect of Strain Rate on BDT in Alloy K5

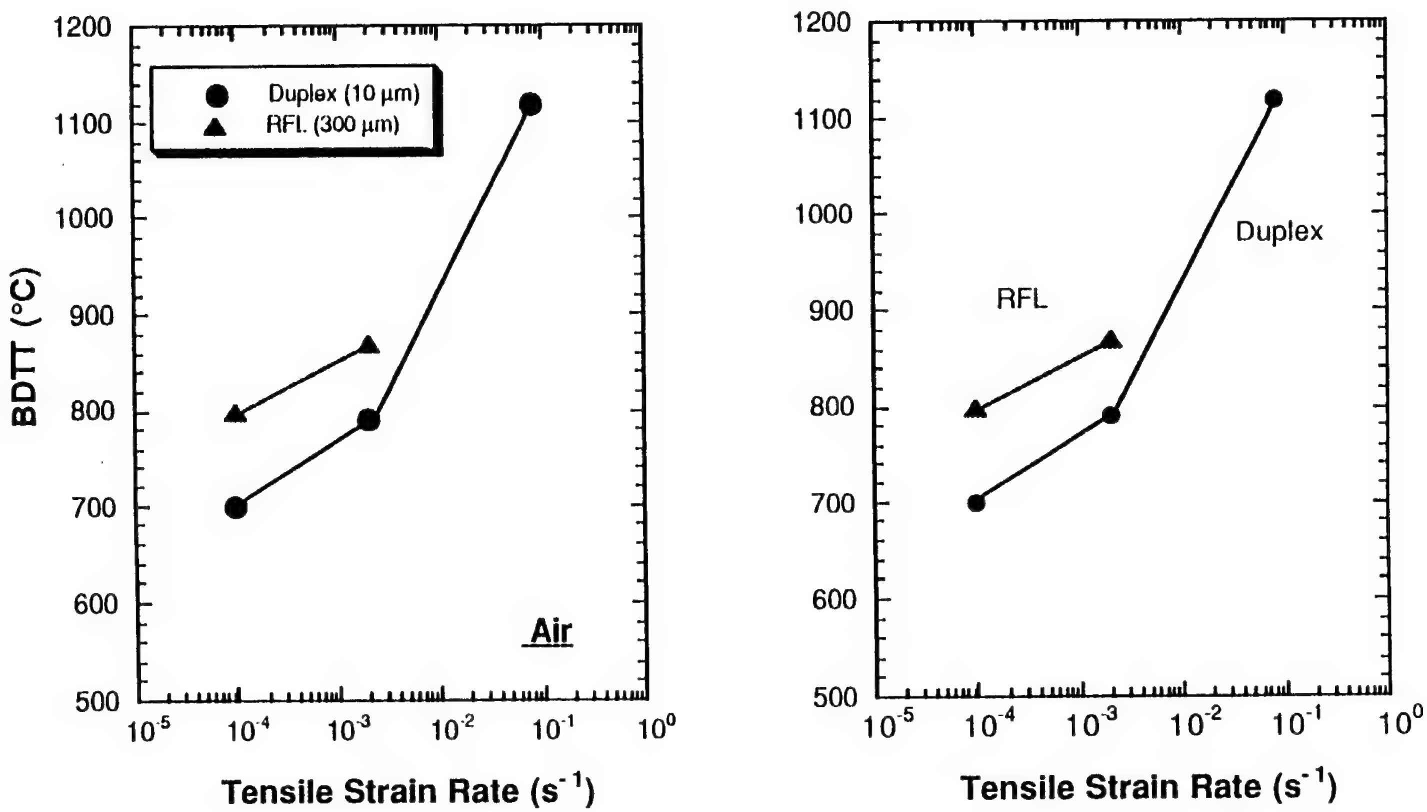

Dependence of Flow Stress on Strain-Rate and Temperature

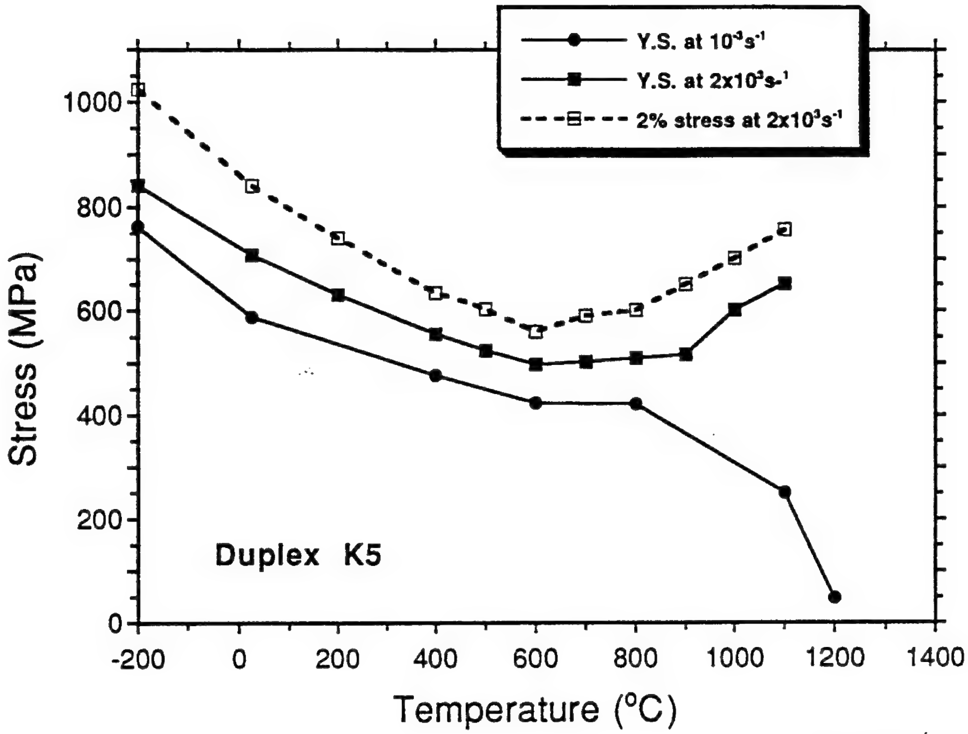

Jin + Kim (95)

Factors Controlling Tensile Properties

Microstructure

Types: Duplex vs. FL

Features

Grain Size and Morphology
GB Morphology
Lamellar Spacing (LS)
α_2/γ Ratio (α_2 vol%)

Uniformity

Composition

α_2/γ Ratio; LS

Cleavage Strength

Interfacial Bond Strength

Grain Size Effects on Tensile and Toughness

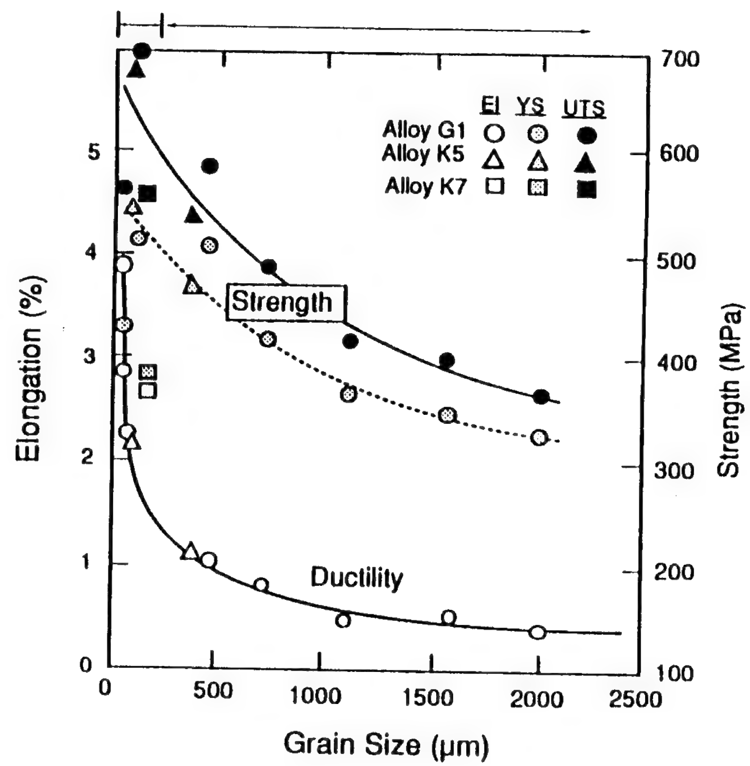

Ductility and Strength

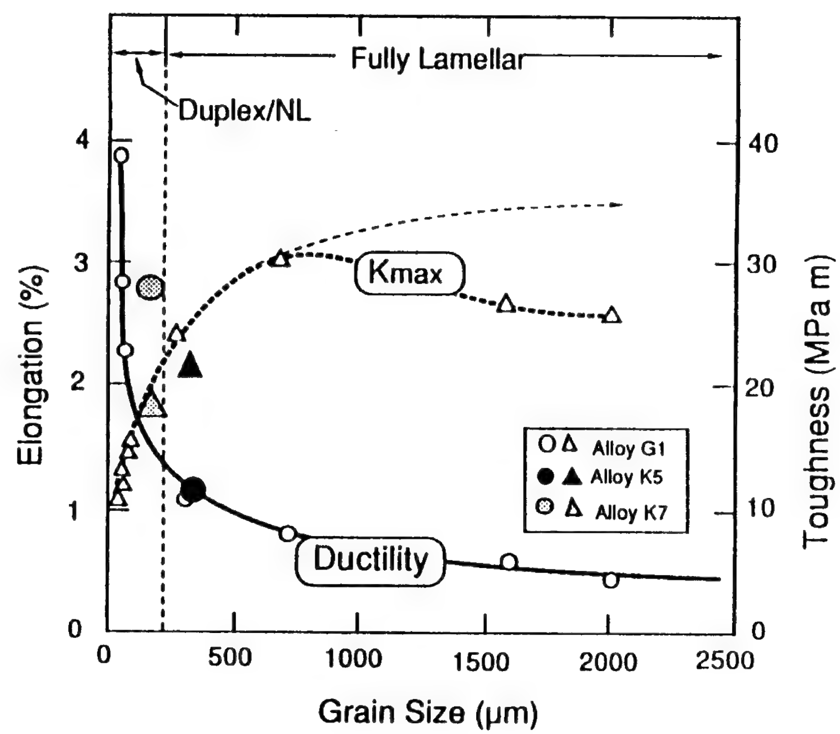

Ductility and Toughness

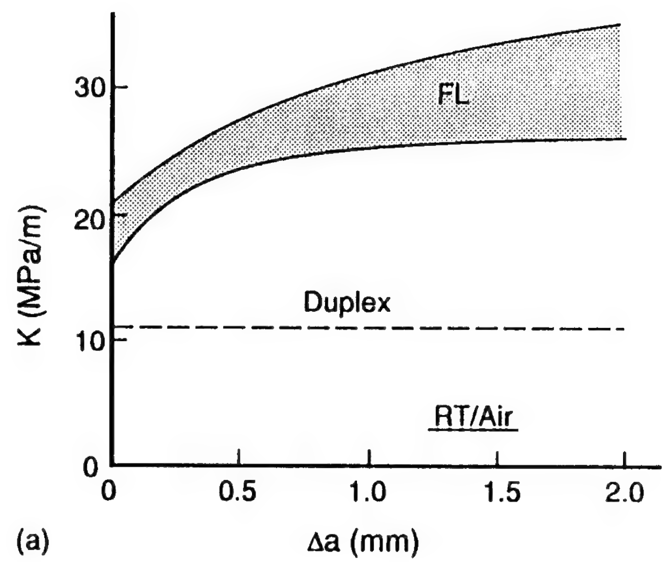

K-Resistance Curves

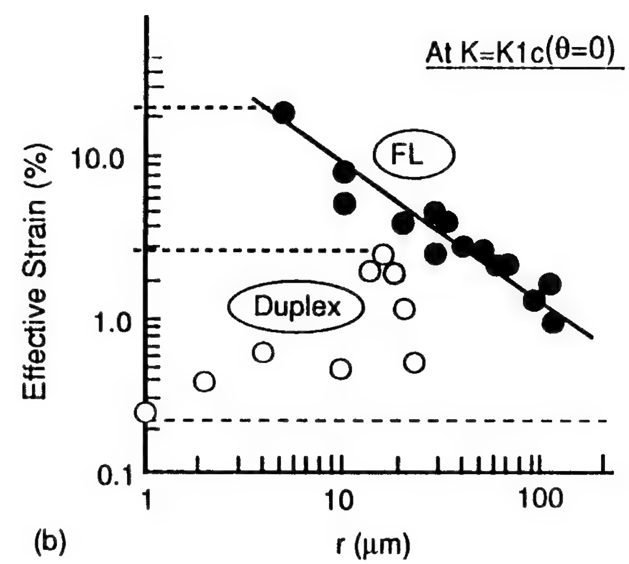

Near-tip Strain Distribution

Fracture Resistance and Near-Tip Plasticity at RT

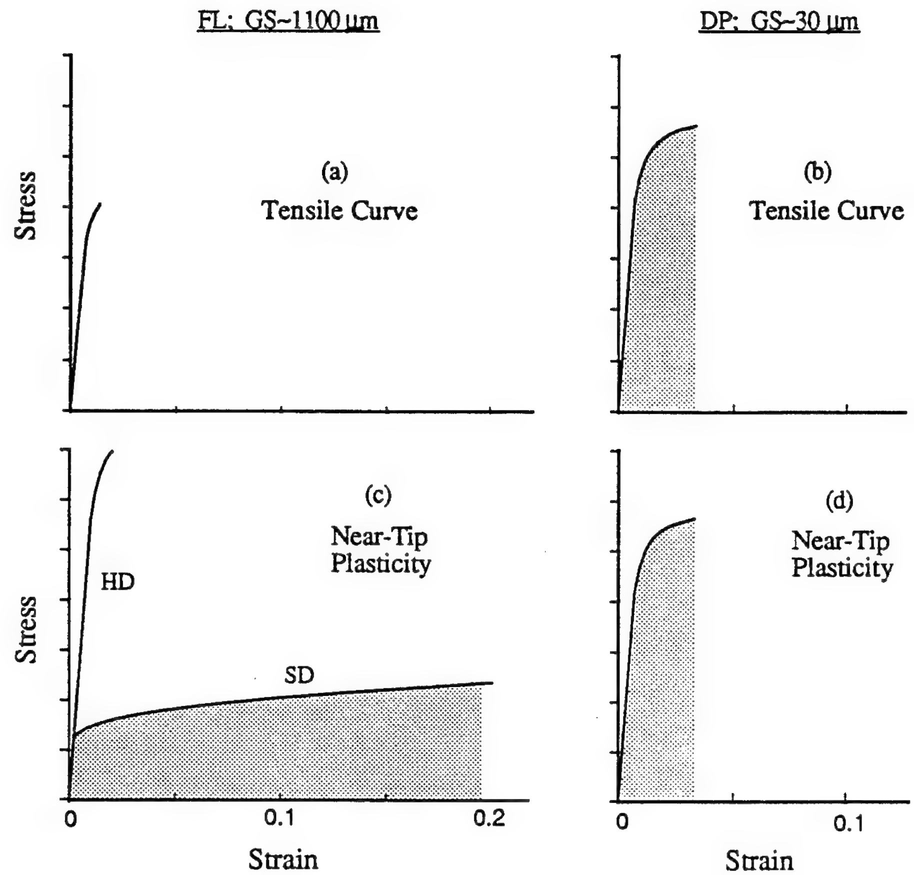

General Tensile Yielding vs. Near-Crack-Tip Plasticity at K_{IC}

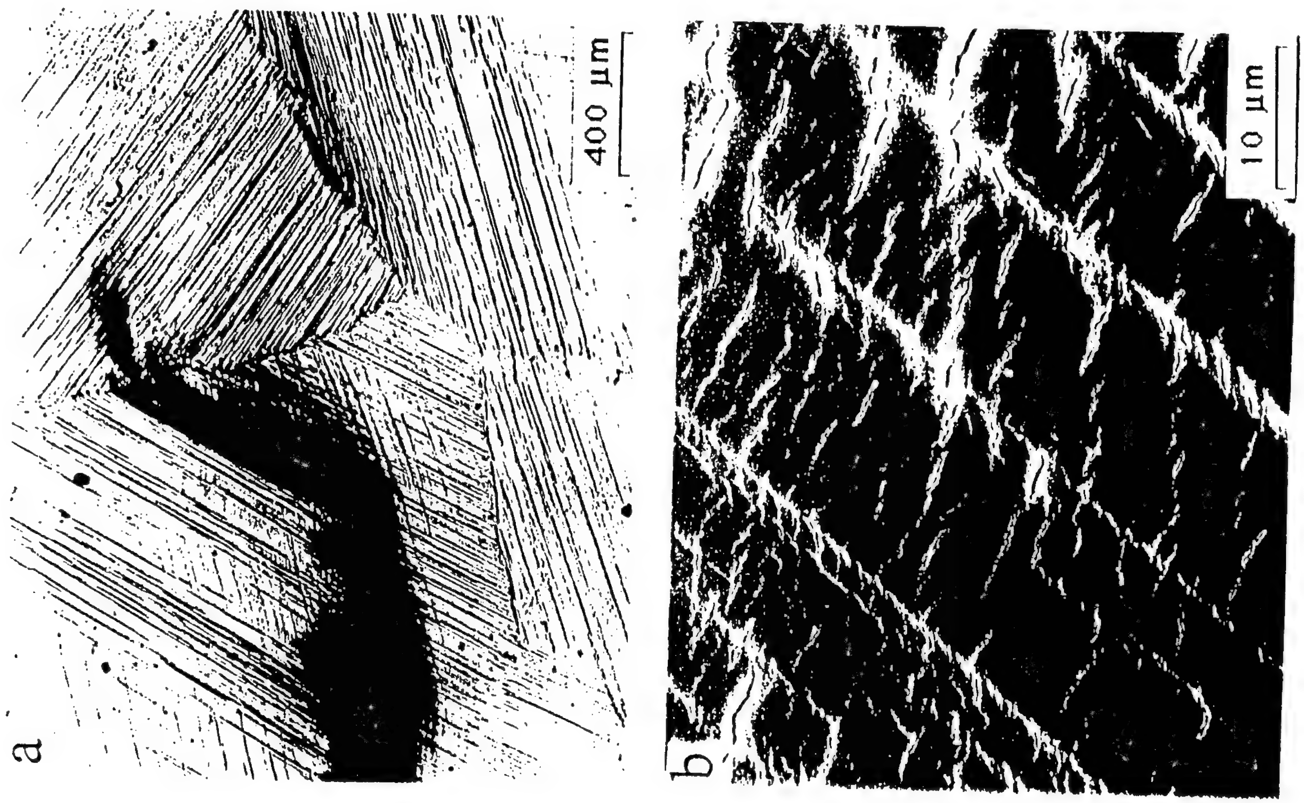

Plastic Deformation and Microcracking Around the Advancing Crack Tip in a FL Alloy G1 CT Specimen under a Monotonic Tension Loading at RT

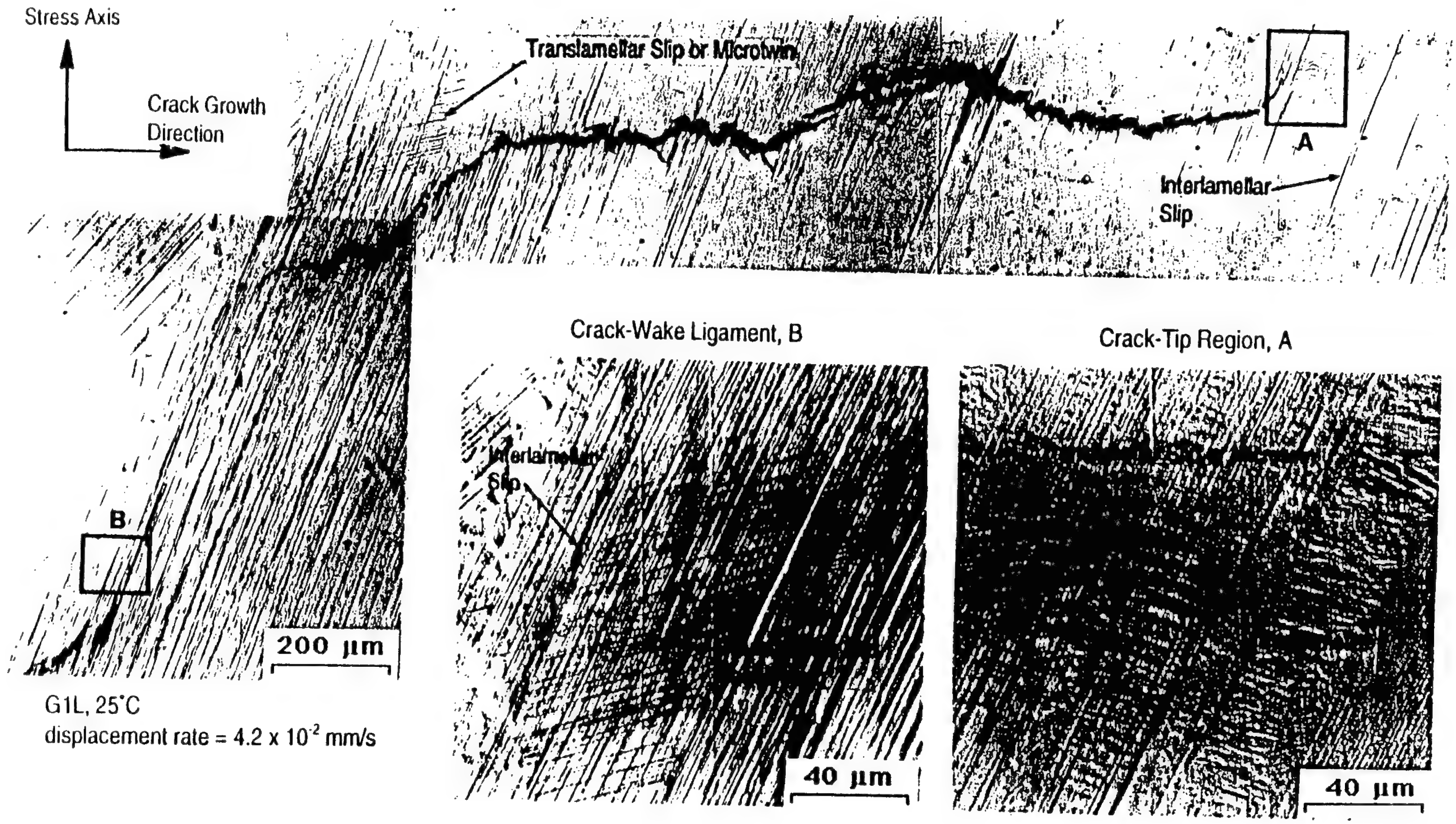

Interlamellar and Translamellar Deformation in Crack-Tip and Ligament Regions

Fracture Toughness

Grain Size Effect

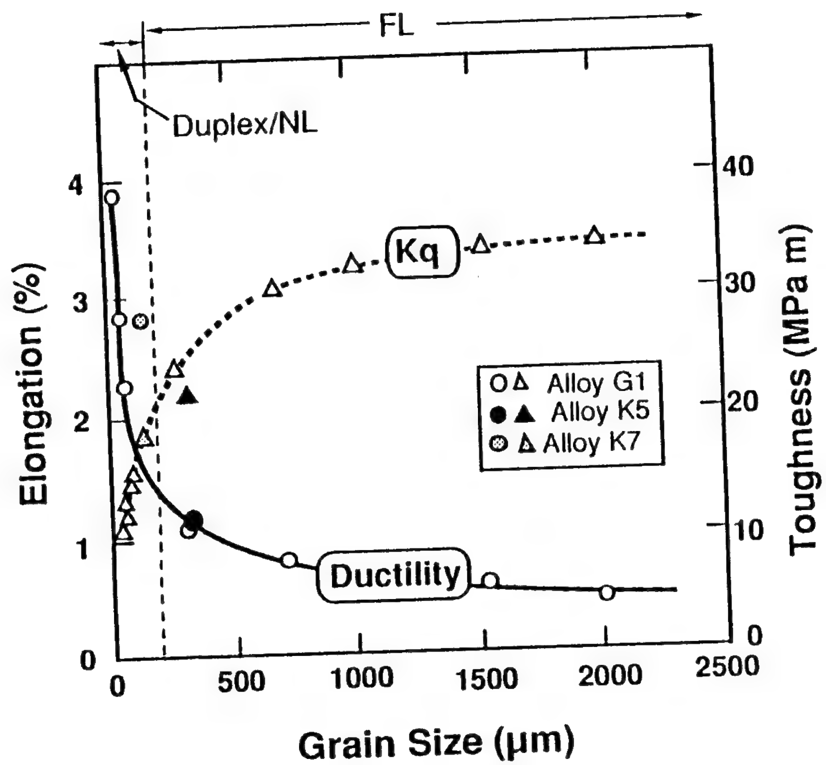

Lamellar Spacing Effect

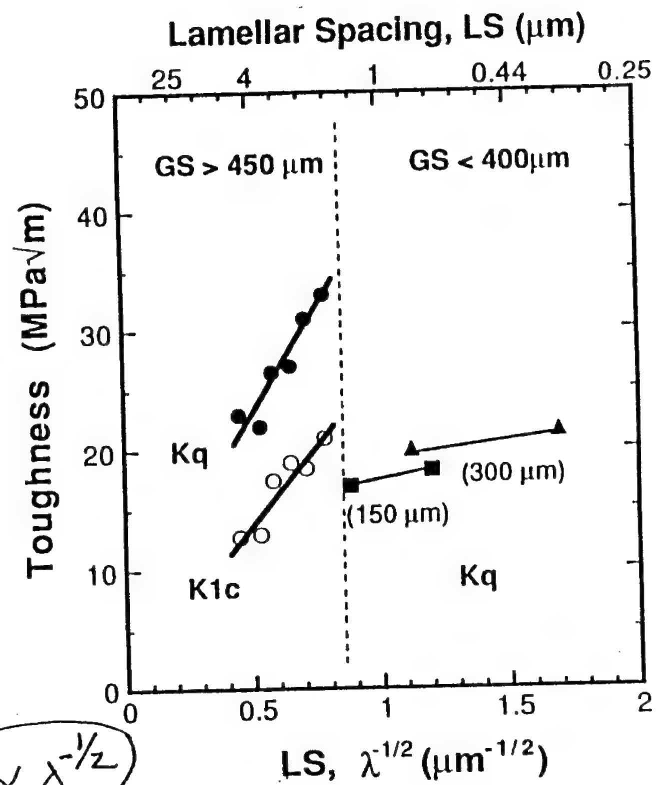

$K \propto \lambda^{-1/2}$

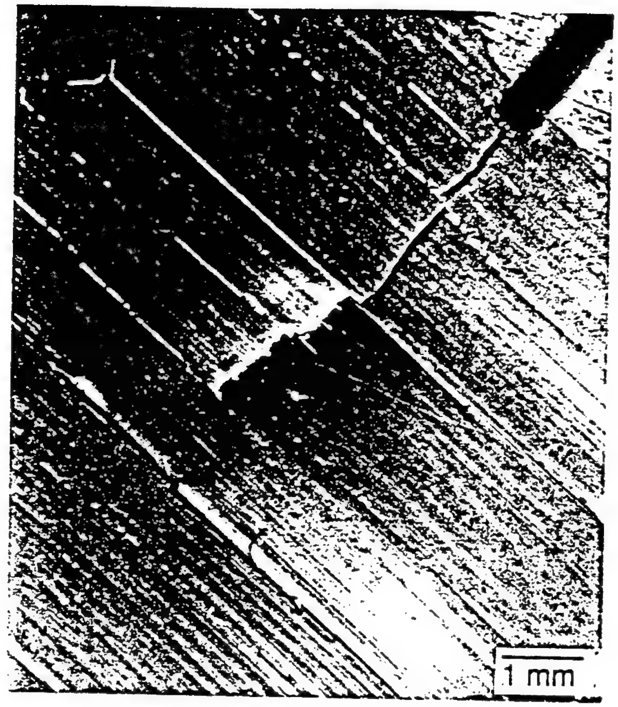

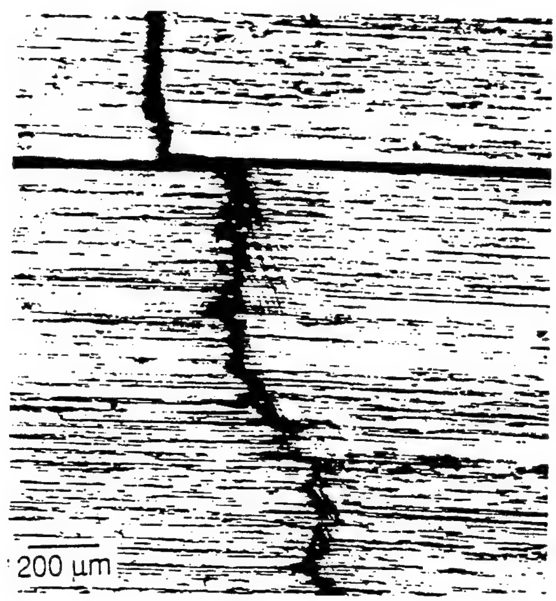

T-Cracks Involving Delamination, and Both Inter- and Trans-lamellar Slip/Twinning

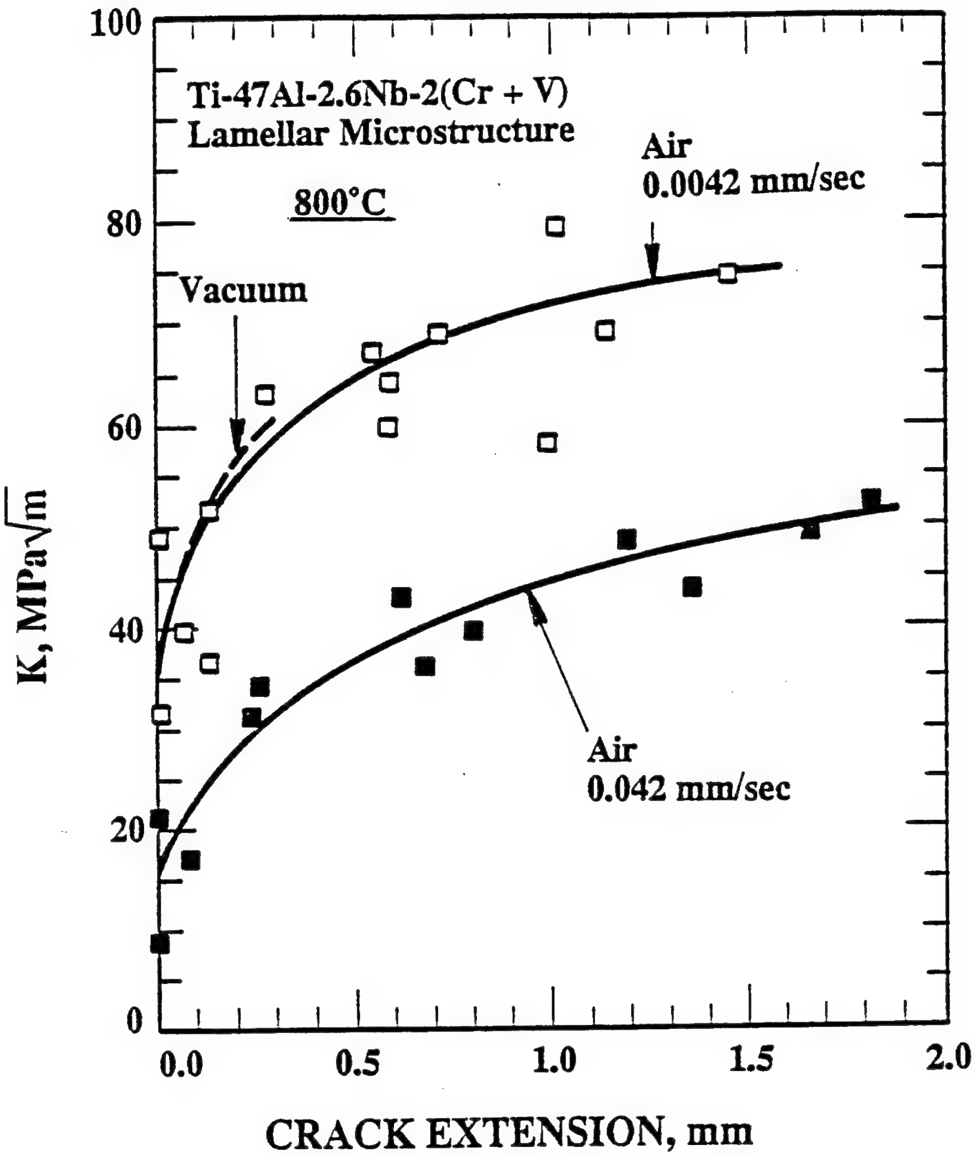

Effect of displacement rate on the K-resistance curves of the G1L alloy at 800°C.

4

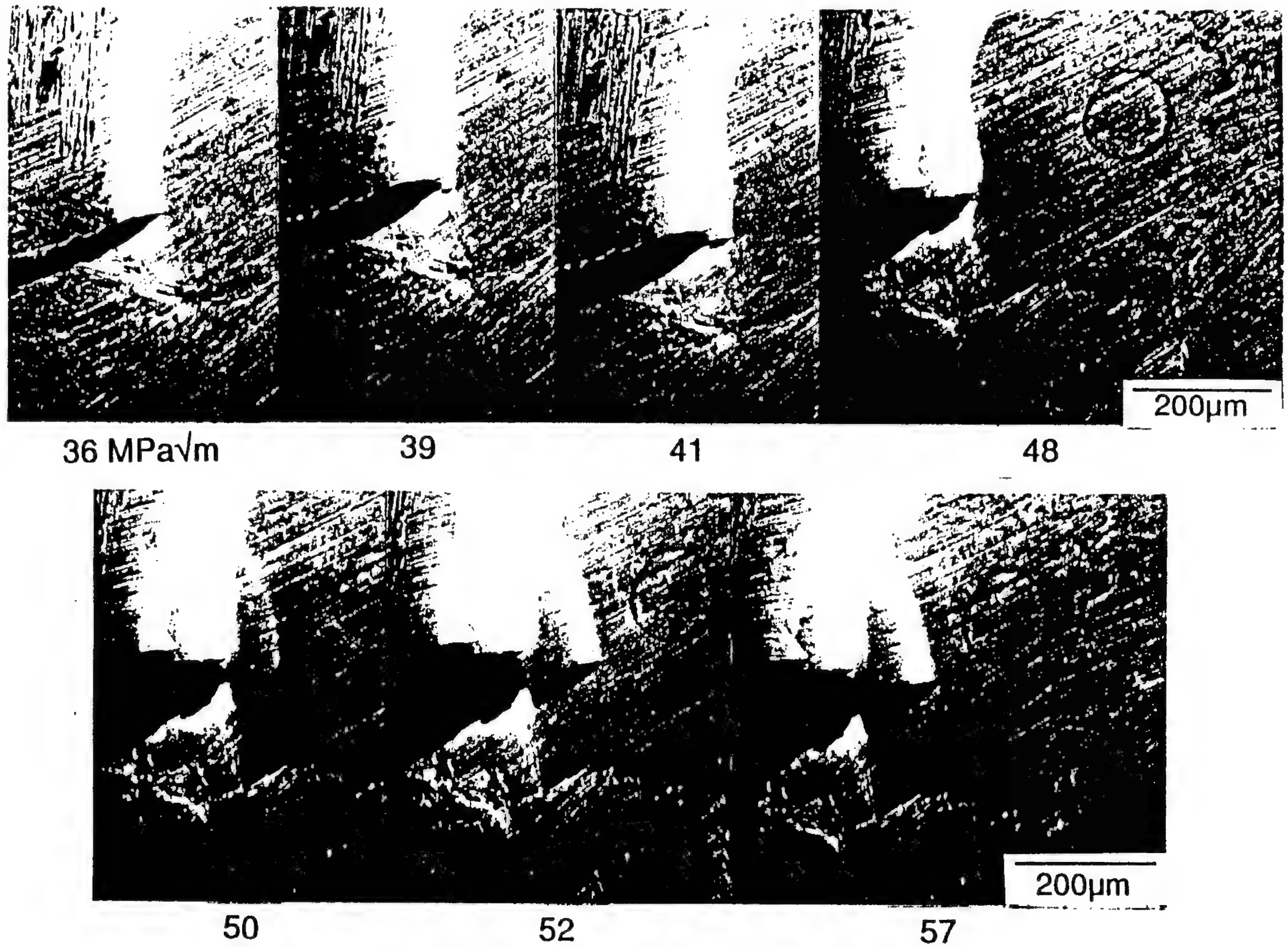

Fracture Process in Lamellar TiAl Alloys at 800°C

4

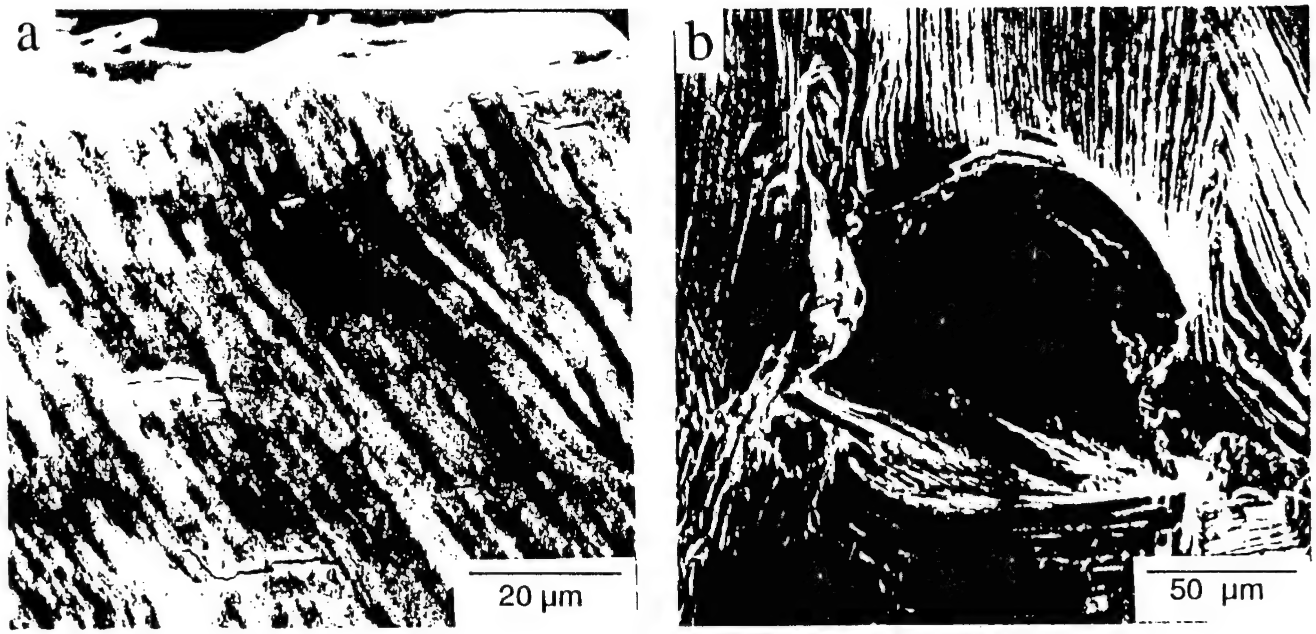

RT 800°C

Crack-Tip Regions of Lamellar TiAl Fracture Specimens

Creep Resistance of Alloy K5

Stress Exponents

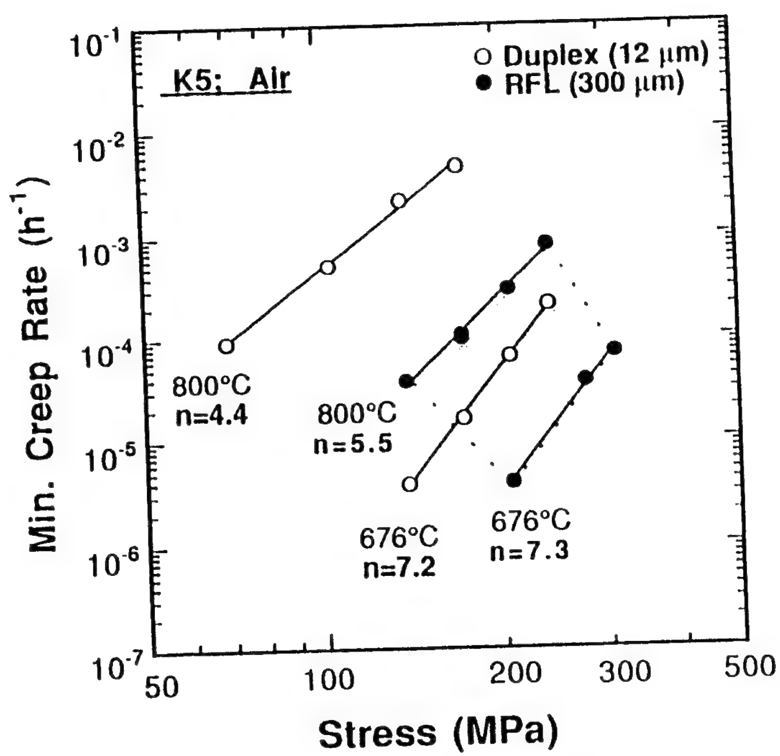

Larsen-Miller Plot

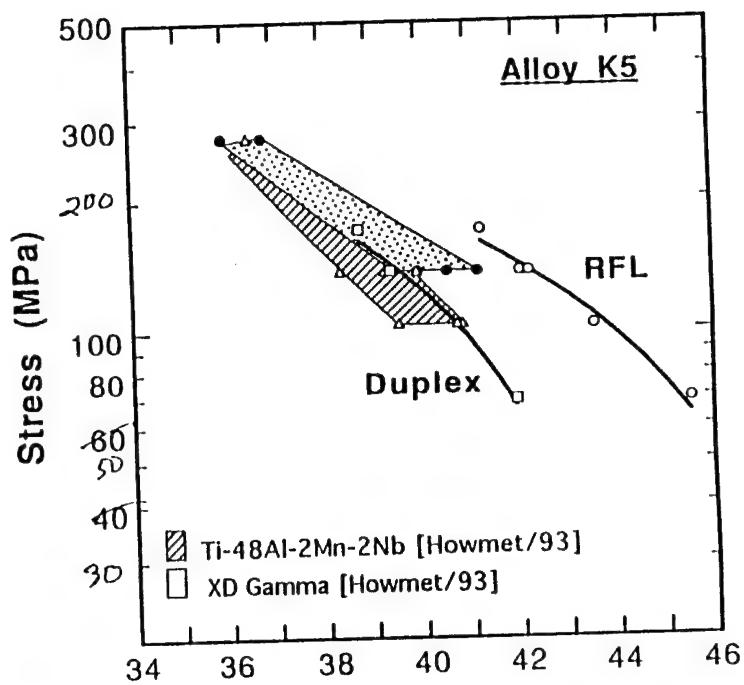

schwenker + Kim (94)

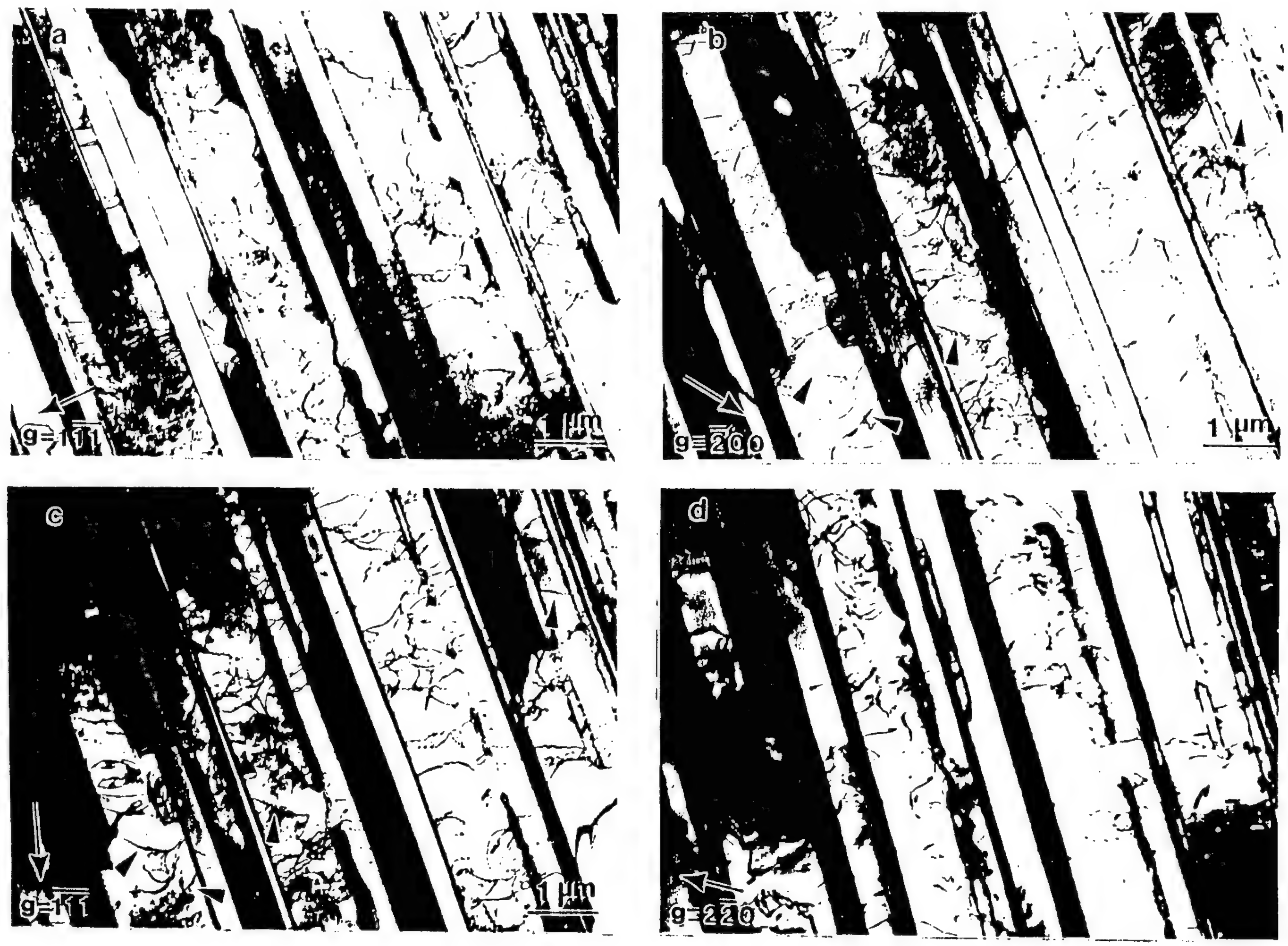

Alloy G1 : Lamellar structure near the fracture surface of the specimen crept in vacuum at 207 MPa

4

Alloy K5 RFL Specimen Crept at 800°C to 18.7% in Air Under
(138-173-207-242-285 MPa) Step Stress Conditions

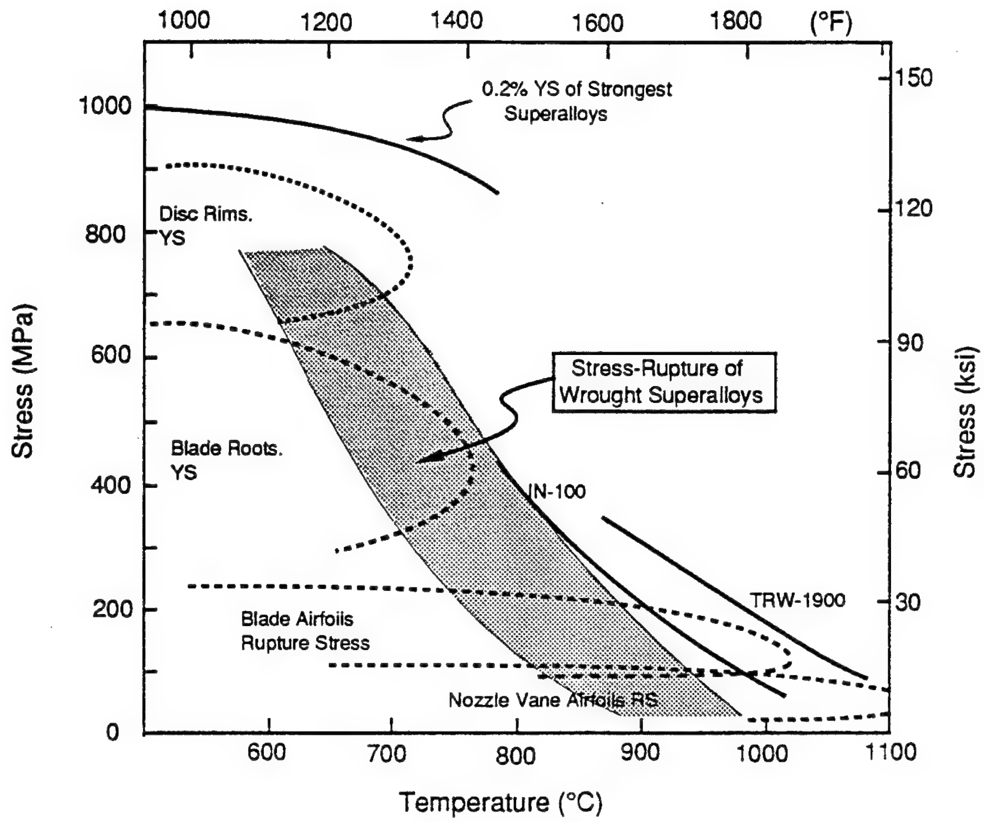

Turbine Blade and Vane Operating Temperatures, Yield Stresses (YS), 1000-h RuptureStresses (RS) for Superalloys

Effect of Al_2O_3 Layer on Creep

Creep of Alloy K5

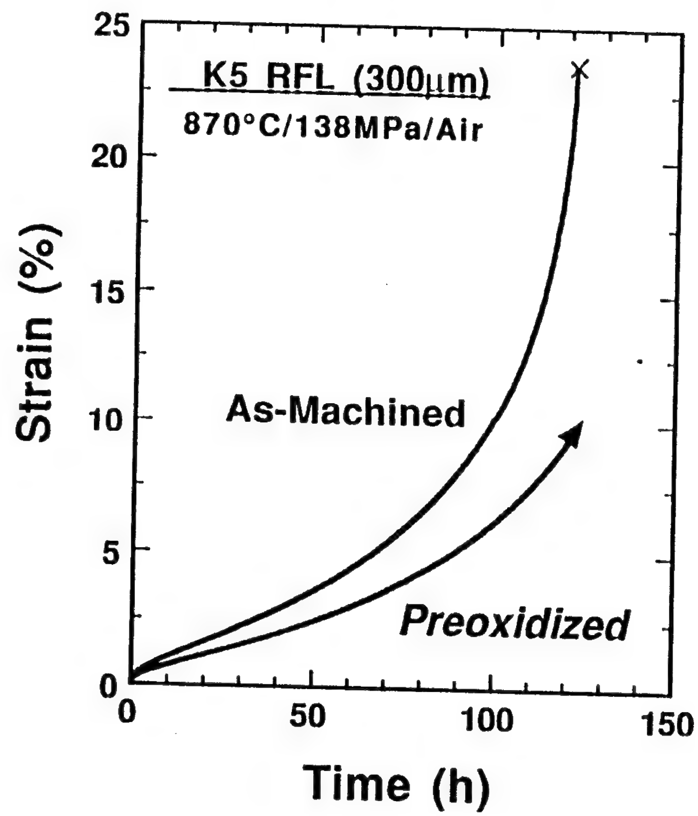

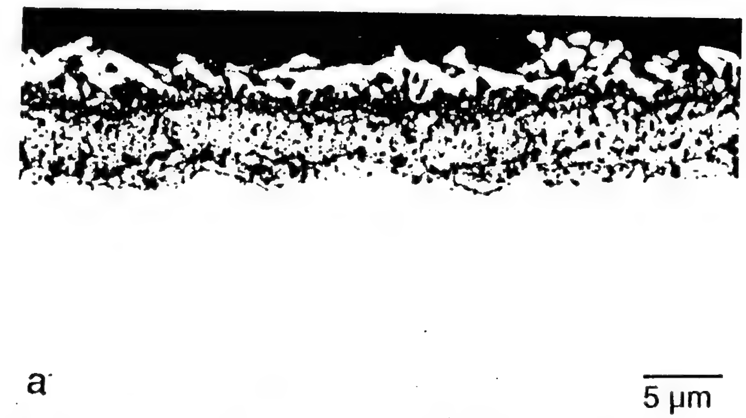

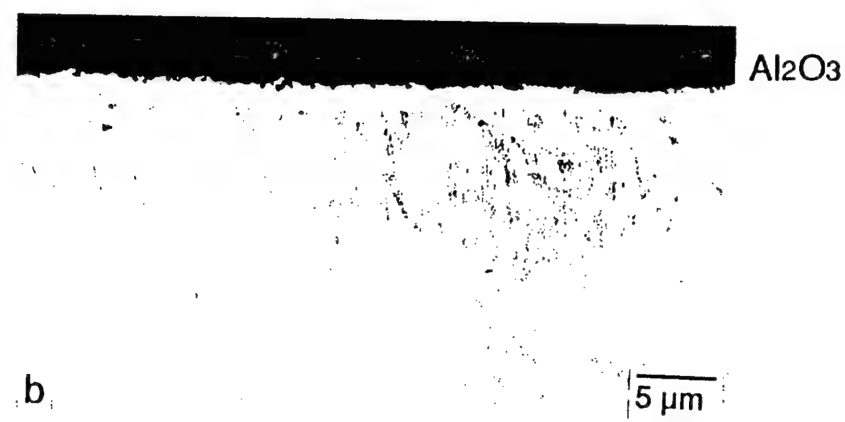

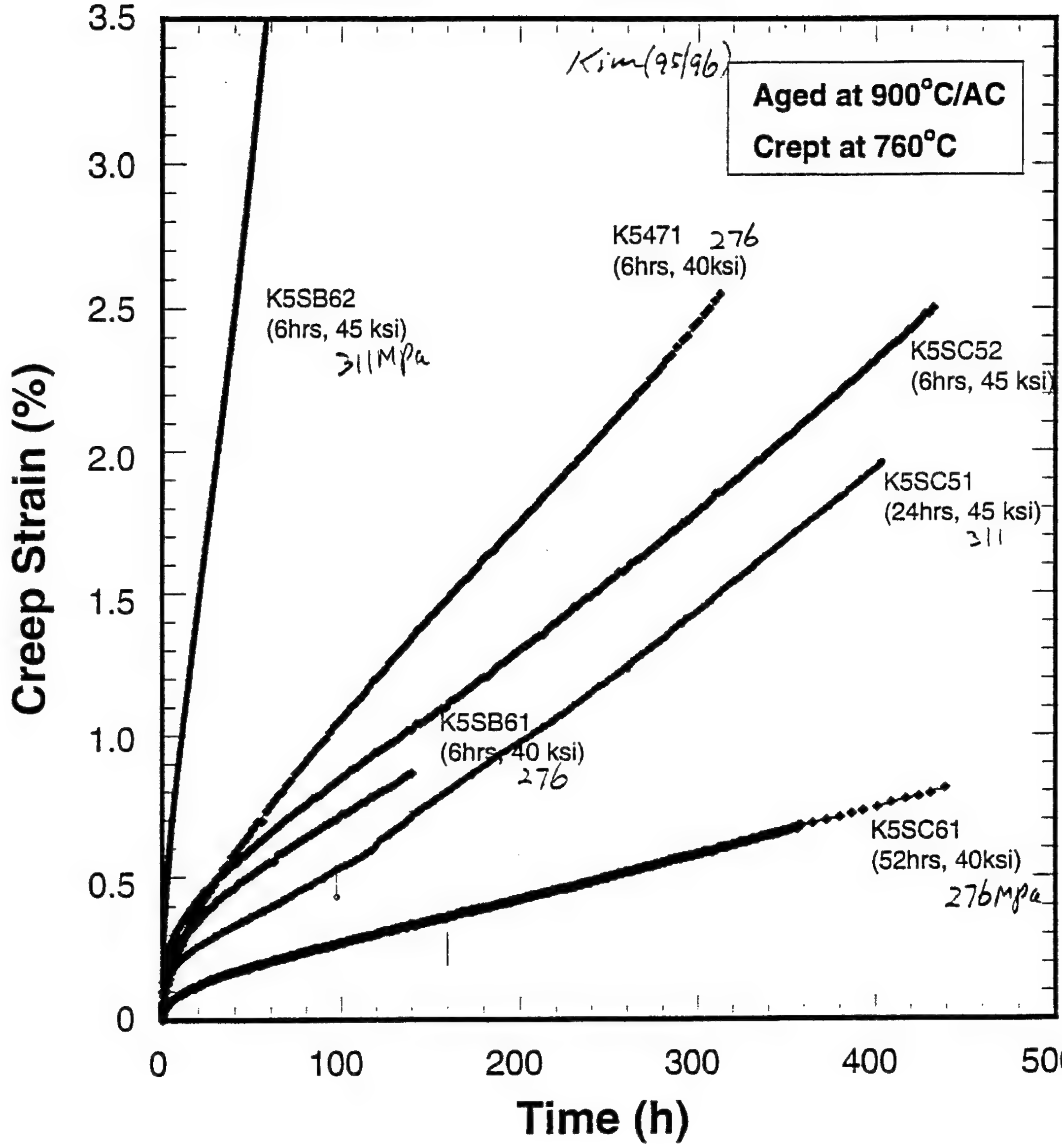

Kim(95/96)
Aged at 900°C/AC
Crept at 760°C
K5SB62
(6hrs, 45 ksi)
311MPa
K5471 276
(6hrs, 40ksi)
K5SC52
(6hrs, 45 ksi)
K5SC51
(24hrs, 45 ksi)
311
K5SB61
(6hrs, 40 ksi)
276
K5SC61
(52hrs, 40ksi)
276MPa
Creep Strain (%)
Time (h)
0
0.5
1.0
1.5
2.0
2.5
3.0
3.5
0
100
200
300
400
500

Creep of Alloy K5 Series

(under severe conditions)

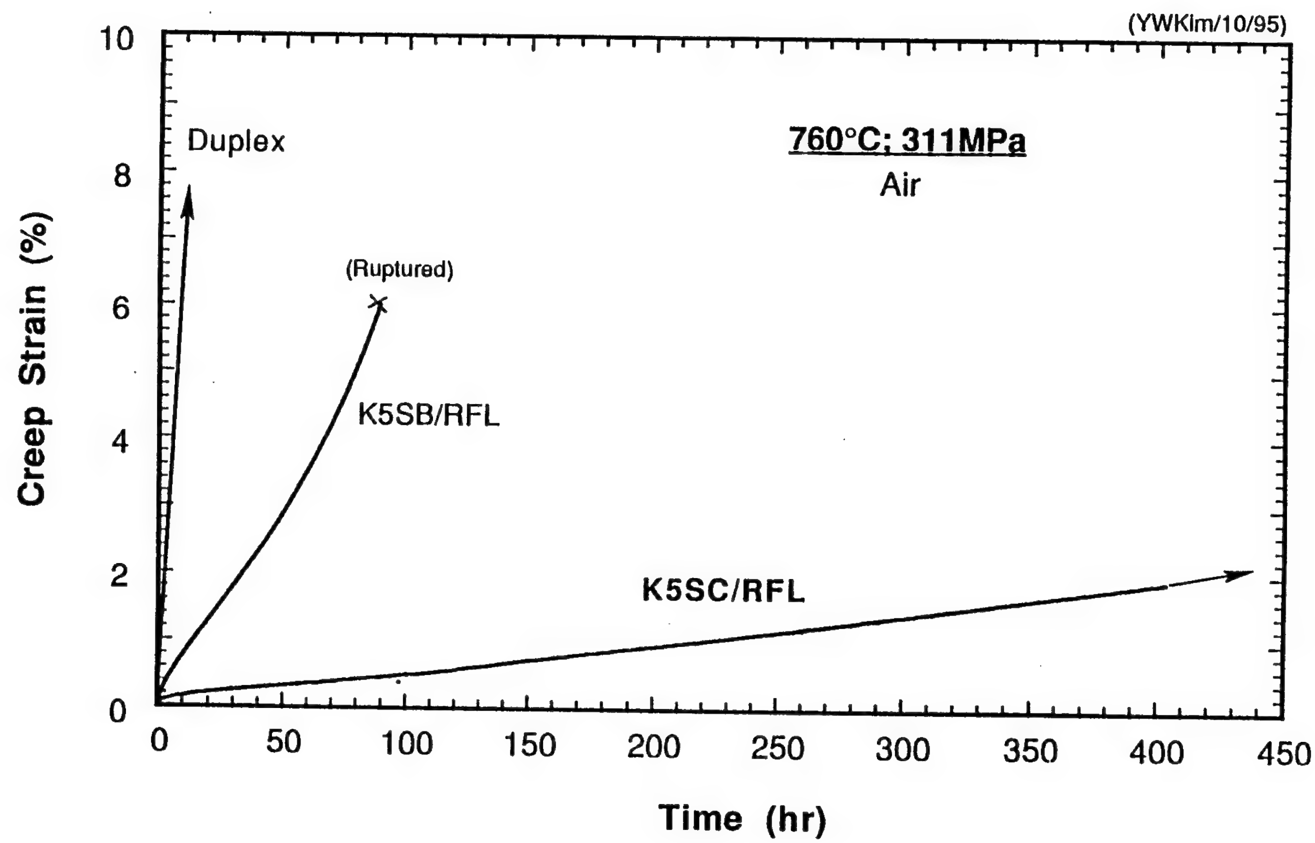

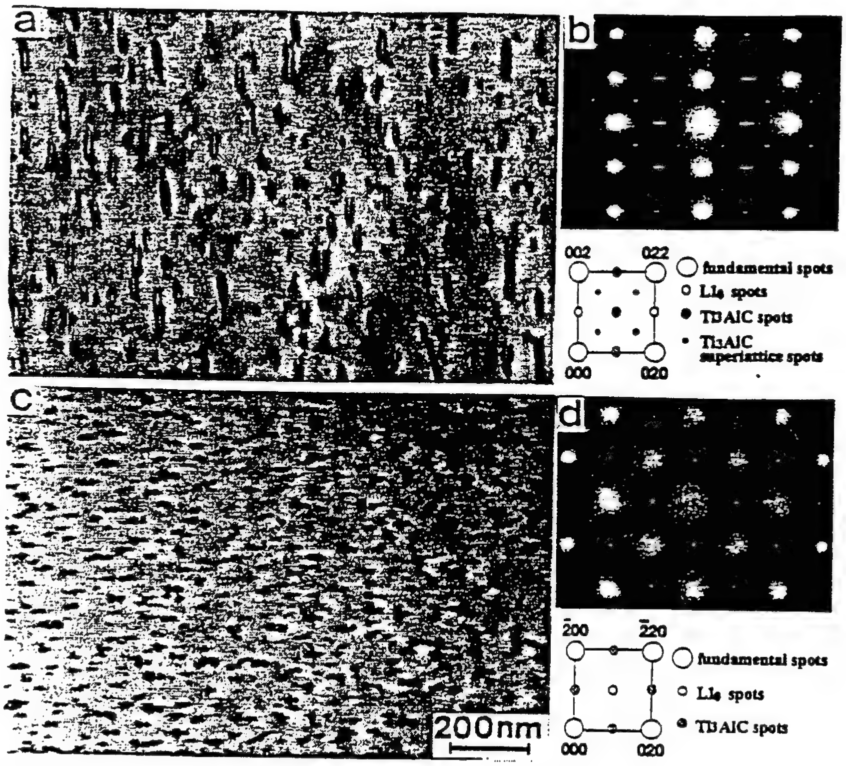

Nemoto (94)

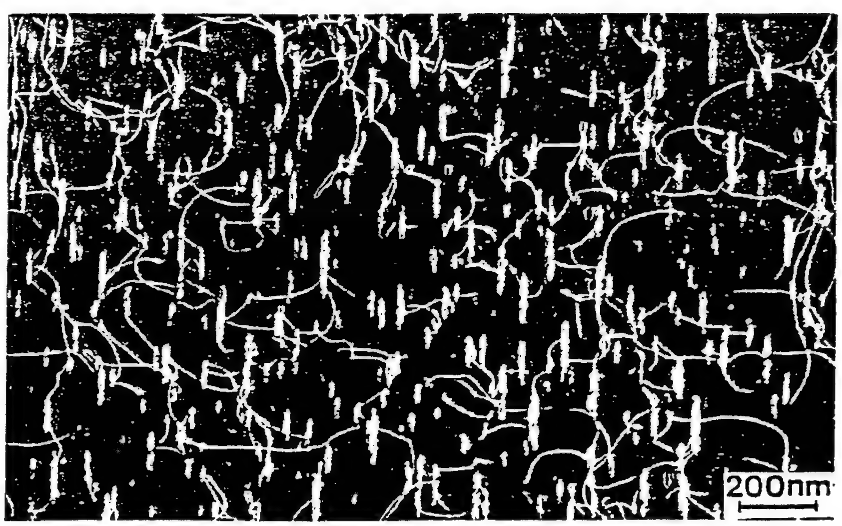

Figure 8 Dark field electron micrograph showing the bypassing dislocations in $(Ti_{0.49}Al_{0.51})_{99.5}C_{0.5}$ aged at 1073 K for $3.6\text{x}10^5$ s (100h/over aged) and deformed to 3% at 873 K. The dislocation loops surrounding needles can be seen.

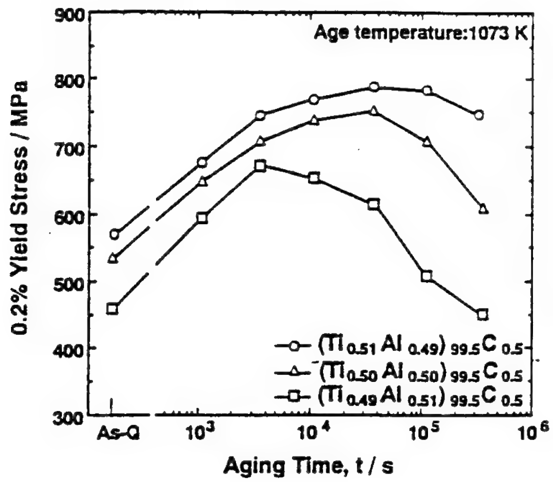

Figure 2 Effects of the deviation from the stoichiometry on the variation of compressive yield strength of $(Ti_{0.51}Al_{0.49})_{99.5}C_{0.5}$, $(Ti_{0.50}Al_{0.50})_{99.5}C_{0.5}$ and $(Ti_{0.49}Al_{0.51})_{99.5}C_{0.5}$ during aging at 1073 K.

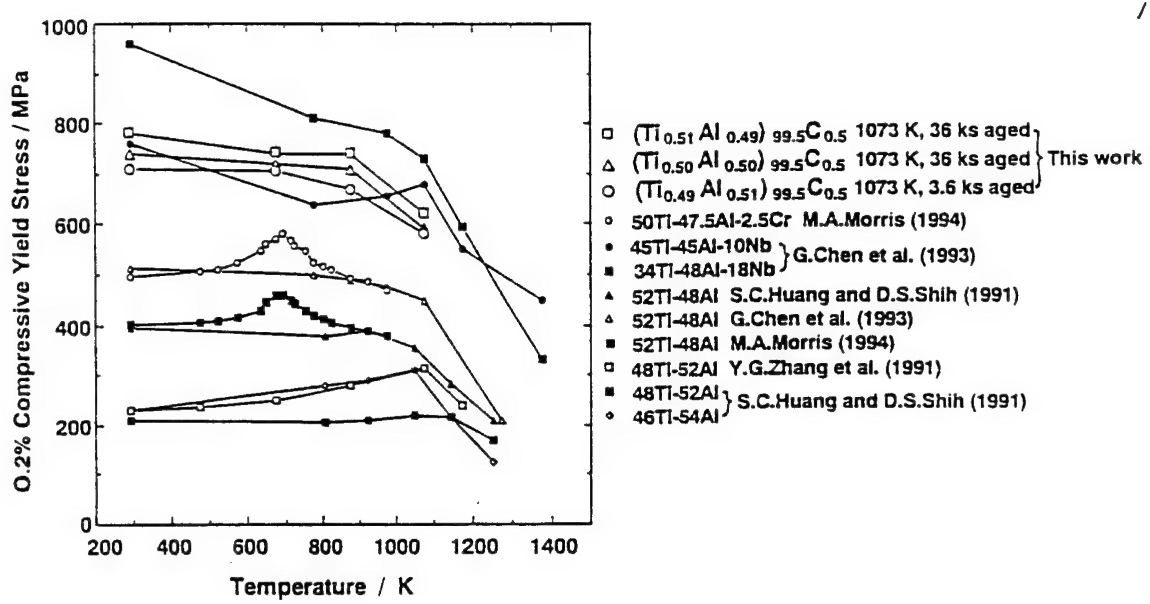

Figure 3 Temperature dependence of compressive yield strength of $(Ti_{0.51}Al_{0.49})_{99.5}C_{0.5}$ and $(Ti_{0.50}Al_{0.50})_{99.5}C_{0.5}$ aged at 1073 k for 3.6×10^4 s (10 h), and $(Ti_{0.49}Al_{0.51})_{99.5}C_{0.5}$ aged at 1073 k for 3.6×10^3 s (1 h). Data for binary and ternary TiAl are also included.

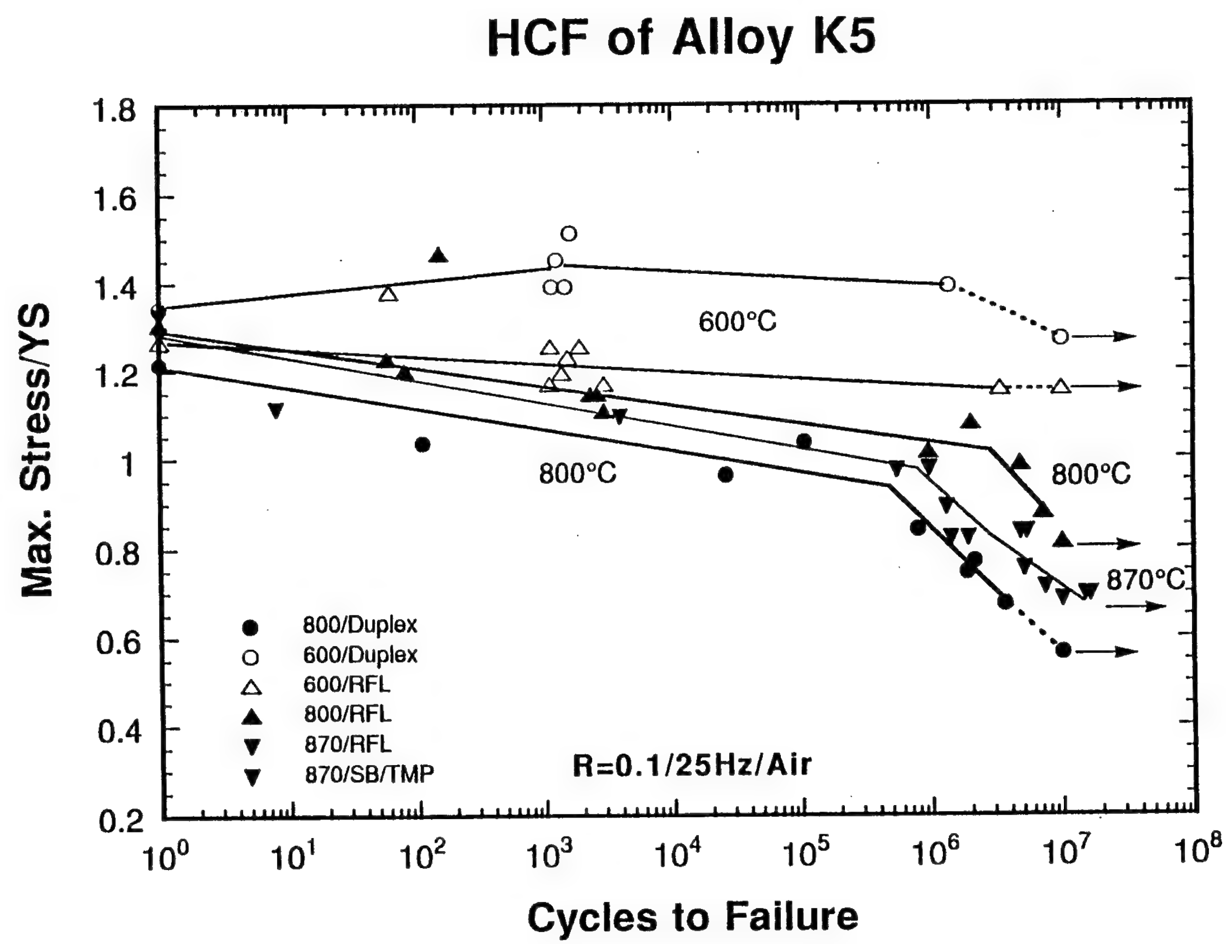
HCF of Alloy K5
Max. Stress/YS
1.8
1.6
1.4
1.2
1
0.8
0.6
0.4
0.2
10^0
10^1
10^2
10^3
10^4
10^5
10^6
10^7
10^8
Cycles to Failure
600°C
800°C
800°C
870°C
800/Duplex
600/Duplex
600/RFL
800/RFL
870/RFL
870/SB/TMP
R=0.1/25Hz/Air

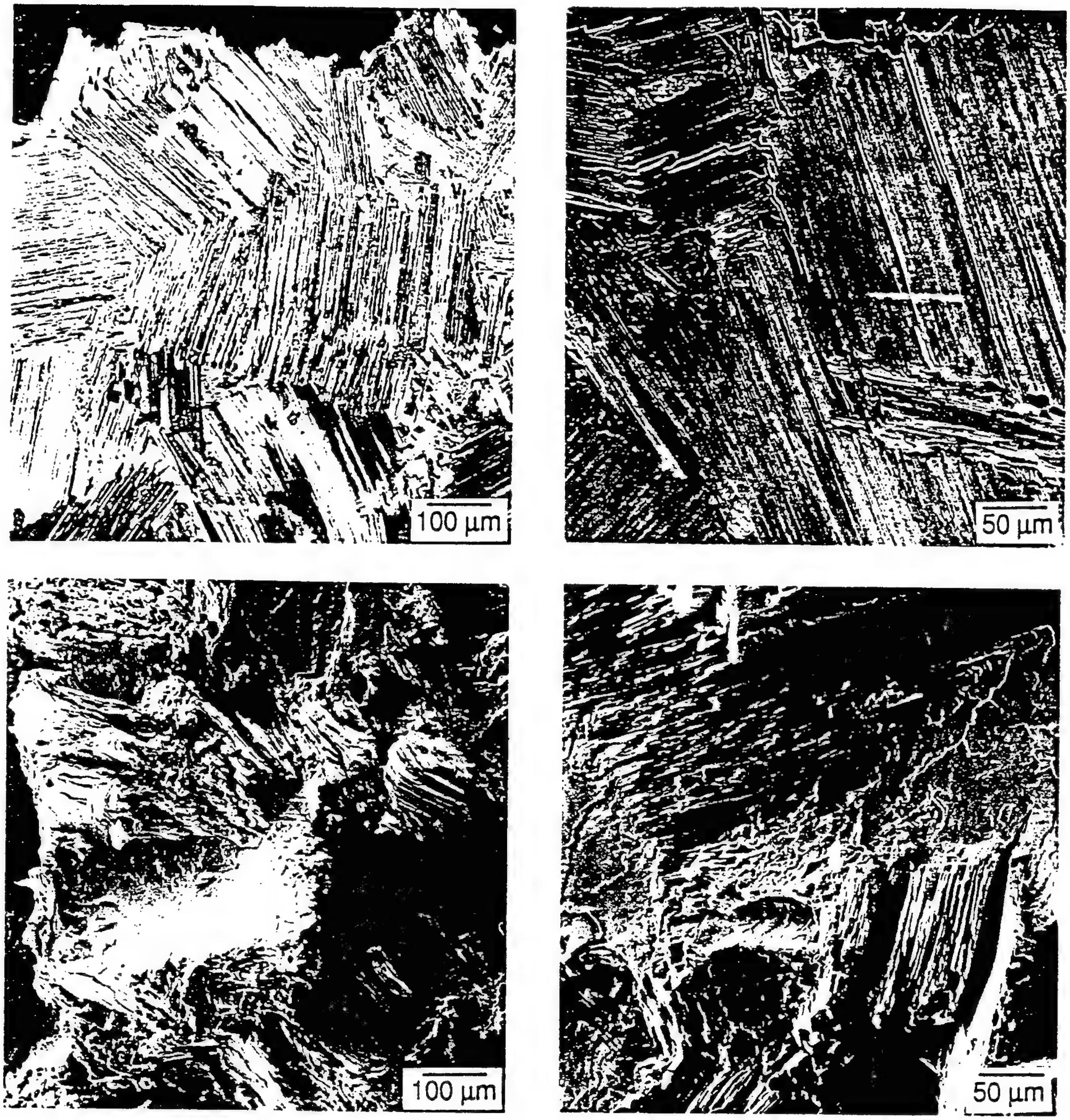

$\sigma_m = 430$ MPa ; $C_f = 2{,}310$ $\sigma_m = 330$ MPa ; $Cf = 7.2 \times 10^6$

Fatigue Deformation and Fracture of FL Alloy K5 at 800°C and R=0.1 in Air (UTS = 500 MPa)

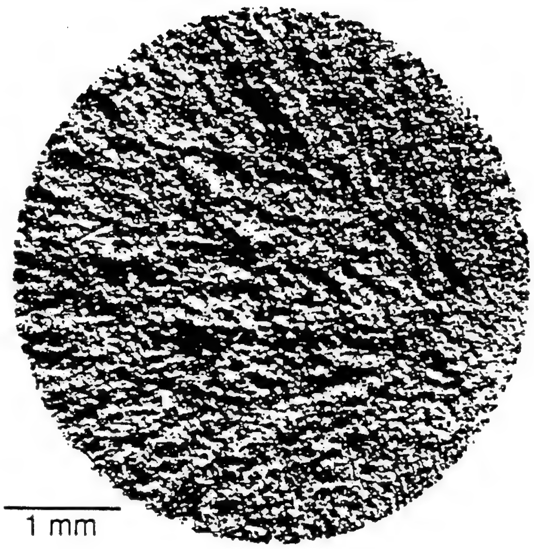

σ_m/UTS=430/505 MPa ; C_f=10,700

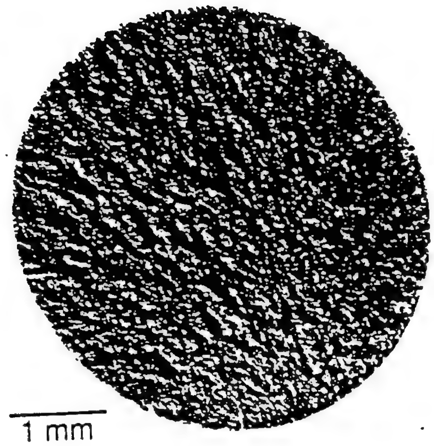

σ_m/UTS=280/505 MPa ; C_f =3.6x10^6

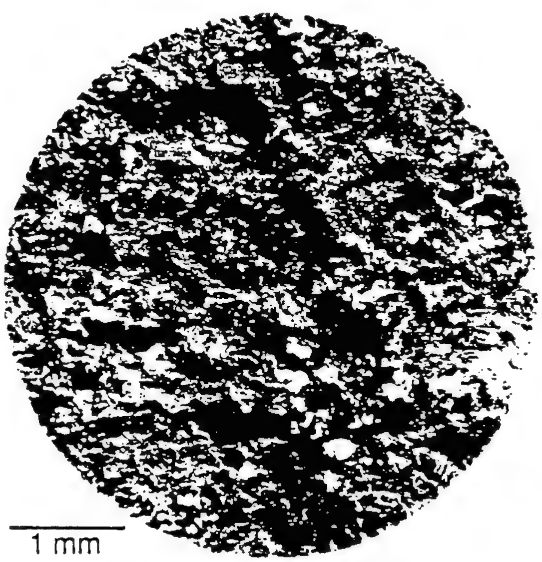

σ_m/UTS=430/500 MPa ; C_f =2,310

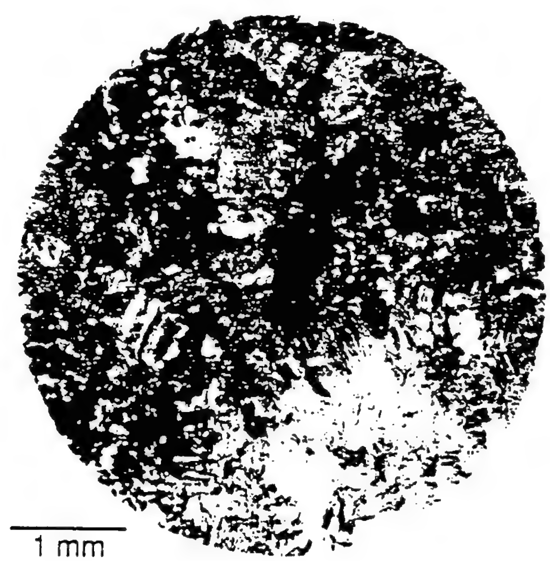

σ_m/UTS=330/500 MPa ; C_f =7.2x10^6

Fatigue Fracture of Alloy K5 in Various Conditions
at 800°C and R = 0.1 in Air

Load-Controlled Fatigue Failure of FL Alloy K5

(R=0.1 / 870°C / Air)

3

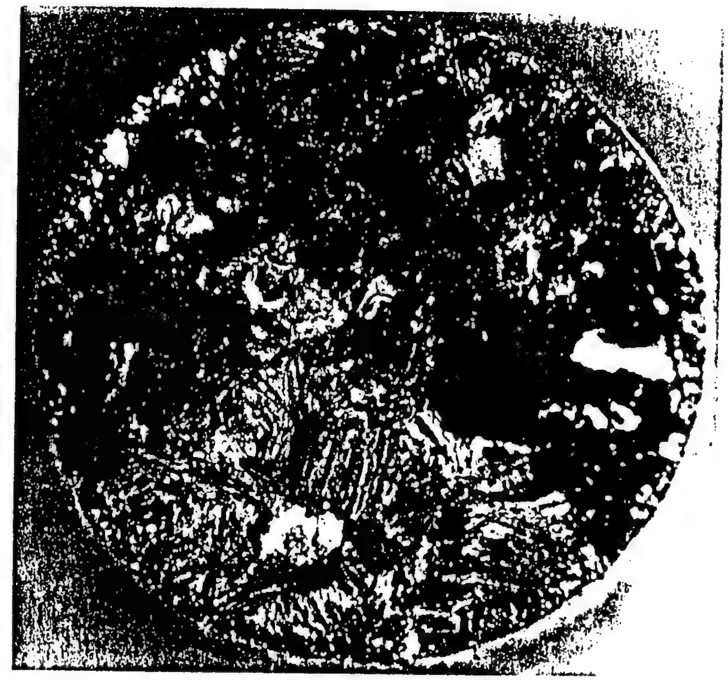

σ_{max}=350 MPa / N_f=9.6×10^5

σ_{max}=250 MPa / N_f=1.63×10^7

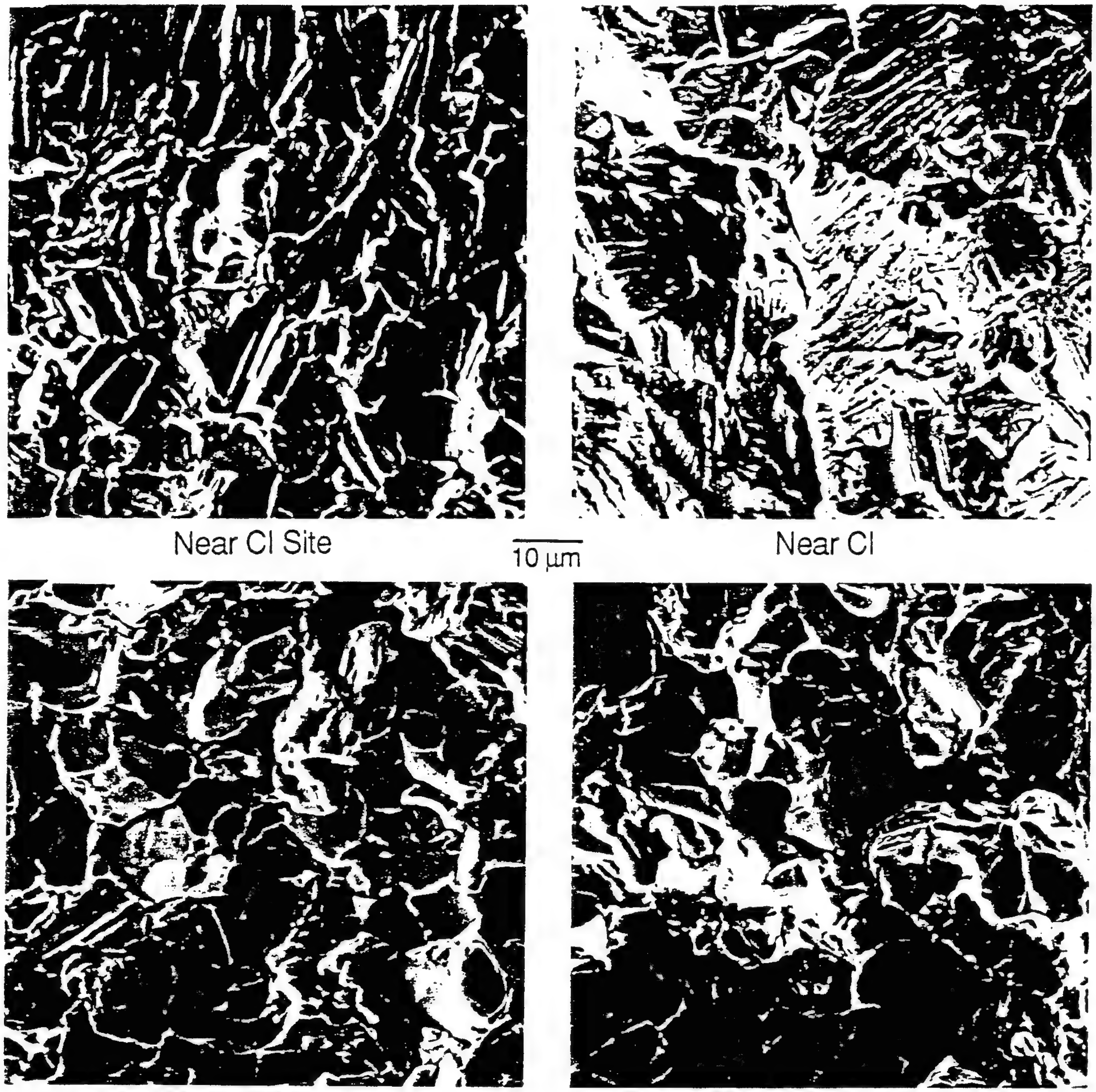

$\sigma_m = 625$ MPa / $c_f = 1629$ $\sigma_m = 575$ MPa / $c_f = 1.36 \times 10^6$

Fatigue Fracture of a Duplex Alloy K5 at 600°C in Air

(R = 0.1; UTS = 583 MPa)

Specimen Geometry Effect at <BDTT

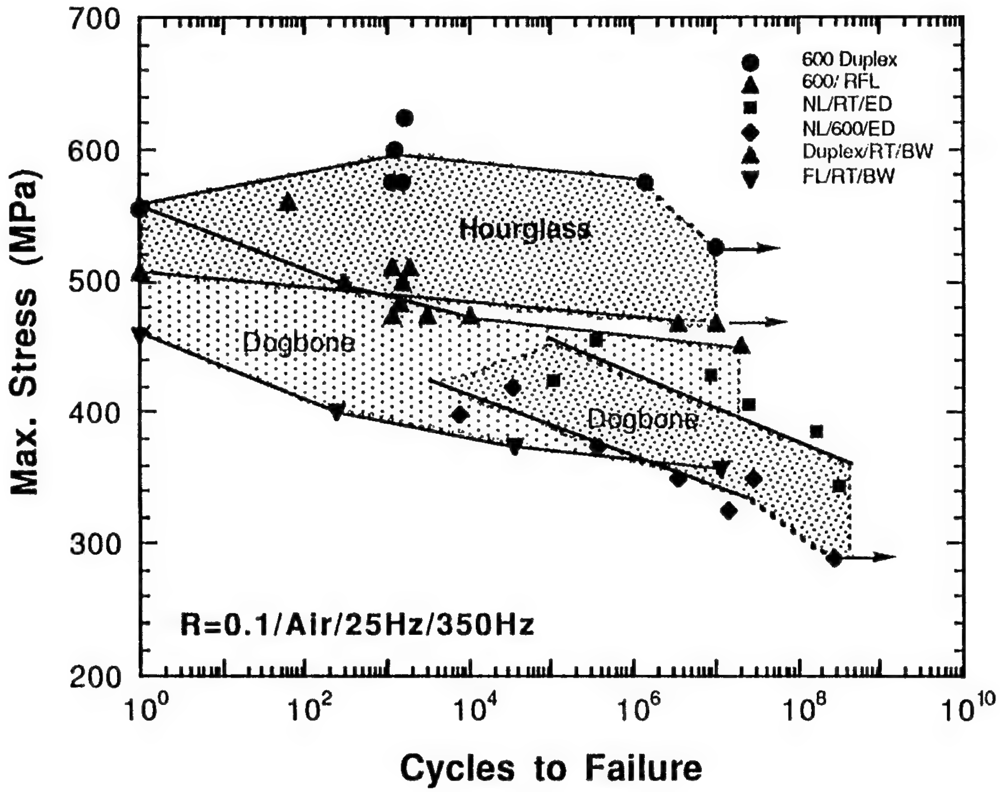

(Hourglass)

(Dogbone)

HCF of Alloy K5 in Duplex at 800°C

(Effect of Frequency and Fatiguing Time)

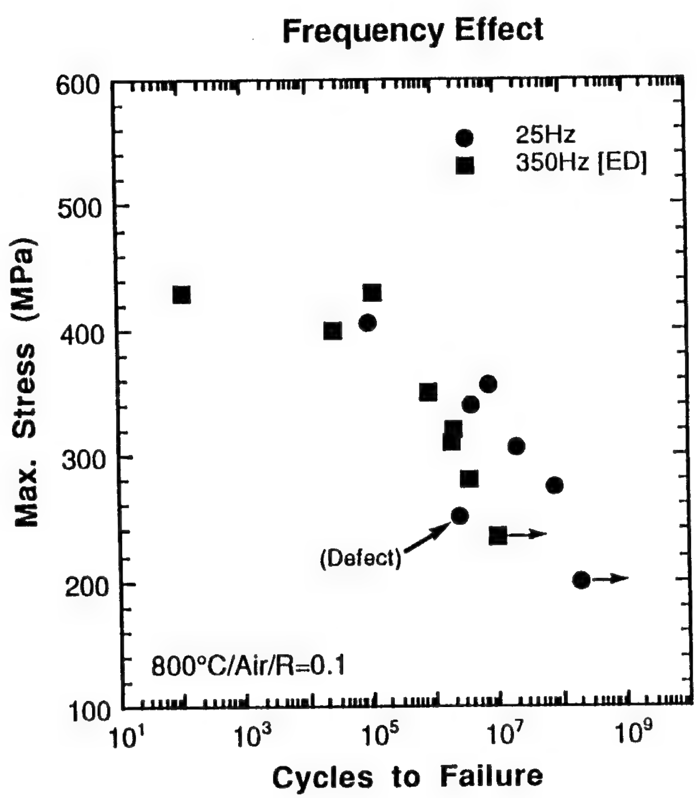

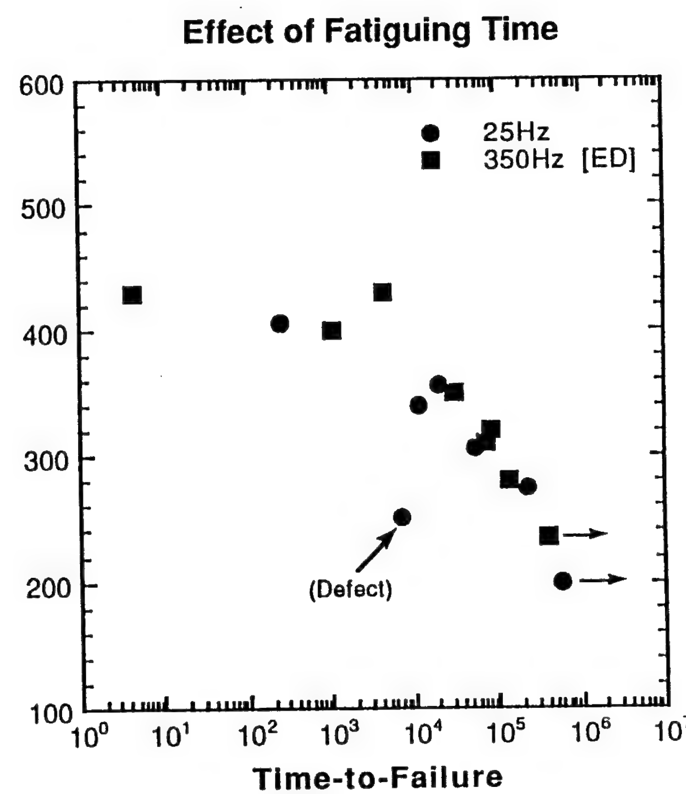

Effect of Frequency on HCF
(at 800°C)

High Stress Regime ($\sigma_{max} > \sigma_y$)

Frequency-dependent (need investigation)
High-rate deformation

Low Stress Regime ($\sigma_{max} > \sigma_y$)

Frequency-independent
Time-dependent
Creep deformation important

Creep Fatigue

Suggested at Low Stresses
Mean Stress: $\sigma_{avg} = (\sigma_{max} + \sigma_{min})/2$

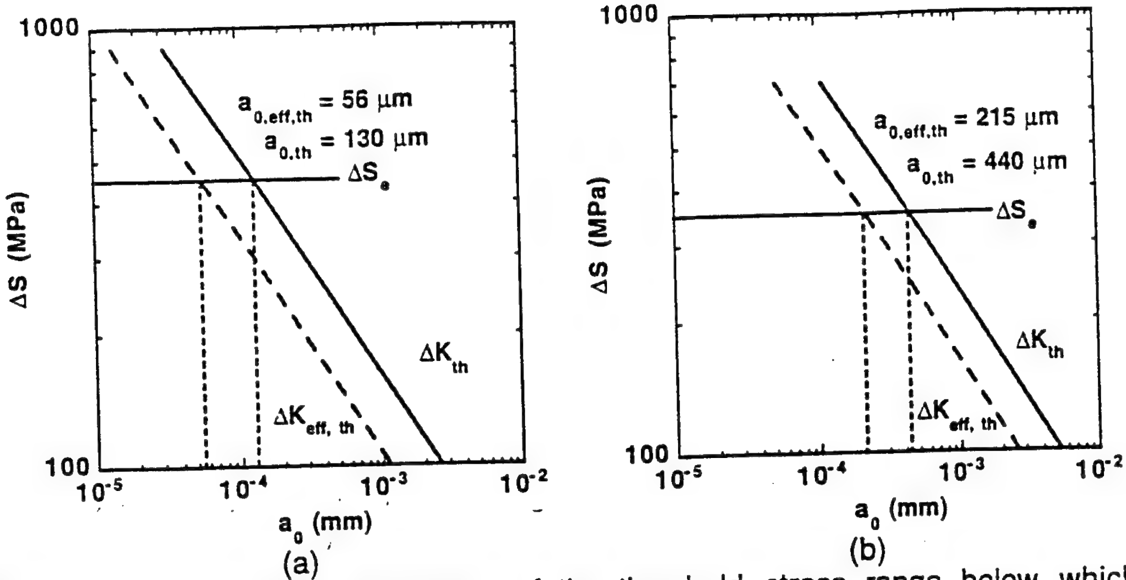

Figure 10. Crack-size dependence of the threshold stress range below which specimen failure will not occur in the alloy K5 in the (a) duplex and (b) lamellar conditions.

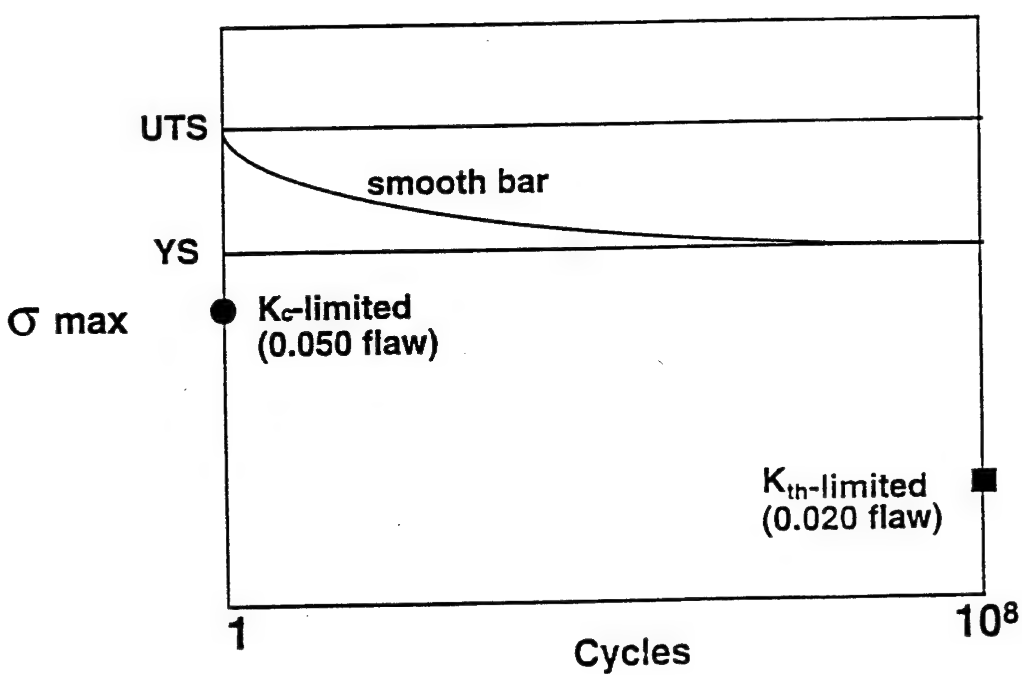

FCG of Alloy K5

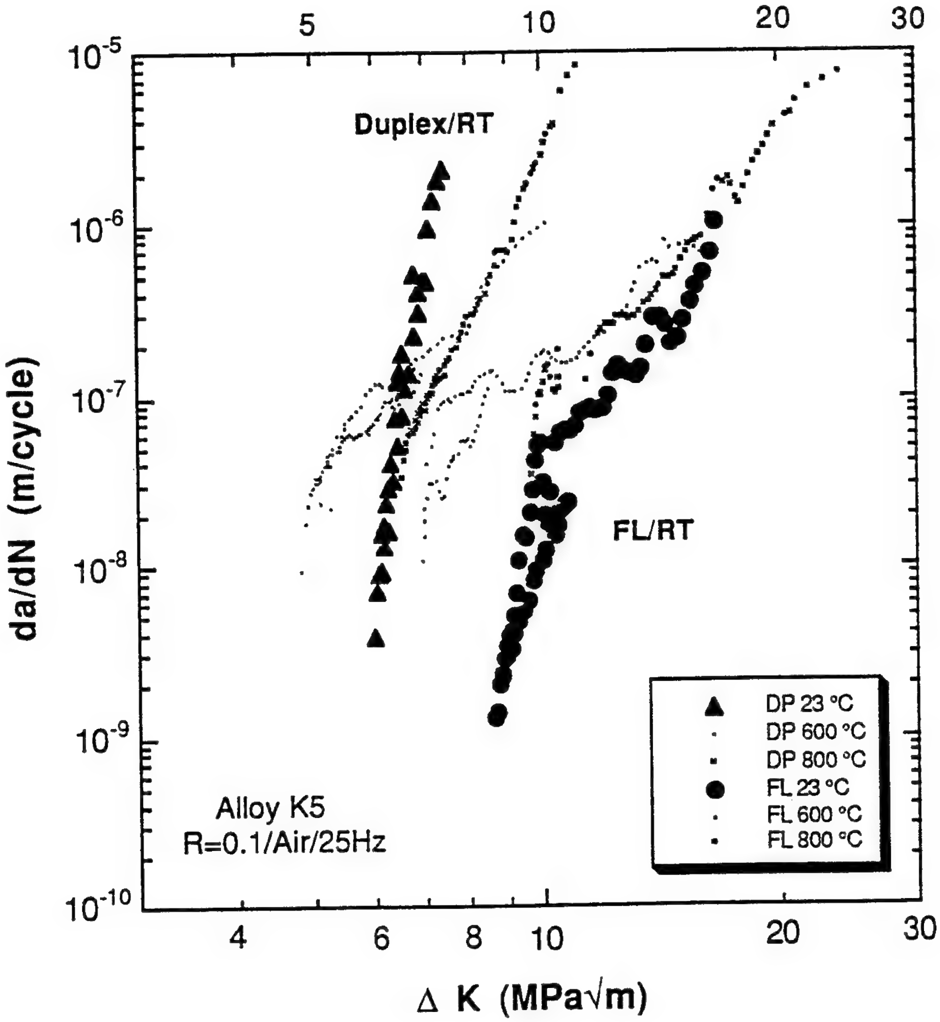

Fatigue Deformation and Failure

- Fatigue behavior in gamma alloys consists of:

  Deformation period (remarkably long),
  Crack initiation and growth (to a critical size)
  Rapid crack propagation (to failure)

- Below BDTT, flat SN curves are observed. The fatigue strength is controlled by tensile properties.

  Duplex microstructure (preferred)

  Above BDTT, fatigue life depends on tensile deformation behavior under high applied stress (>YS). Under low stresses (<YS), fatigue strength appears related to creep resistance.

  Fully-lamellar microstructure (preferred)

- Fracture takes place transgranularly below BDTT and boundary fracture becomes predominant at higher temperatures.

Fatigue Behavior

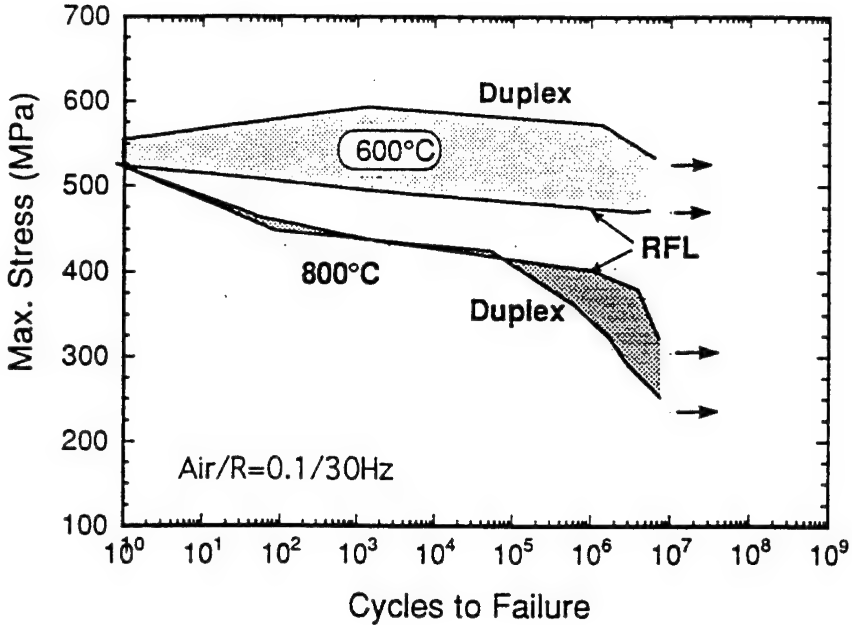

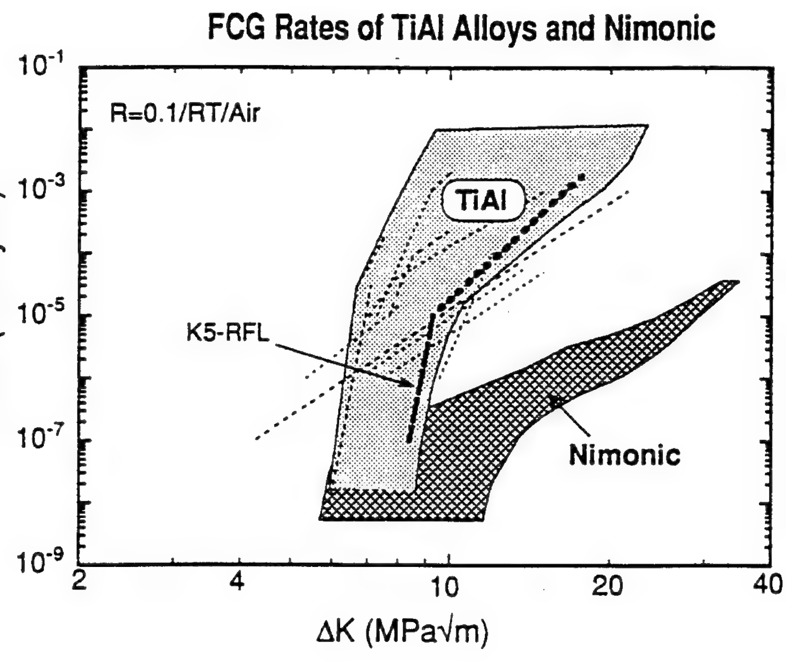

Alloy K5 vs. Disk Superalloys

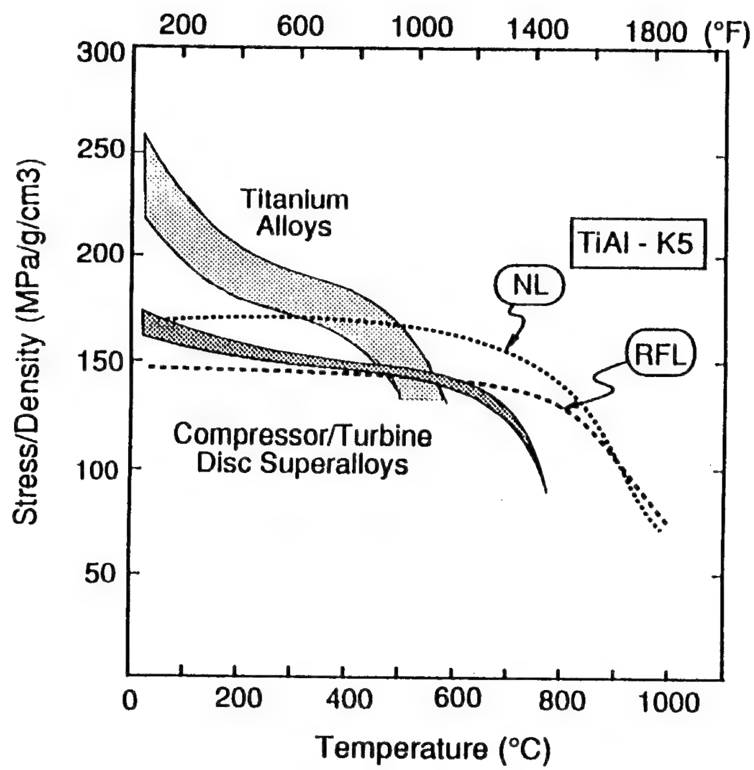

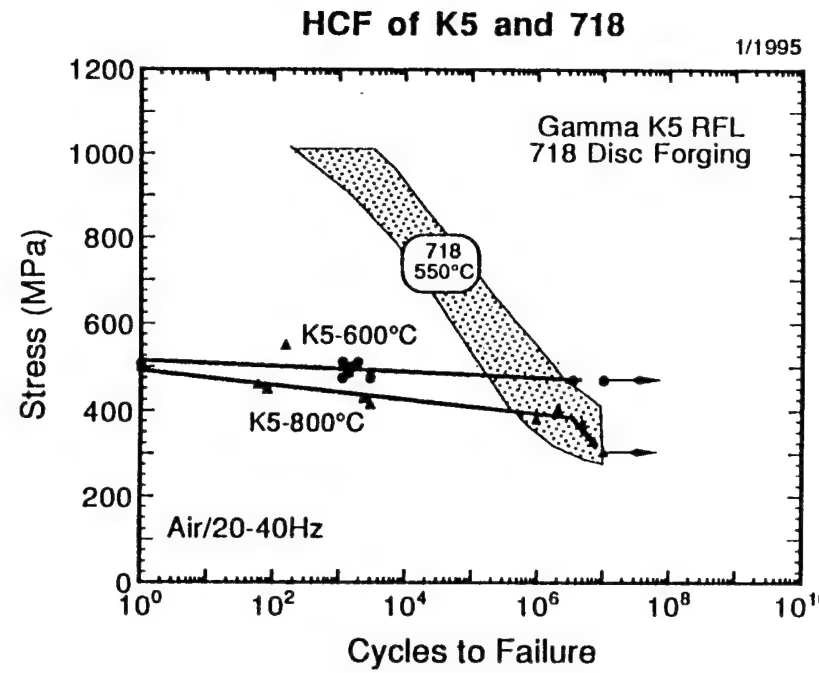

Alloy Design

Alloy Selection

Microstructural Optimization

Considerations

- Mechanical Data and Behavior
- Damage-Tolerance & Life-Prediction
- Microstructural Controllability

Derive Optimum Microstructures

Devise Process & Treatment Schemes

Chemistry Modification

Promote Desired Microstructures

Improve Mechanical Behavior

Enhance Environmental Resistance

Design of Microstructures

Property Requirements

Dimensional Considerations

Component-Specific Microstructures

Scaled-up Process Development

Designed Microstructures

Refined FL (RFL)

Alloy Modification
Innovative Heat Treatments

TMT Lamellar (TMTL)

Boron Addition
Heat Treatments

TMP Lamellar (TMPL)

Extrusion
Forging
Aging

****Aligned Lamellar****

Directionally Solidified (DS)
Directionally Worked : DELM; DFLM

Other Types: Under Exploration

Chemistry Modification

(Standard: NG, DP, NL and FL)

Optimized
Microstructural Features
(Wrought Alloys)

Lamellar Structure Base

Grain Size: 50-400 μm

GB Morphology

Slip Transmission
Bond Strength

Lamellar Spacing < 2μm

Strength; Strain-to-Failure
Toughness; Creep

α_2 Volume Fraction: 5-30 %

Strength; Ductility; Toughness
Anisotropy

Texture Consideration

Duplex Microstructures (?)

3

RFL vs. TMTL Microstructures

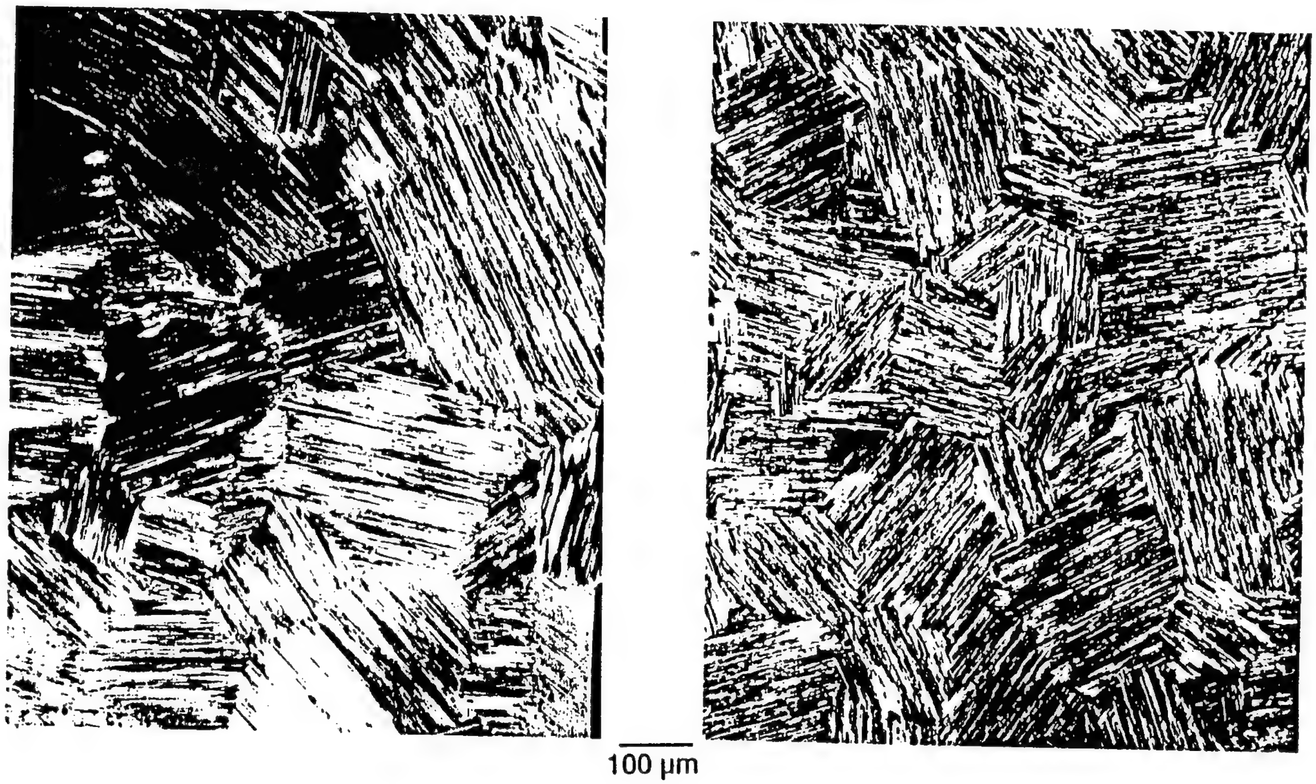

TMT Lamellar Microstructures

Wrought Processed Alloys
Boron Additions: 0.05-0.5 %
HW plus Alpha Treatment
Advantages/Disadvantages

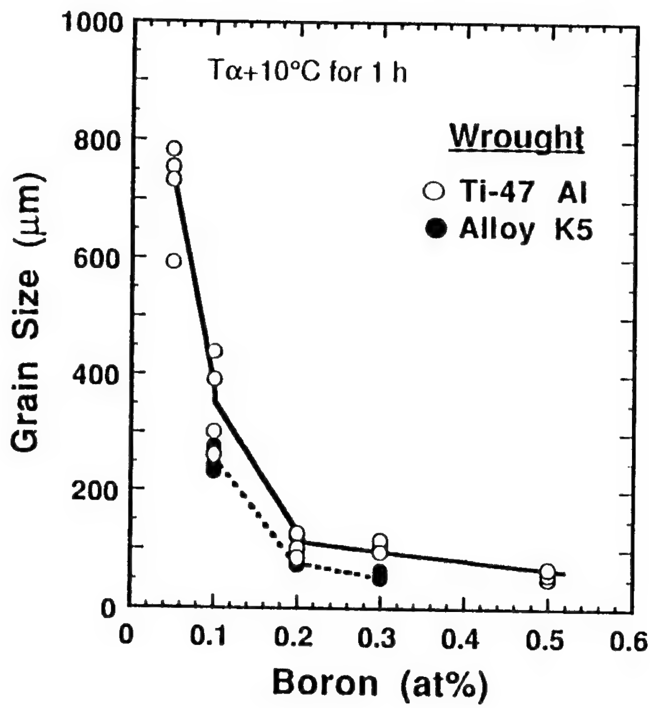

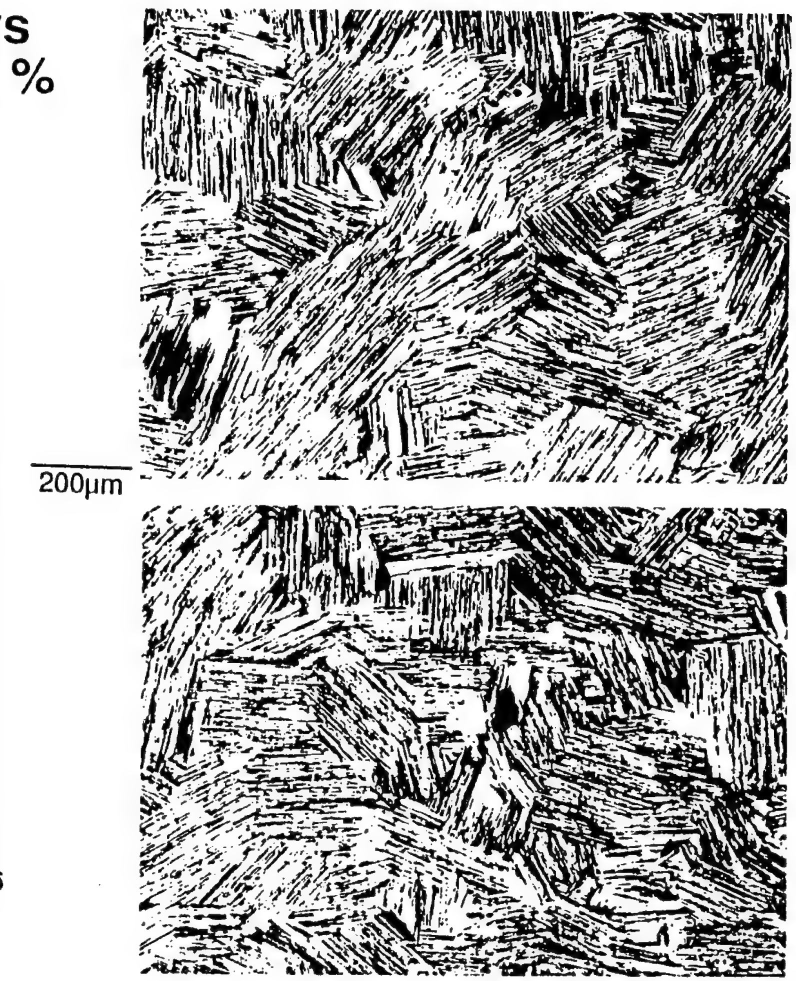

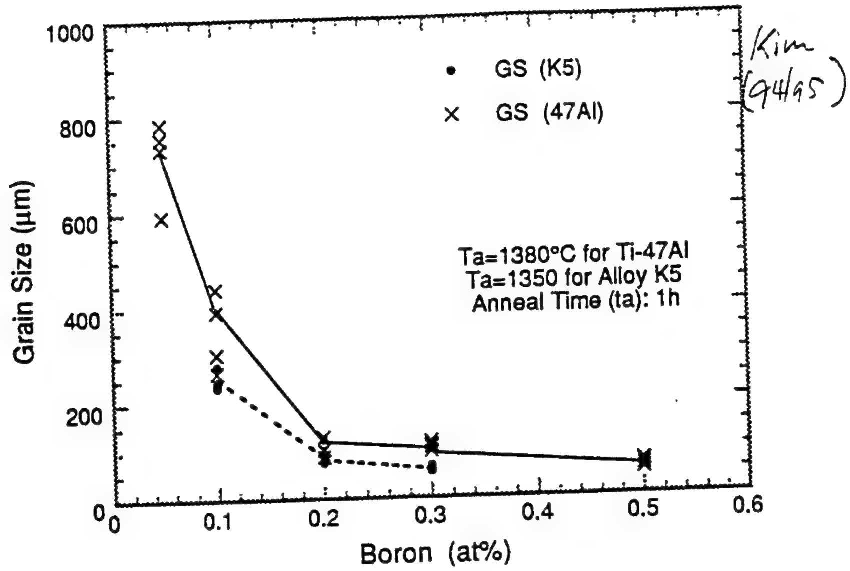

GS vs Boron Content in Gamma Alloys

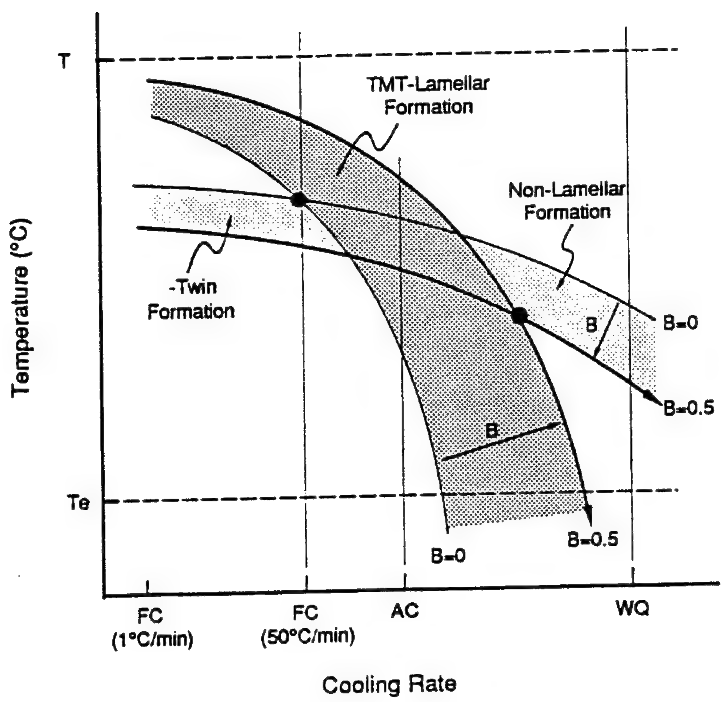

Cooling-Rate and Boron -Content on Alpha Decomposition

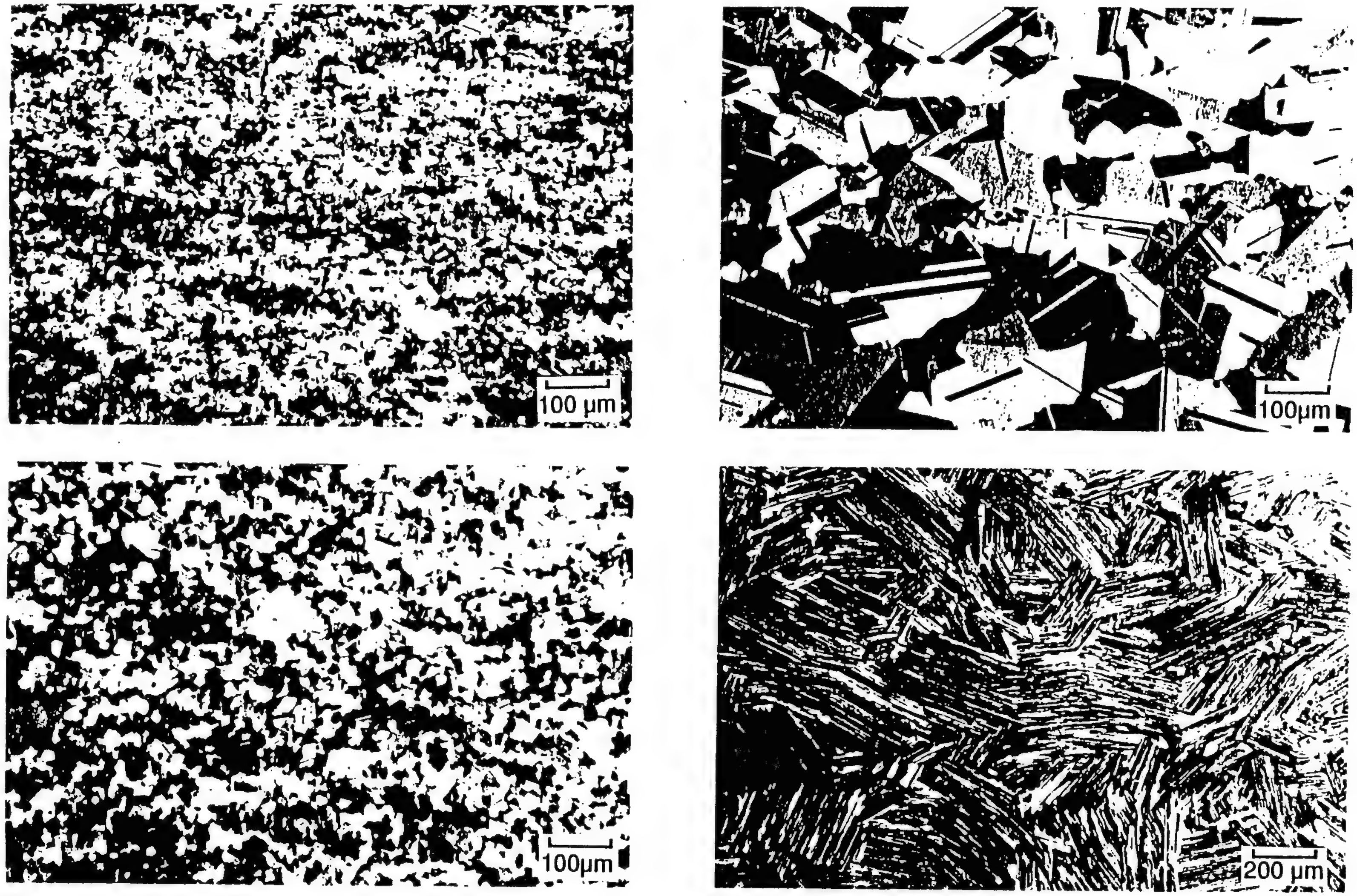

Alloy K1: **As-Forged; Near Gamma; Duplex; and TMTL microstructures**

Ti-47Al-0.05B

Ti-47Al-0.10B

Ti-47Al-0.24B

Forged and **TMT-Lamellar Treated** (1370°C/1h/FC/1000°C/AC)

100 μm

FC/900°C/AC

FC/1300°C/AC

AC

Alloy K7: **Alpha-Treated** (1390°C/30min) **and Cooled Differently**

FC/1200°C/AC

AC

Alloy K6: **Alpha-Treated** (1370°C/1h) **and Cooled Differently**

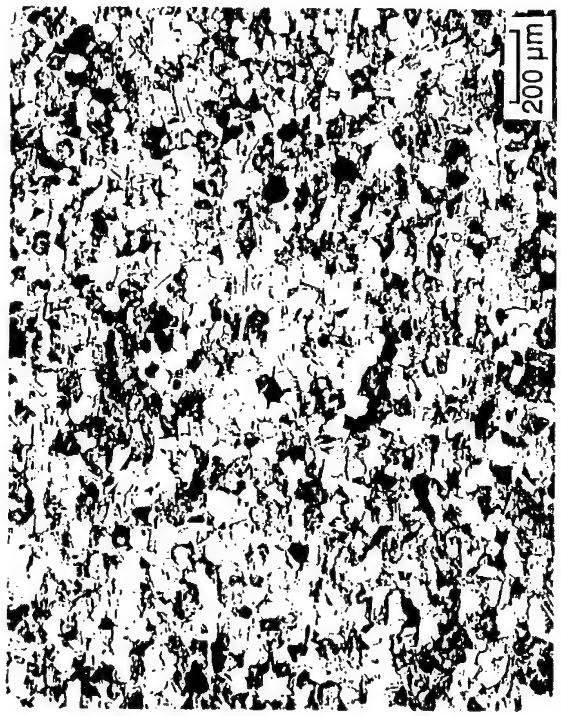

Duplex

200 μm

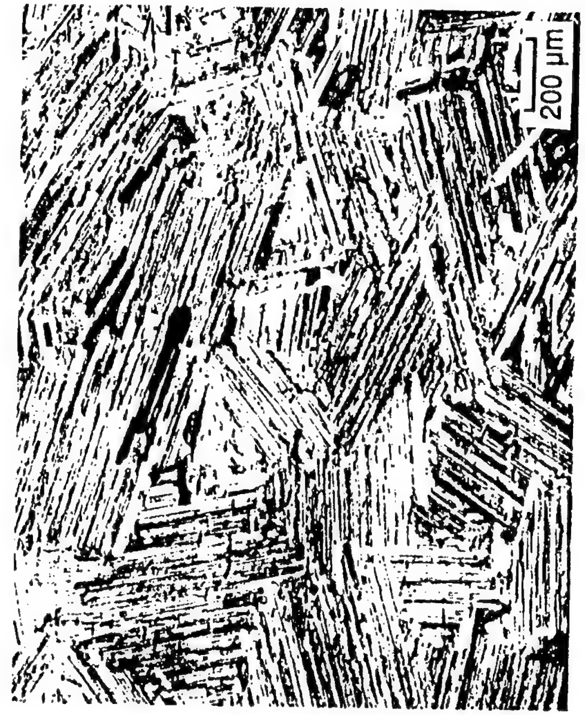

TMTL

Alloy K2 (Ti-46.8Al-2Cr-4.0Nb-0.3B): **Boride Distribution**

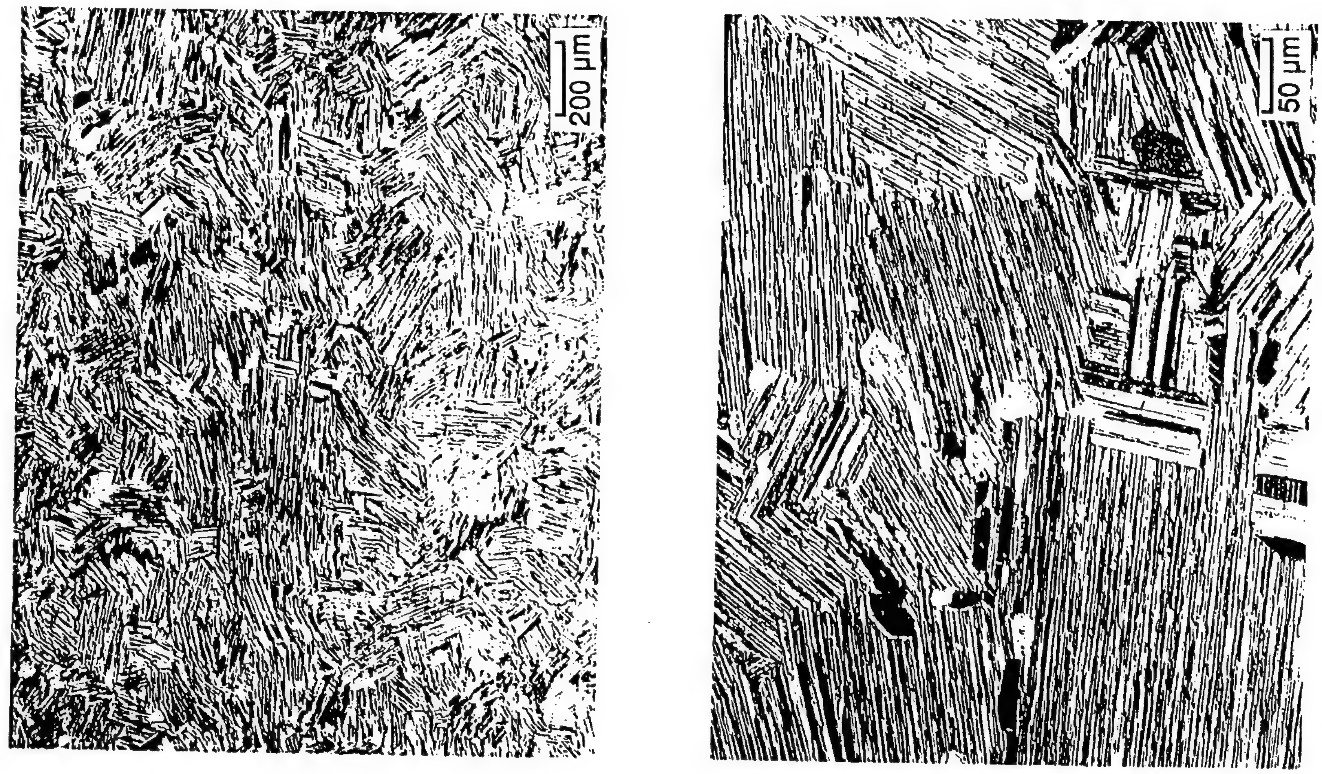

Alloy K7: **TMT-Treated** (1390°C/1.5h/AC) **and Annealed** (1300°C/24h/AC)

TMP Lamellar Microstructures

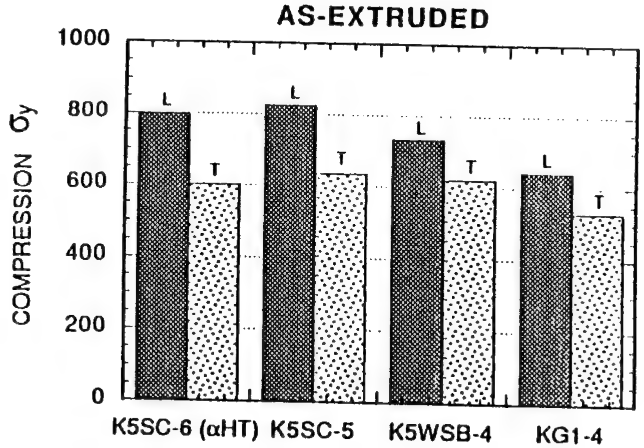

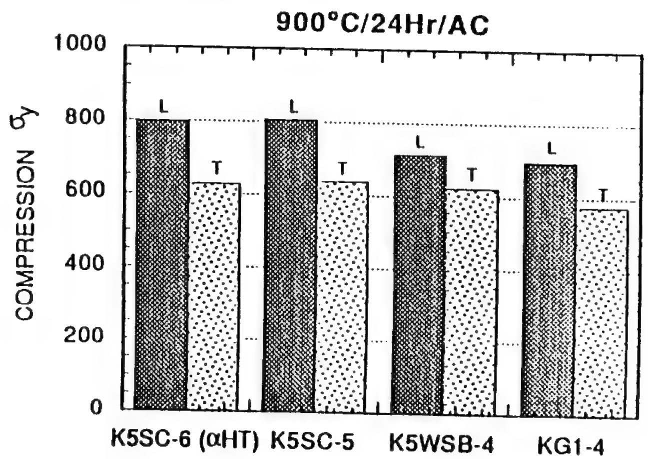

Kim (95)

L

50 μm

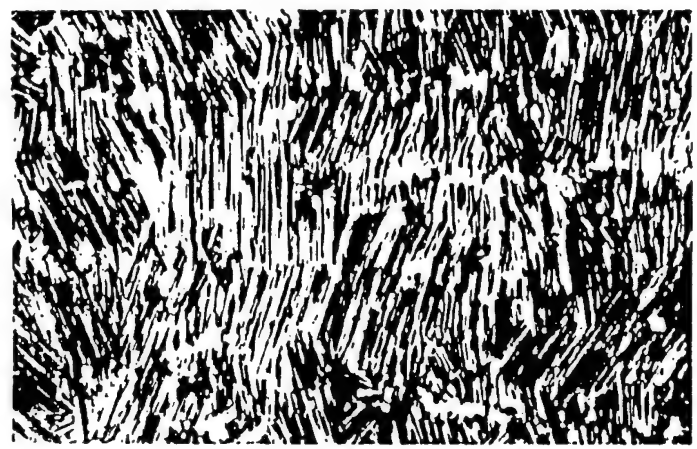

T

K5SC Alloy TMPL Extrusion LT-Section

5

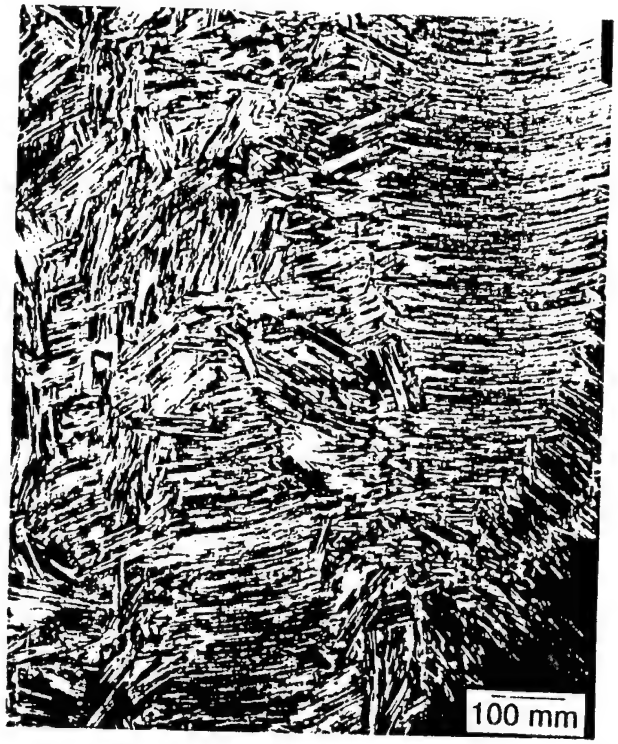

Transverse

Longitudinal

A TMP Microstructure in a 4822 Extrusion

Thermal Stability of TMP Lamellar Extrusions

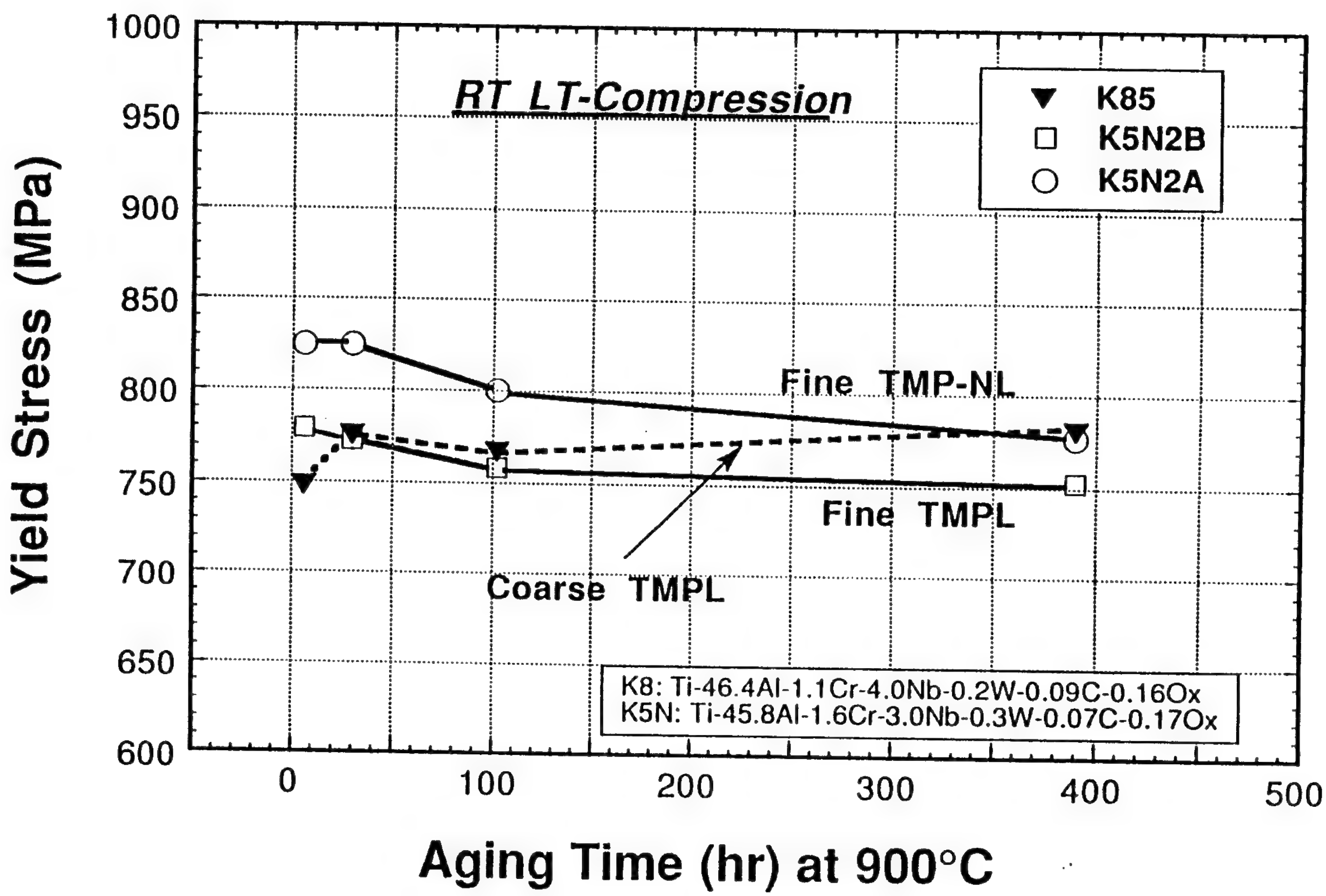

Flow Curves of Lamellar Alloys

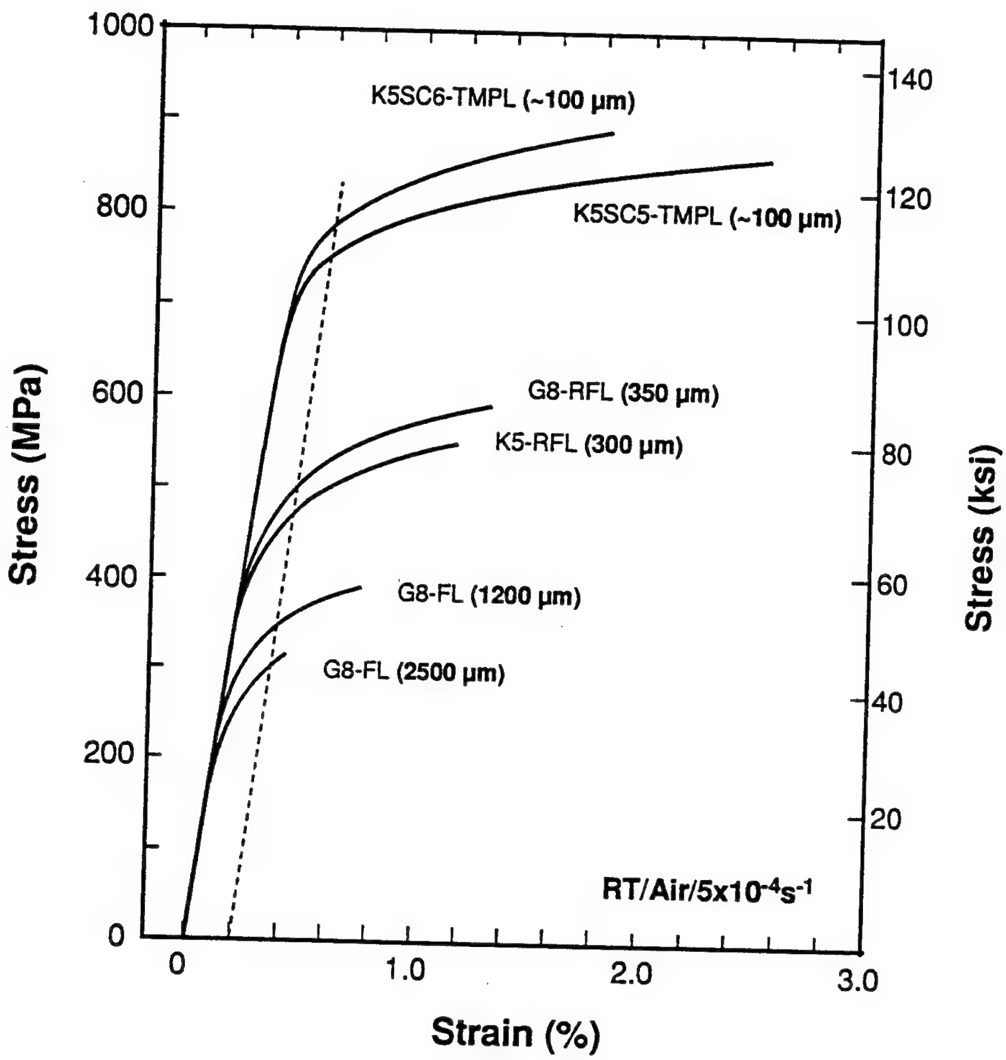

Strengths of RFL/TMPL Gamma Alloys

Kim (95)

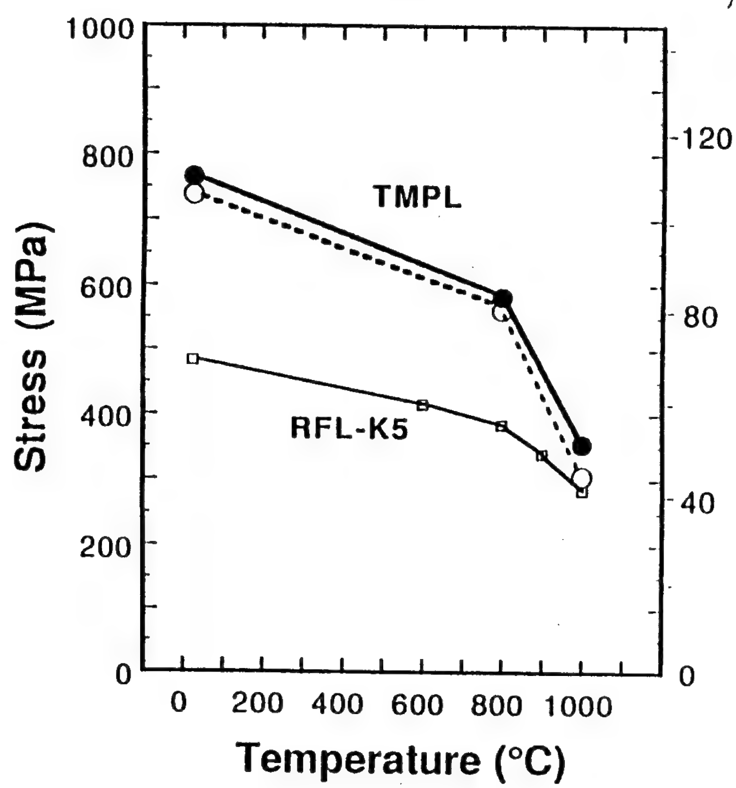

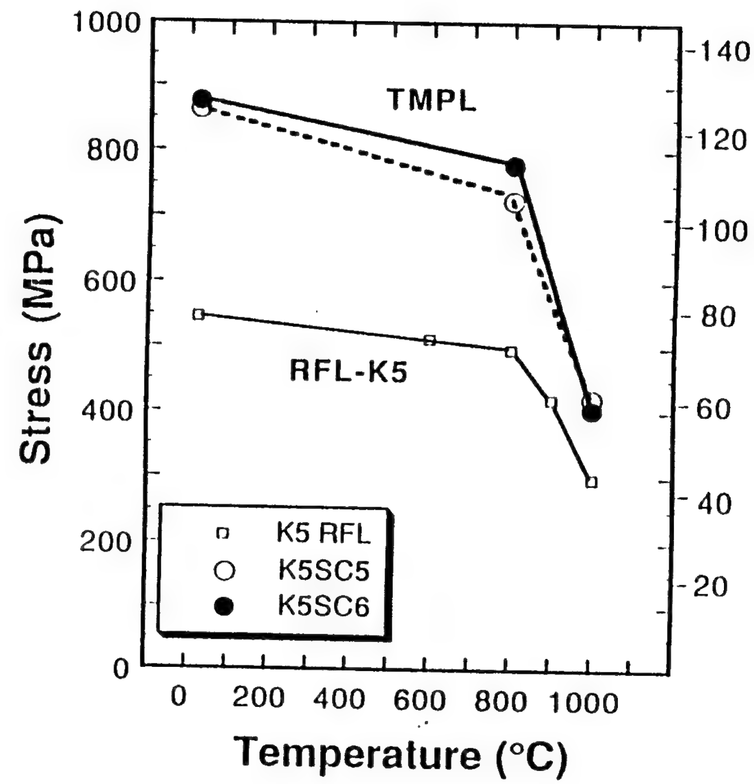

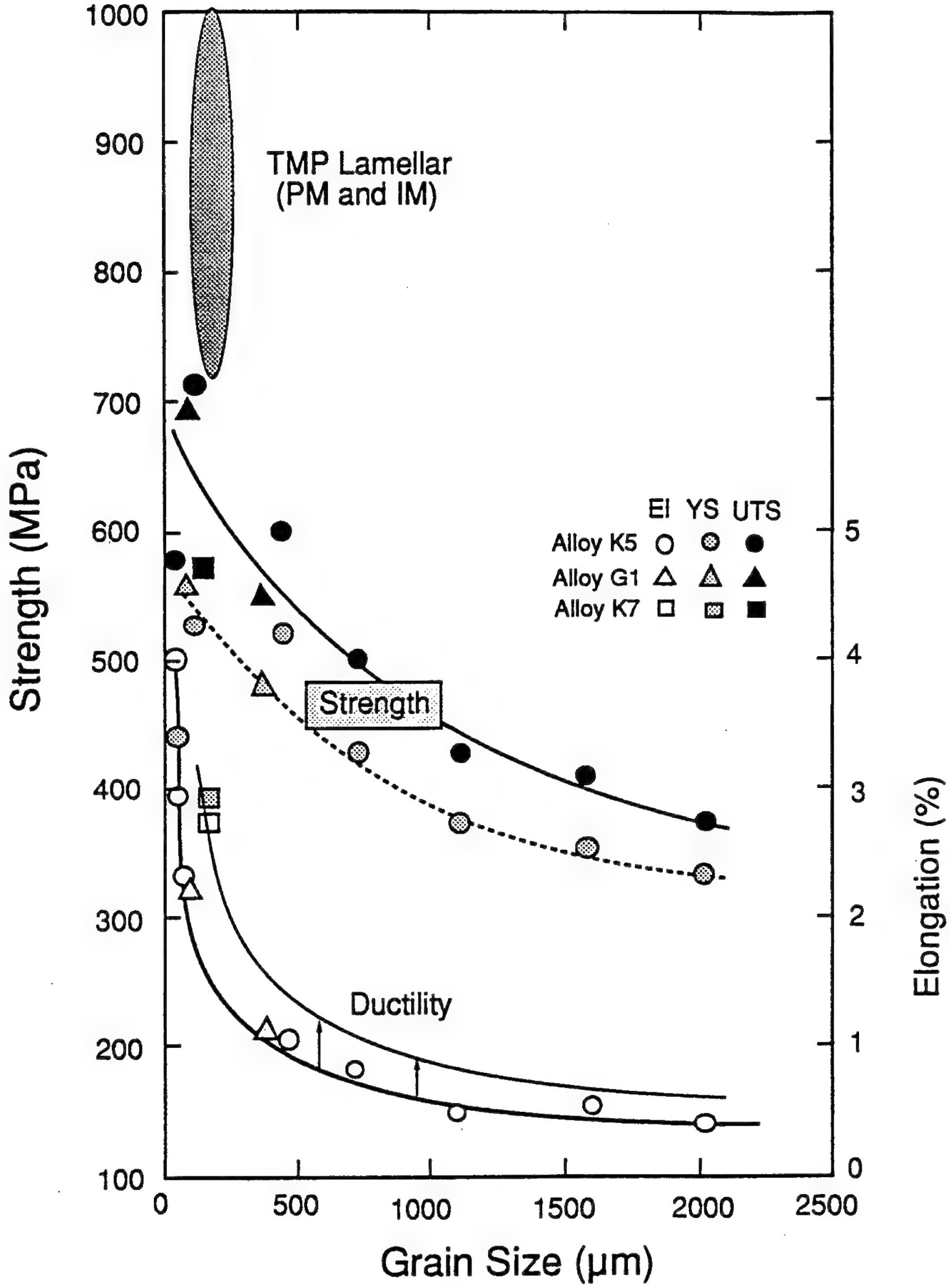

MIcrostructure on RT Tensile Properties

GS/LS/YS Relations in TiAl FL Alloys

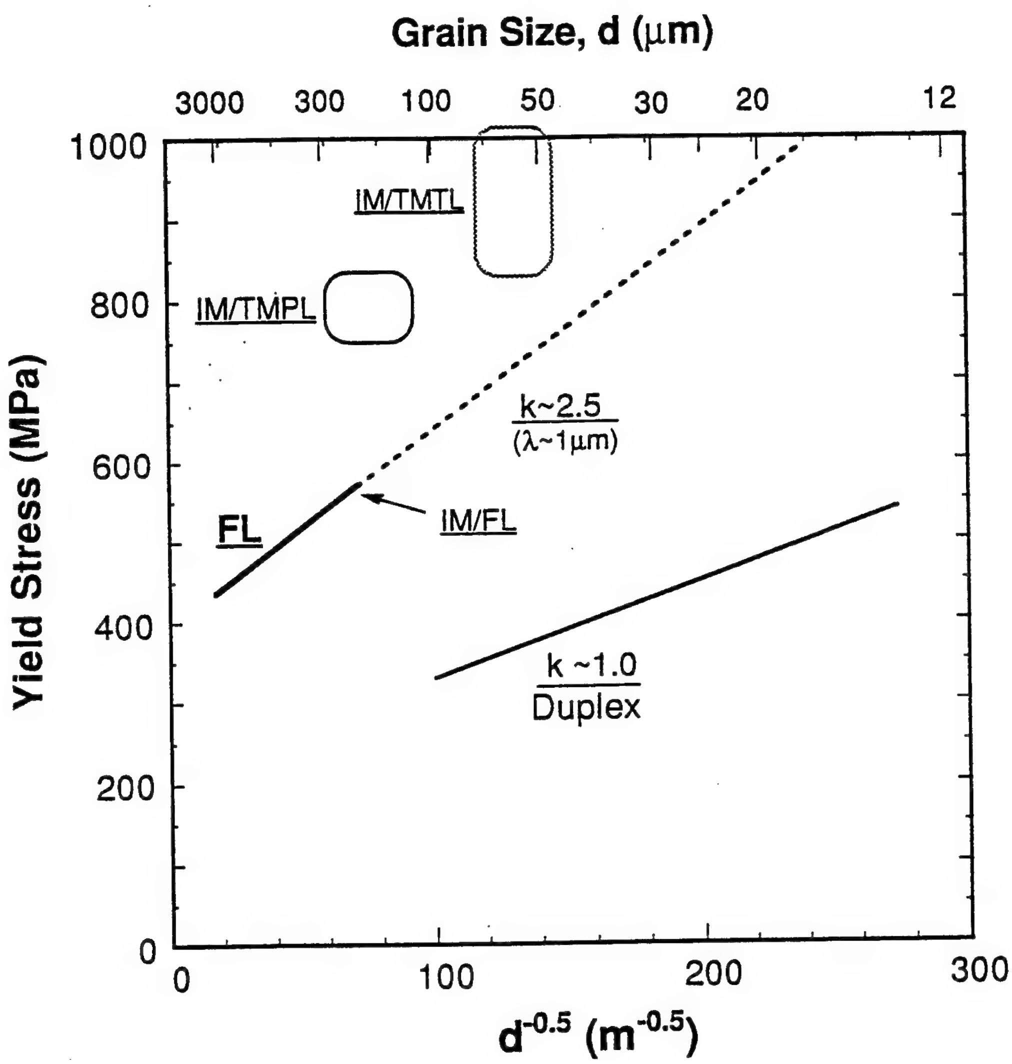

5

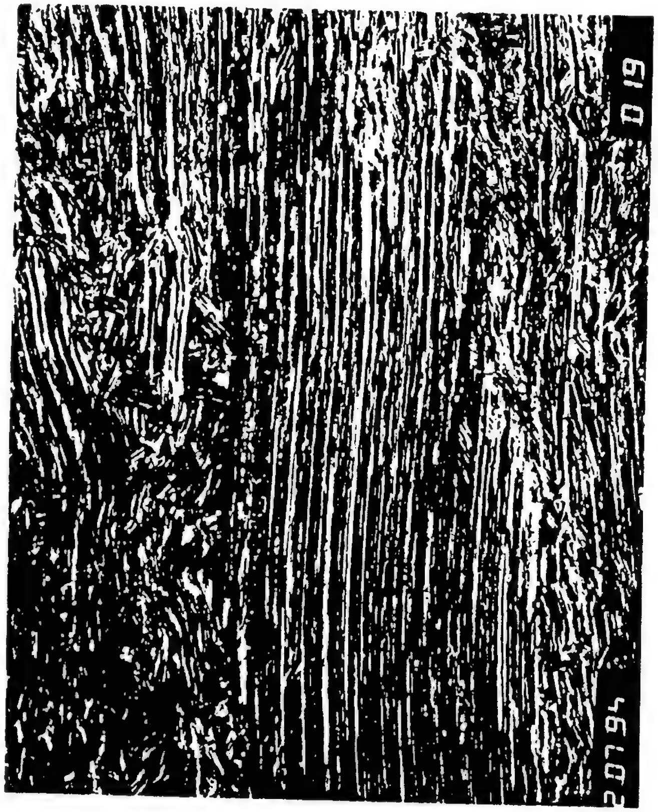

Longitudinal (L)

100 µm

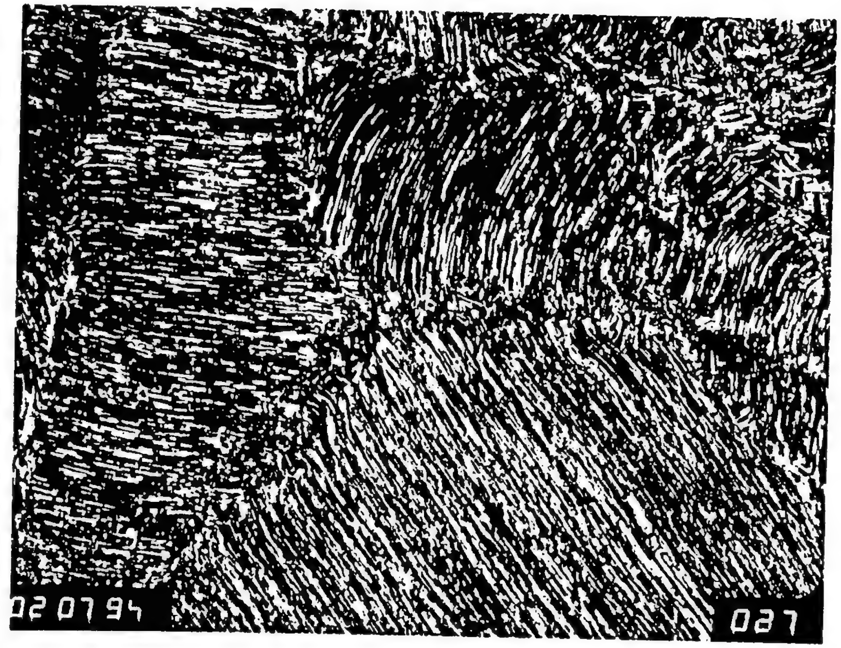

Long-Transverse (LT)

Alloy K8 TMP-Lamellar Extrusion

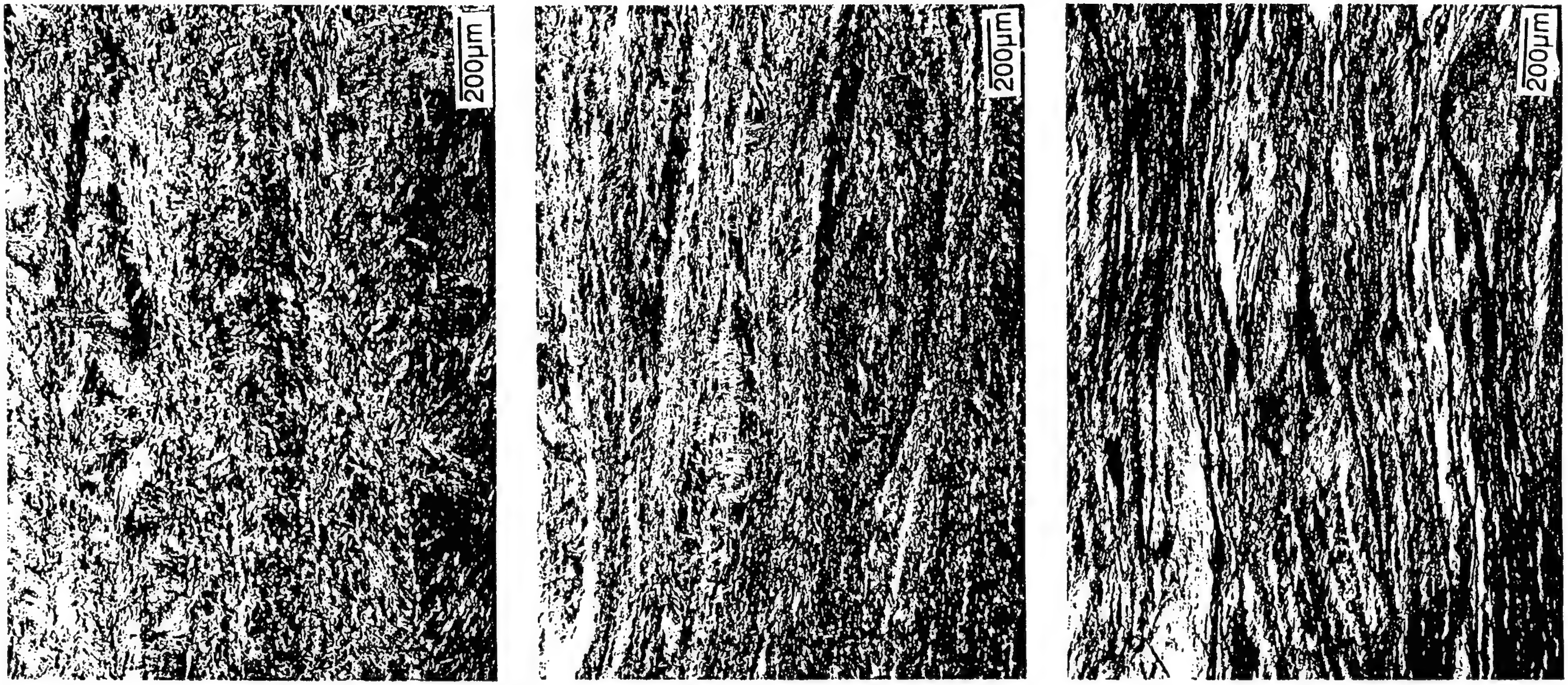

60 18 6

Alloy K5S: Effect of Ram Speed on the Alpha-Forged Microstructure

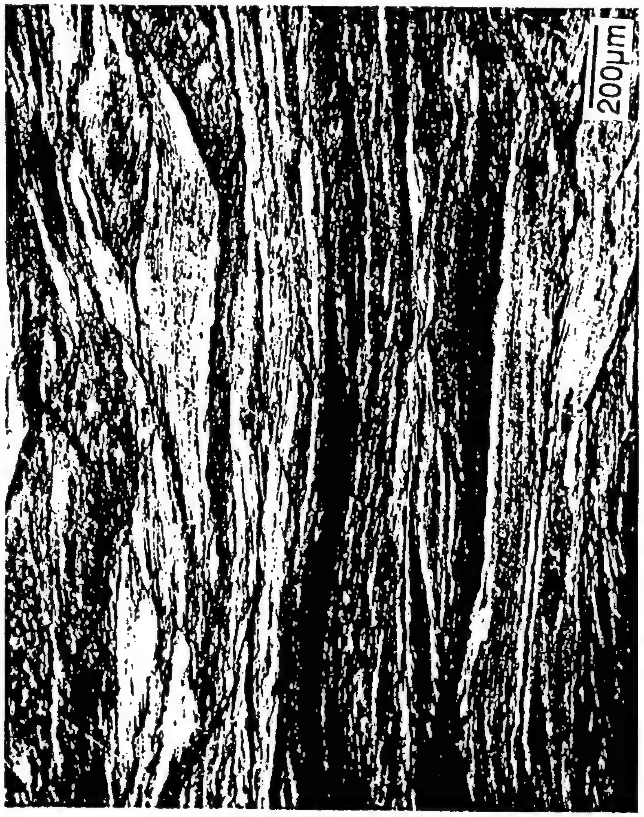

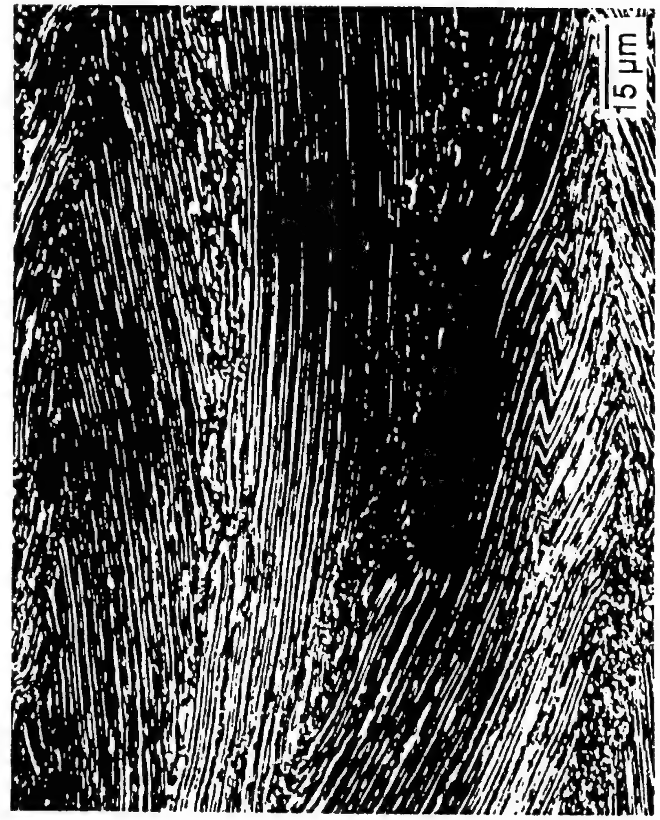

K5S (Ti-46.2Al-2Cr-3Nb-0.2W-0.2Si): **Directionally Alpha-Forged**

3

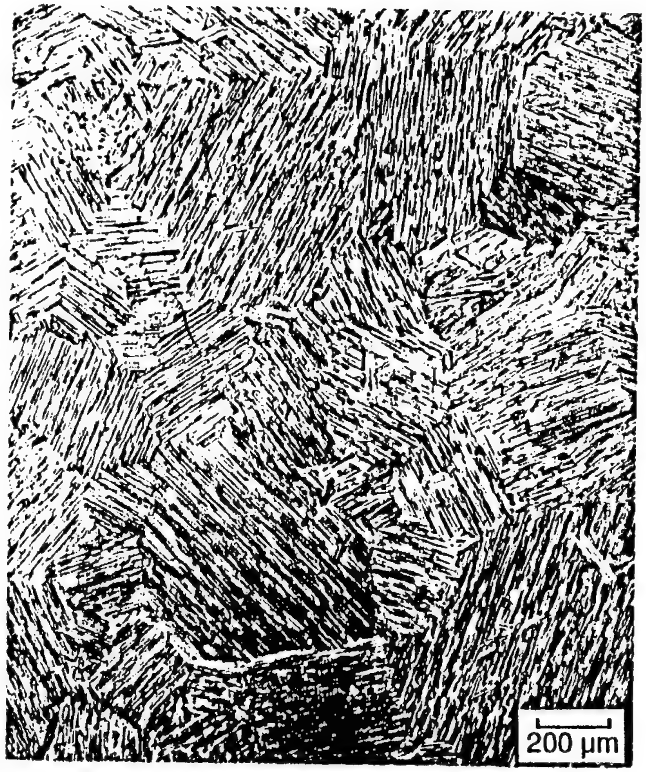

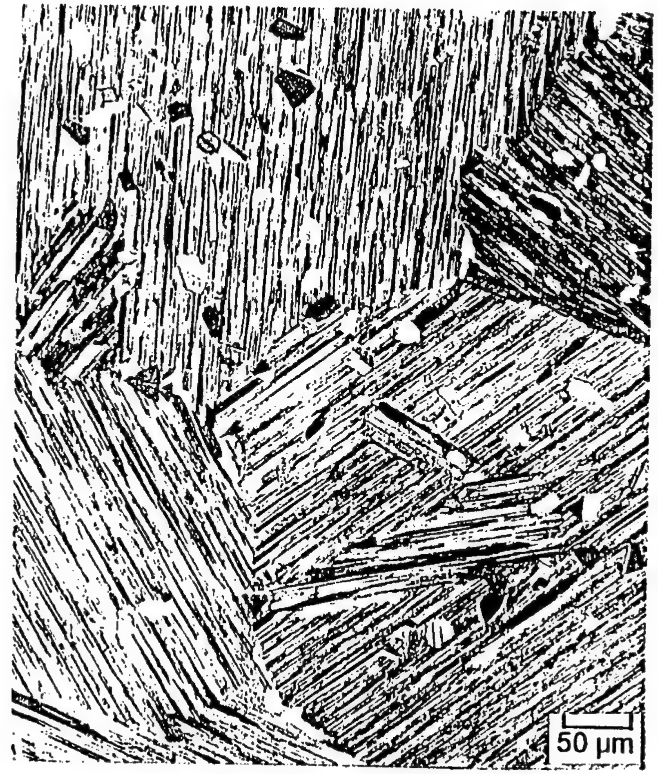

A Discrete Lamellar Structure in Alloy K5

3

250 μm

FC: YS/UTS/e_f=293MPa/310MPa/0.14%

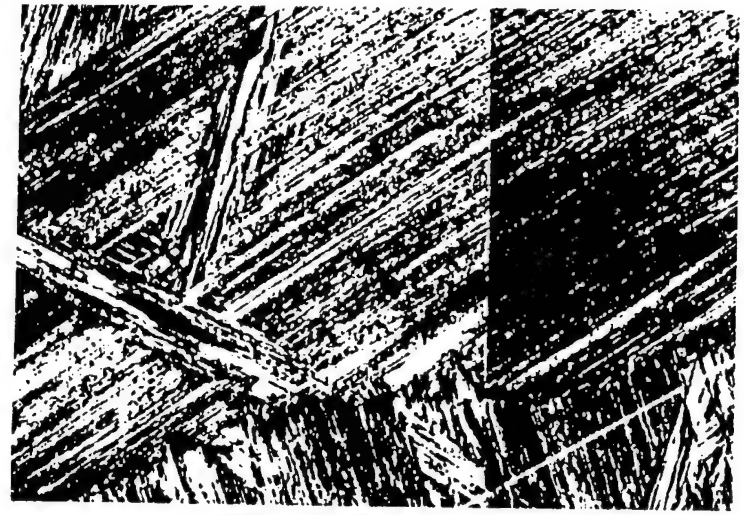

FC: 297/360/0.36

AC: 460/543/0.82

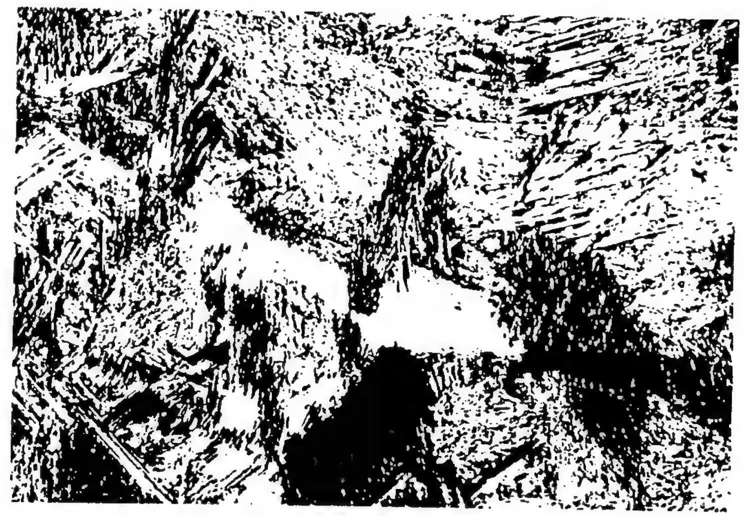

WQ: 516/579/0.5

Cooling Rate vs Microstructure/Tensile-Properties in α-Treasted Alloy G8

4

HIGH TEMPERATURE MATERIALS

Advances in Microstructural Control

Gamma Microstructure/Property Relationships:

STRUCTURE	YEAR	YS (ksi)	UTS (ksi)	EL (%)	K $(ksi\sqrt{in})$	CREEP (<950°C)
Duplex (G+L)	1988	65	80	**3-4**	12	Fair
Nearly Lamellar	1990	**90**	**105**	2-2.5	14	Fair
Fully Lamellar	1990	50	75	0.4-0.9	**22-30**	**Very Good**
Cast Nearly Lamellar*	1991	43	58	1.4-2.0	23-28	Good
TMP Lamellar	1991	**85**	**100**	**2-2.5**	**25-30**	Good

*Howment Co,
Cast Ti-48Al-2Mn-2Nb

TMP LAMELLAR STRUCTURE HAS BEST BALANCE OF PROPERTIES

Properties of Titanium-Base Alloys and Superalloys

Property	Ti-Base	Ti_3Al-Base	TiAl-Base	Superalloys
Structure	hcp/bcc	DO19	L1o	fcc/L12
Density (g/cm^3)	4.5	4.1-4.7	3.7-3.9	7.9-8.5
Modulus (GPa)	95-115	110-145	160-180	206
Yield Strength (MPa)	380-1150	700-990	350-600	800-1200
Tensile Strength (MPa)	480-1200	800-1140	440-700	1250-1450
Ductility (%) at RT	10-25	2-10	1-4	10-25
Ductility (%) at HT(°C)	12-50 (550)	10-20 (660)	10-60 (870)	20-80 (870)
Fracture Toughness (MPa/m) at RT	30-60	13-30	12-35	30-90
Creep Limit (°C)	600	750	750^a-950^b	800-1090
Oxidation Limit (°C)	600	650	800^*-950^+	870^*-1090^{**}

^{a} Duplex; ^{b} Fully-lamellar microstructures; * Uncoated; + ** Coated; + Expected

Component Forming
(Wrought Processing)

Turbine Engine Components

Blades

- Alloy/Microstructures
- Mill product + Machining
- Impression Forging to NNS
  - Isothermal
  - Hot-Die Forming
- Heat Treatment

Disks

- Mill Product + Machining
- Impression Forging to NNS
  - Isothermal
  - Hot-Die Forming
- Heat Treatment

Engine Valves

Automotive Engines

Aircraft Engines

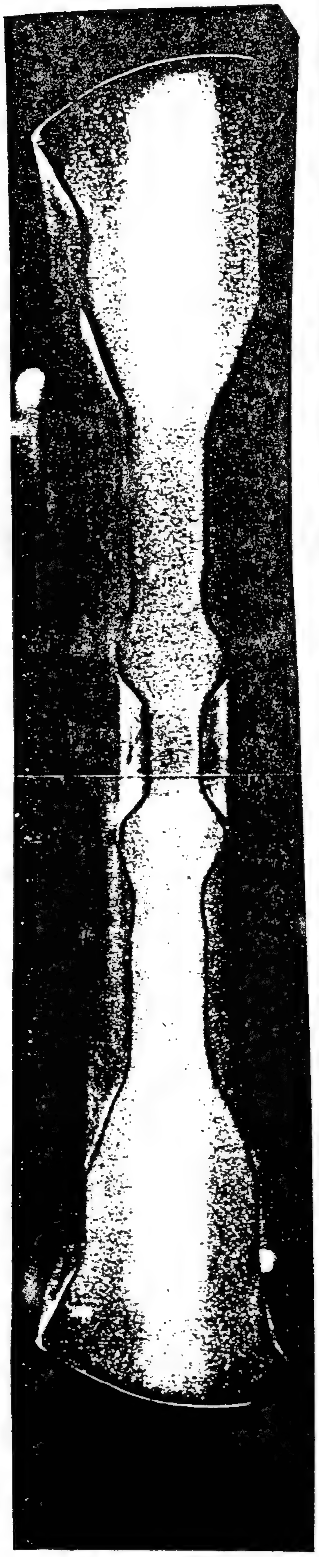

G87

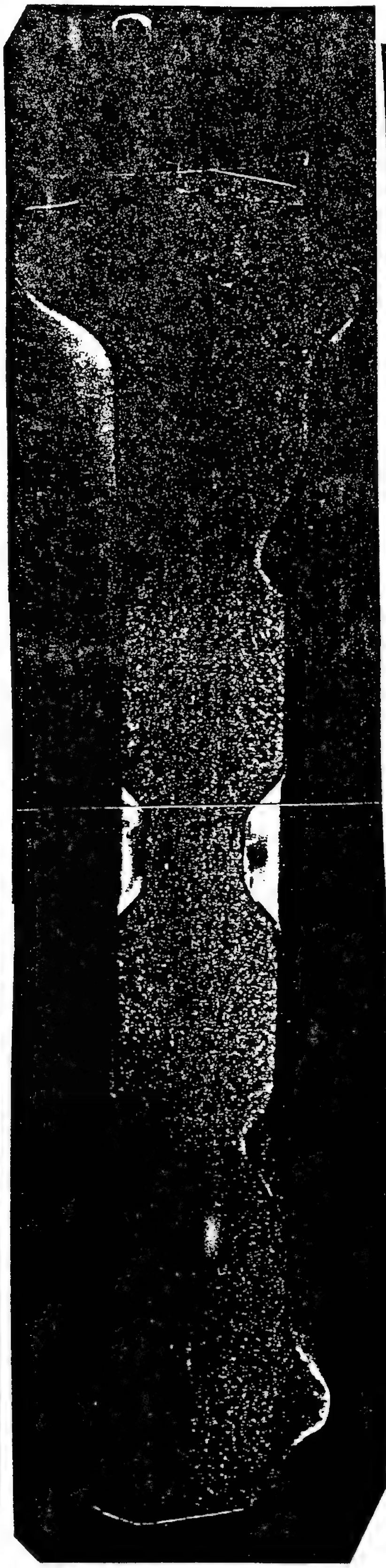

3882

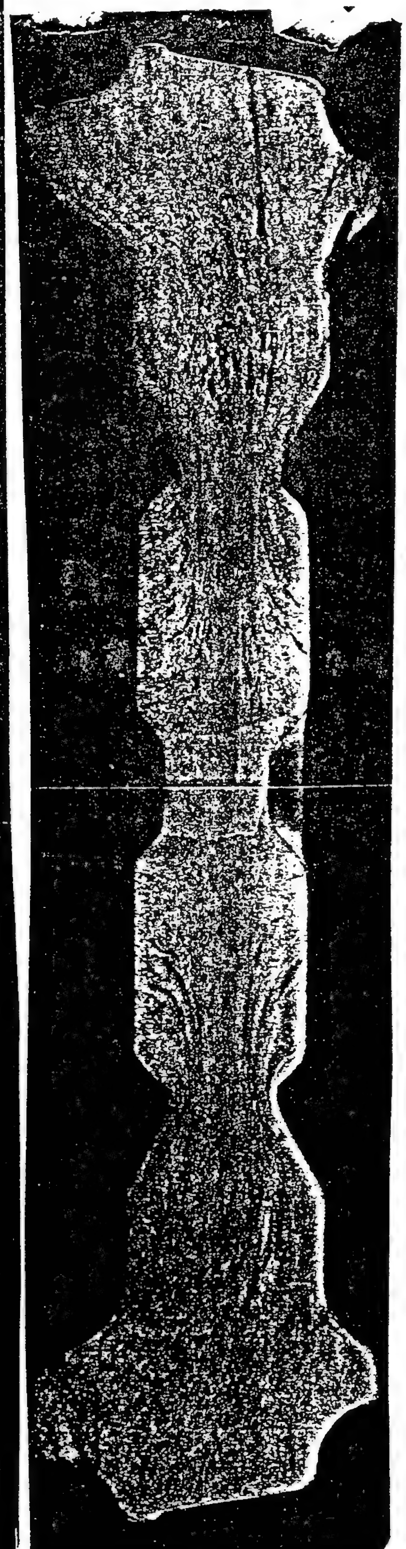

3880

W

Automotive Valve Forming

Cast Valve

Casting

Hipping

Passenger Car

Wrought Valve

Isothermal Forging

Production Die Extrusion/Forging

- Preconditioning: IM; PM
- High Rate Extrusion of Preforms
- High Rate Head Forging
- Microstructure Control

Head/Stem Joining

High Performance

6

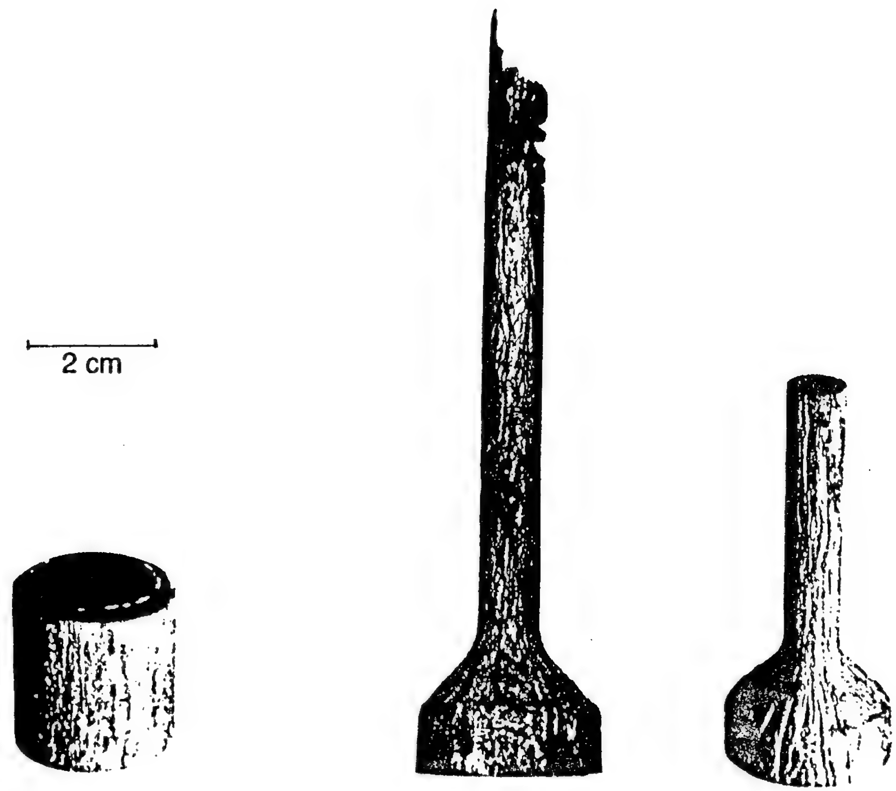

Preform

1st Step: Partial Extrusion

Wrought Gamma Engine Valve

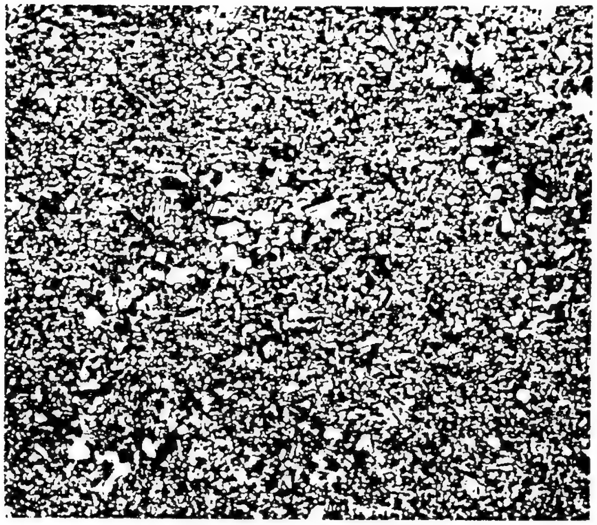

Stem

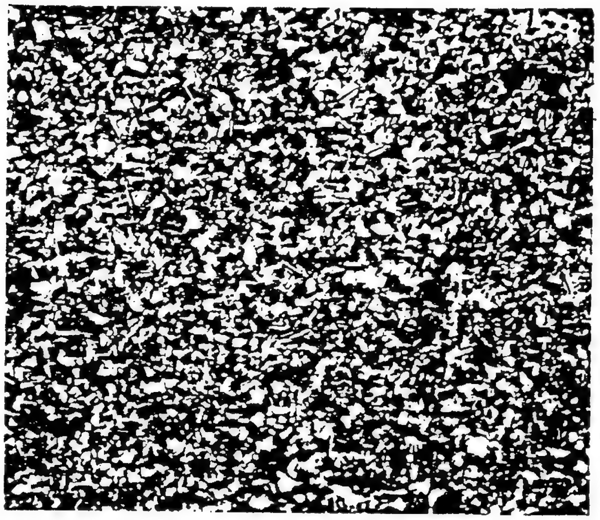

Neck

Base

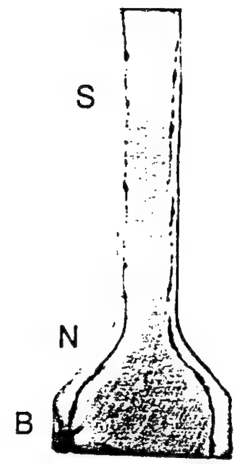

50 µm

G10 Valve Extrusion:
Transverse Sections

6

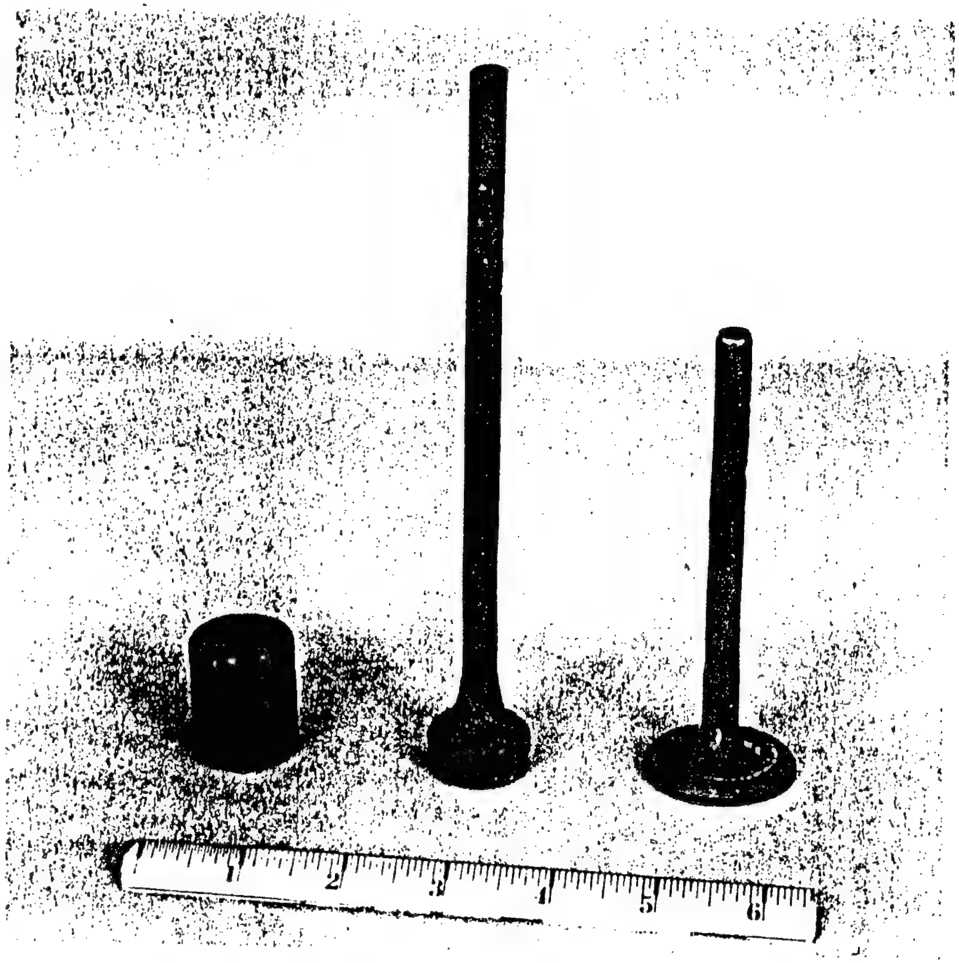

High-Rate (80 cm/sec)
Warm-Die (250°C)

Valve Extrusion
Head Coining

Commercial Steel Valve
Production Press (TRW)

Wrought Gamma Exhaust Valves

Applications

Aircraft Gas Turbine Engines

Automotive Engines

Land-Based Gas Turbine Engines

Others

6

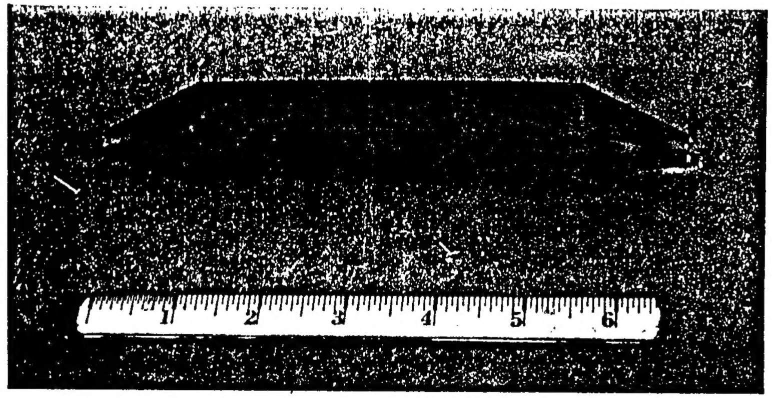

Cast 4822 Gamma Transition Duct Beam

GE-90 Engine for Boeing 777

CAESAR
Program

COMPONENT AND ENGINE STRUCTURAL ASSESSMENT RESEARCH

Gamma Titanium HPC 6th Stage Blades

Participants:

P&W	Cast "XD" Ti-47Al-2Nb-2Mn-0.8%TiB_2
Rolls Royce	Cast "XD" Ti-45Al-2Nb-2Mn-0.8%TiB_2
Allison ADC	Wrought Alloy 7
GE	Wrought Ti-48Al-2Cr-2Nb

Schedule:

Design and fabrication	[redacted] 96
Delivery to P&W	[redacted] 96
Proof spin (P&W)	[redacted] 96
~~F119 Core test 100 hrs (AEDC)~~	[redacted] 96
~~Engine tests 2000 TAC cycles (P&W)~~	[redacted] 97
~~Spin pit test to failure (P&W, UK)~~	[redacted] 97

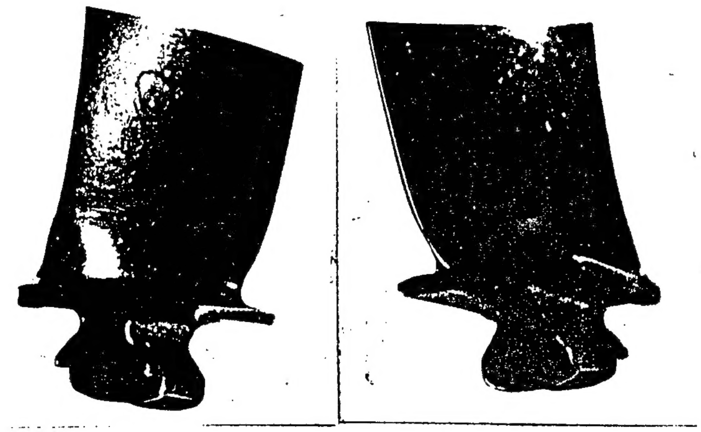

Other gamma Ti components:

- ~~HPC inner shroud~~
- ~~combustor swirlers~~
- ~~nozzle tiles~~

6

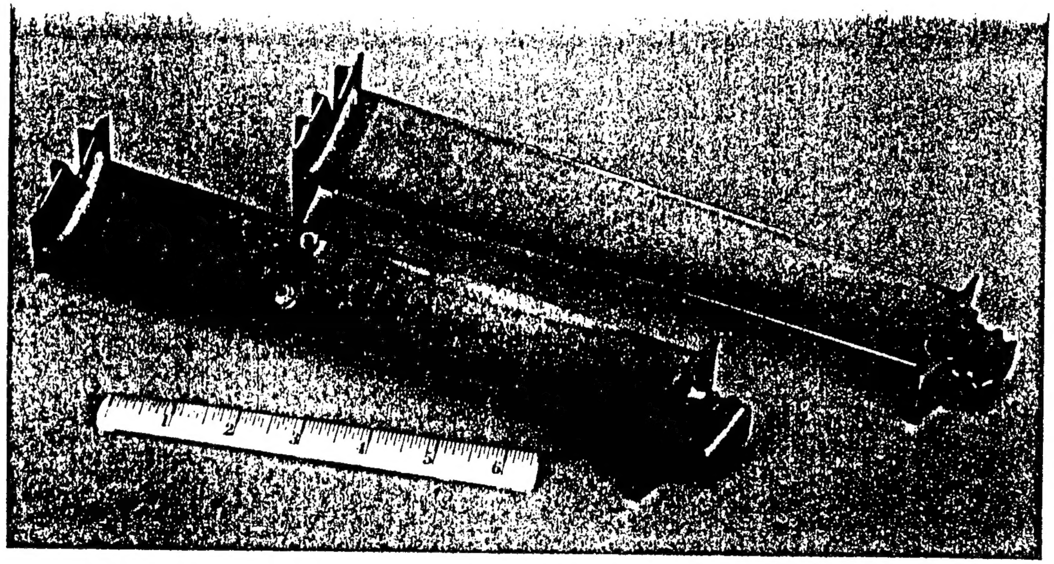

4822 Cast Gamma LPT Blades for GE CF6-80C2

Cast and Chem-milled

Engine Tested for over 1000 cycles

Summary and Future

Continuous Alloy Exploration/Design

Casting vs Wrough Alloys

Continuous Search for Fundamentals

Process Development

Component-Specific Alloy Design

Search for Application Areas

Understand Practicality

Collaboration/Exchange